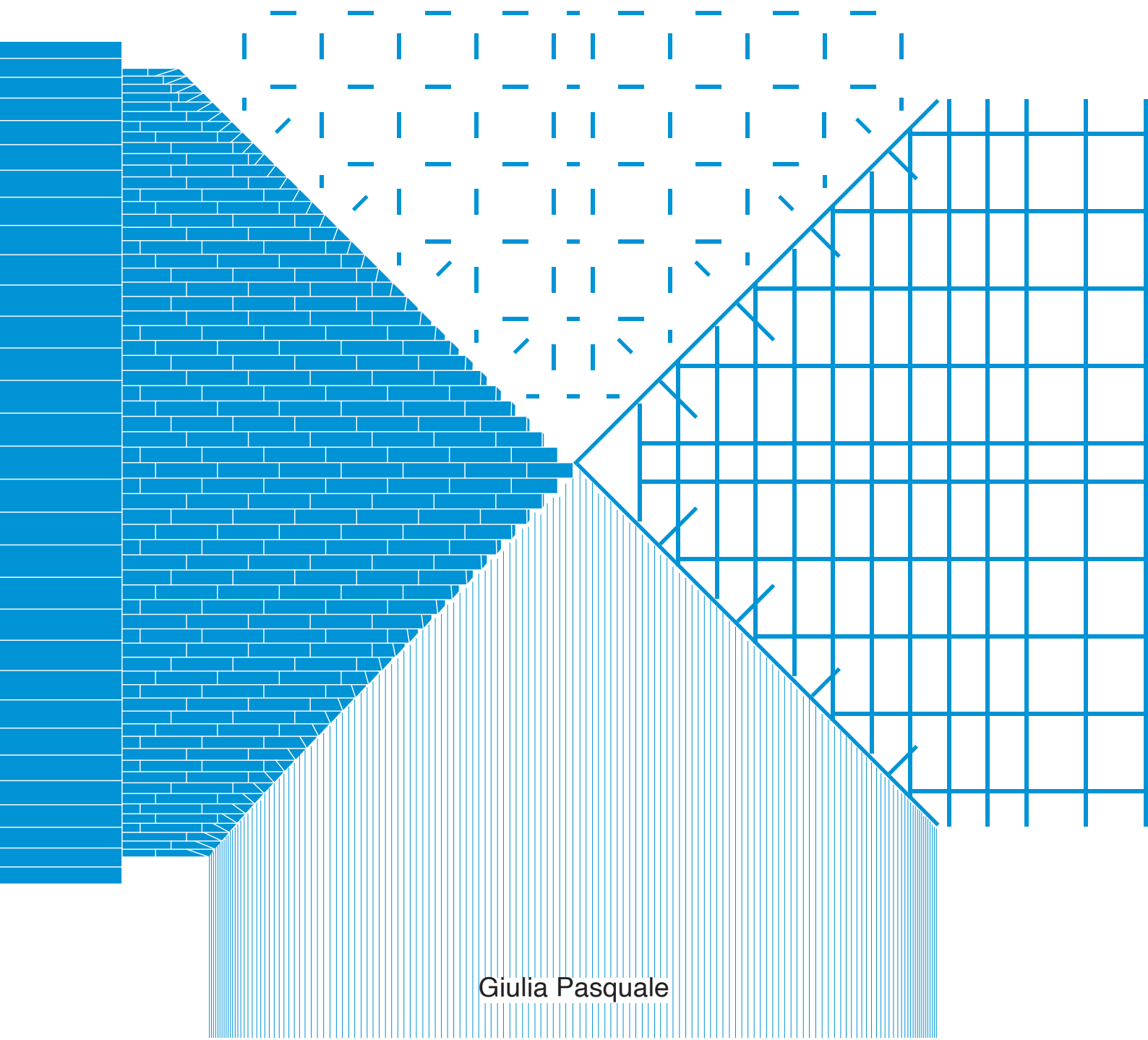


Design of physical models for the analysis of vaulted structures:

prototyping the testing setup for a small-scale cross-vault



Giulia Pasquale



**Politecnico
di Torino**

DAD - Dipartimento di Architettura e Design
Master degree in Architettura costruzione città
A.Y. 2023/2024
Graduation period December 2024

***Design of physical models for the analysis
of vaulted structures:
prototyping the testing setup for a small-scale cross-vault***

Supervisors:

Alessia Monaco
Fiammetta Venuti

Co-supervisors:

Marco Alforno
Chiara Ferrero

Candidate:

Giulia Pasquale
S310765

Ringraziamenti

*Grazie alla mia famiglia,
per l'incondizionato supporto, per avermi sempre spinta ad essere
curiosa e a conseguire gli obiettivi con determinazione.*

*Grazie agli amici,
per avermi accompagnato in questo incredibile viaggio di crescita
personale che si chiama università.*

*A Matindi,
compagna di progetto fidata, per aver sempre rallegro con
spensieratezza anche le giornate più difficili.*

*A Sara,
compagna di una giostra di alti e bassi che si chiama quotidianità,
per aver condiviso con me avventure d'alpe e d'oltralpe.*

*Ai miei professori,
guide essenziali nella scoperta del mondo dell'architettura.
In particolar modo ai miei relatori e correlatori,
Alessia Monaco, Fiammetta Venuti, Marco Alforno e Chiara Ferrero,
grazie per avermi accolta nel loro gruppo di ricerca e per essere
stati con me sempre disponibili e disposti a rivolgere parole di
gratitudine.*

*Grazie al ModLab Arch,
Francesca Ronco e Giulia Bertola,
per avermi aperto le porte del laboratorio ed avermi pazientemente
seguita nella realizzazione del progetto.*

*Grazie ai tecnici di laboratorio del ModLab Design e del Lastin,
per essere stati disponibili a dedicare tempo e spazio a questo
progetto di tesi.*

*Alla professoressa Laura Burul,
un grazie speciale
per avermi trasmesso alle scuole medie la passione per il
disegno tecnico.*

*Ad Alberto,
un grazie unico
per avermi saputa ascoltare, per aver sempre creduto in me ed
avermi sempre sostenuta da vicino e da lontano.*

*Grazie a tutti,
a tutti coloro che hanno contribuito, in grande e in piccola parte,
al raggiungimento di questo traguardo.*

*Grazie a me stessa,
che ho avuto la forza di cambiare direzione
ed intraprendere questo percorso che mi ha regalato enorme
soddisfazione.*

Abstract

Since masonry vaults are among the most common structural elements within European cultural heritage buildings, understanding their behavior is essential for accurately assessing how entire buildings respond to cracks and instability phenomena caused by poor maintenance, ineffective retrofitting interventions, changes in loading conditions and earthquakes.

Considering the importance of this topic and the growing interest in safety and conservation of historical heritage, many architecture research studies focus on this area.

The present work contributes to the *REVHEAL* research project, a national research initiative coordinated by the Department of Architecture and Design of Politecnico di Torino and developed in collaboration with University of Brescia.

REVHEAL focuses on assessing the safety of cross-masonry vaults and designing risk mitigation strategies in line with traditional conservation principles. The primary research goal is cross-referencing previous numerical analyses conducted on cross-vaults with the results of a new experimental campaign performed on both small-scale and full-scale cross-vault specimens.

This thesis is part of the initial phase of the above-mentioned extensive research. In particular, the design and building process of a testing setup for the analysis of small-scale vaulted structures is here presented.

The research begins with an outline of the thesis objectives, followed by an overview on the role of small-scale models of arches and vaults and an excursus on the state of the art regarding the topic of experimental campaigns on masonry vaults. This introductory part is followed by the main core of the thesis, which is divided into two parts: the design of the testing setup and its prototype building process.

Particularly, the present work focuses on the design of two different setups for conducting structural tests on a 1:5 scale model of a cross-vault. Moreover, a prototype of a plywood centering system is developed in order to be able to build the cross-vault on which shear

and opening tests will be performed. The centering system, designed to be adaptable to both testing setups, is characterized by a modular geometry composed of three separate pieces which will be removed from beneath the cross-vault.

In conclusion, the present work analyzes the process of designing a functional and precise assembly, maneuvering and extraction system for the cross-vault's centering. A 1:5 scale model of the plywood centering and other components of the testing setup are then built and assembled.

Index

1.	Introduction	p. 11
	1.1 General purpose	p. 11
	1.2 Identification of the case study	p. 12
2.	Small-scale models of arches and vaults	p. 17
	2.1 Scale laws	p. 17
	2.1.1 Concept of similarity in structural engineering	p. 17
	2.1.2 Heyman's scale law hypothesis	p. 22
	2.2 State of the art	p. 23
	2.2.1 The use of physical models in architecture	p. 24
	2.2.2 Comparison table on small-scale masonry vaults testing campaigns	p. 27
	2.3 Considerations on the selected case studies	p. 28
3.	Design of the testing setup	p. 35
	3.1 Design of the cross-vault	p. 35
	3.1.1 The cross-vault's geometry and its boundary conditions	p. 35
	3.1.2 Design of the 3D-printed blocks	p. 37
	3.1.2.1 The issue of blocks' density	p. 40
	3.1.2.2 Rhinoceros "pockets" modelling	p. 41
	3.2 Evolution of the conceptual design of the testing setup	p. 44
	3.2.1 Step 1: first approach to the problem	p. 45
	3.2.2 Step 2: prototype with an internal lowering mechanism	p. 48
	3.2.3 Step 3: prototype with an external lowering mechanism	p. 54
	3.3 Design of the plywood centering	p. 60
	3.3.1 Excursus on the centering's design	p. 60
	3.3.2 Final centering prototype	p. 62
	3.4 Design of the centering moving system	p. 70

4.	Building process of the testing setup	p. 77
	4.1 Manufacturing of 3D-printed components	p. 77
	4.2 Building process of the centering	p. 81
	4.2.1 First prototype	p. 81
	4.2.3 Final assembly	p. 82
5.	Conclusions	p. 99
6.	References	p. 105

1. Introduction

1.1 General purpose

The present work is part of a research project that aims to develop a better understanding of historical unreinforced masonry vaulted structures. Masonry arches and vaults, representing one of the most important structural topologies within European cultural heritage buildings, are particularly vulnerable and often show signs of damage or collapse due to multiple factors, including poor maintenance, ineffective retrofitting interventions, changes in loading conditions, or, in the worst-case scenario, catastrophic events such as earthquakes.

The interest in safety and conservation has been growing in the last few decades, not only because of a cultural awareness factor towards historical heritage, but primarily because unreinforced masonry buildings are the most common form of civil construction around the globe and there is still a lack of knowledge about their structural behavior due to their constructive complexity [1].

The present work contributes to the *REVHEAL* research project, a national research initiative coordinated by the Department of Architecture and Design of Politecnico di Torino and developed in collaboration with University of Brescia, with Alessia Monaco and Emanuele Gandelli as respective coordinators.

REVHEAL focuses on assessing the safety of cross masonry vaults and designing risk mitigation strategies in line with traditional conservation principles. The project will analytically identify collapse mechanisms using innovative technologies with the support of 3D user-oriented digital models [2].

The primary goal of the research is to compare the results of previous numerical analyses of cross-vaults with both physical and numerical structural analyses conducted on small-scale and full-scale physical models of cross-vaults. Subsequently, researchers will design *ad*

hoc reversible and natural reinforcements to strengthen the vaults following the logic of minimum intervention.

This experimental thesis is part of the initial phase of this extensive research. It focuses on the design of small-scale physical models for the analysis of vaulted structures. A preliminary setup of a specimen and scaled-down samples are designed and built to better understand the assembly and maneuvering process of its components. In other words, this research aims to design and build a testing setup that would be used as the starting point for future structural experiments and tests on scaled cross-vaults.

The future developments of this research will proceed with an experimental and numerical study on the structural behavior of cross-vaults under the effects of quasi-static displacements such as shear displacement, opening test and tilting test.

In conclusion, understanding the behavior of masonry vaults using small-scale models is crucial to comprehend cracks and instability phenomena of real case studies. Therefore, the knowledge of cross-vaults' behavior under load is fundamental for the planning of structurally compatible, cost-effective and targeted consolidation interventions.

1.2 Identification of the case study

Focusing on the research conducted by Politecnico di Torino, the goal is to study the structural behavior of small-scale models of masonry cross-vaults with different bricks patterns under various load conditions.

Geometrically the cross-vault is made of blocks disposed in a radial or diagonal pattern, three boundary arches and a back wall. In order to build and conduct structural tests on the vaults, a plywood centering, a manual lowering system and support elements are designed for

this specific case study.

The present thesis focuses on the design and 3D modelling of the entire 1:5 small-scale prototype, excluding the vault itself, as well as the physical realization of the centering mechanism and other components of the testing setup.

Talking about the case study references, the investigated cross-vault follows the vaults' geometries identified by Marco Alforno in his doctoral research [3].

He numerically investigated how different brick patterns influence the instability of full-scale masonry cross-vaults (Fig. 1.1, 1.2). In particular, the research started by focusing on ideal cross-vaults geometries, referencing the case study analyzed by Michela Rossi. Subsequently, a correspondence between the numerical analyses and the case study of the Sanctuary of Vicoforte was identified. This Renaissance building is entirely constructed in brickworks, apart from stone pillars, and all its vaults are built with bricks, regular in shape and arranged in a diagonal or radial pattern.

As a result, it was highlighted how the recurring geometry of a diagonal cross-vault confined by head arches has a structural explanation. While a cross-vault with a radial pattern is stable under its self-weight, the diagonal one is not, so a perimetral confinement is needed.

The cross-vault assembly process and centering removal, instead, takes inspiration from Michela Rossi's doctoral research conducted on masonry cross-vaults [4]. She tested both numerically and experimentally a small-scale model of a masonry cross-vault with the aim of evaluating its response under seismic damage mechanisms, such as horizontal shear distortion and longitudinal opening/closing of the abutments (Fig. 1.3, 1.4).

The purpose of the present research is to design a testing setup that allows for multiple tests on vaulted structures. The testing setup is a functional tool as long as it is resistant enough to withstand multiple

tests. Repetitive tests are necessary to validate the obtained results, as the small-scale model is highly susceptible to environmental changes and human error. A smooth process of centering maneuvering is needed to perform as many tests as possible in the shortest time possible.

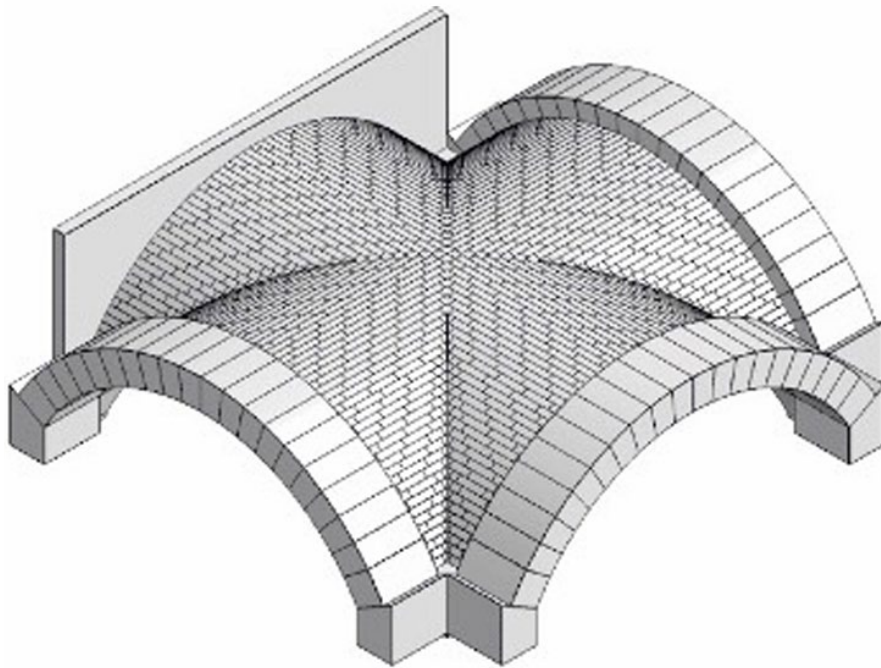


Fig. 1.1 – Full-scale radial cross-vault with head arches and back wall (From: Alforno 2021 [3]).

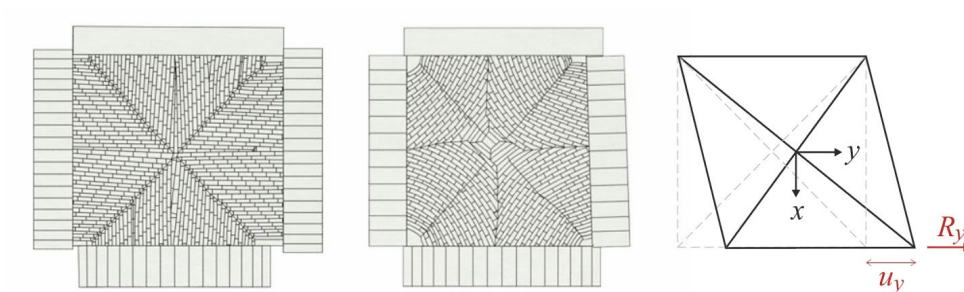


Fig. 1.2 - Radial and diagonal cross-vault and the scheme of the imposed shear displacement (From: Alforno 2021 [3]).



Fig. 1.3 - Testing setup for small-scale cross-vault, focus on the centering system (From: Rossi 2015 [4]).

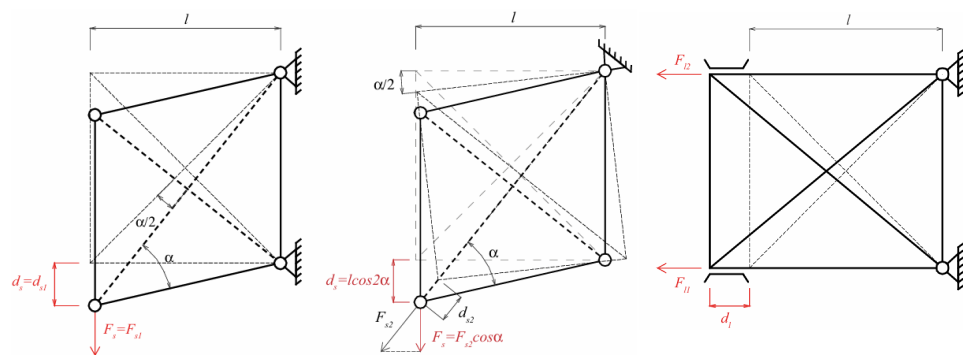


Fig. 1.4 - Scheme of the imposed shear displacements and opening test (From: Rossi 2015 [4]).

2 . *Small-scale models of arches and vaults*

In this second chapter, an overview on the role of small-scale models of arches and vaults, in the field of assessing and retrofitting the architectural heritage, is presented.

Firstly, the principles that allow reduced scale experimentation are investigated, then the state of the art on the theme of small-scale models of masonry cross-vaults will be summarized and reviewed using comparison tables.

2.1 Scale laws

2.1.1 Concept of similarity in structural engineering

Thanks to the concept of scale laws, complex problems can be studied through small prototypes which are more feasible and less expensive than full scale models.

The concept of similarity in engineering refers to the relationship between two systems or models, where one is a reduced or simplified representation of the other but retains the same fundamental physical characteristics. This technique is often used to study complex phenomena in a more manageable way, by creating scaled physical or mathematical models that replicate the behavior of the real system [5].

Similarity is based on the following parameters [6]:

1. Geometric similarity: the different parts of the model and the real system must have the same geometric shape, with all linear dimensions such as lengths, widths and heights in proportion.
2. Kinematic similarity: the relative velocities of particles in the model and the real system must be proportional. This implies that the model

and the real system must have the same ratio between velocity and spatial dimensions.

3. Dynamic similarity: the dynamic forces acting in the model must be proportional to the forces in the real system. This type of similarity is often expressed in terms of dimensionless numbers, such as the Reynolds number or the Froude number, which must be the same in both the model and the real system.

When these different types of similarity are respected, the model is said to be similar to the real system, and thus the results obtained from studying the model can be applied to the real system, with appropriate scaling. This concept is fundamental in many fields of engineering, such as aerodynamics, hydraulics and structural mechanics.

Reduced scale experiments, which are relatively economic and feasible, provide insights into the expected performance of full-scale machines. But not all the results can be scaled up by multiplying the model results by a scaling factor.

For example, material properties such as mass, density, friction coefficient or strength and stiffness cannot be scaled linearly [7].

Another topic concerns those geometries that are independent of scale, a fundamentally important issue in structural engineering.

Among form-active structures, we find arches, vaults and domes. Following Robert Hooke's law, the ideal shape for which an arch is stable is represented by the geometry of an inverted catenary, acting in pure compression. The arch is a structural element capable of channeling the stresses produced by loads along its curved path, transforming them into predominantly compressive forces. This also occurs with vaults and domes, but in three dimensions and with more complex geometries. Hence, the stability of masonry arches, vaults and domes under gravity loading is a characteristic independent of scale [8].

This observation explains how masonry structures managed to evolve so impressively, long before there was any scientific or mathematical comprehension of structural behavior. Consider that the first dome in history, the Treasury of Atreus in Mycenae (Fig. 2.1), was built in XIV BC. [7].

Giovanni Poleni, called in 1748 to work on the structural consolidation of St. Peter's dome, was probably the first to provide a scientific explanation for the stability of a dome using the concept of the thrust line (Fig. 2.2). Many other historical architectures were designed in reverse as tensile structures and then inverted to act in pure compression. Examples like these include the Sagrada Familia and the Church of Colònia Güell designed by Gaudì (Fig. 2.3), as well as Isler's concrete shells (Fig. 2.4).

This said, the similarity concept is very difficult to respect in the design of small-scale models because some structure's properties can be easily scaled up, such as linear dimensions and shape, whereas other cannot, such as mass, strength and stiffness.

For this reason, it is not possible to design a small-scale model that is similar in every aspect to the full-size structure. Therefore, it is important to highlight which properties are going to be scaled and which are not in relation to the purpose of each case study. By doing so, the results will be understood depending on the chosen scale factors [7].

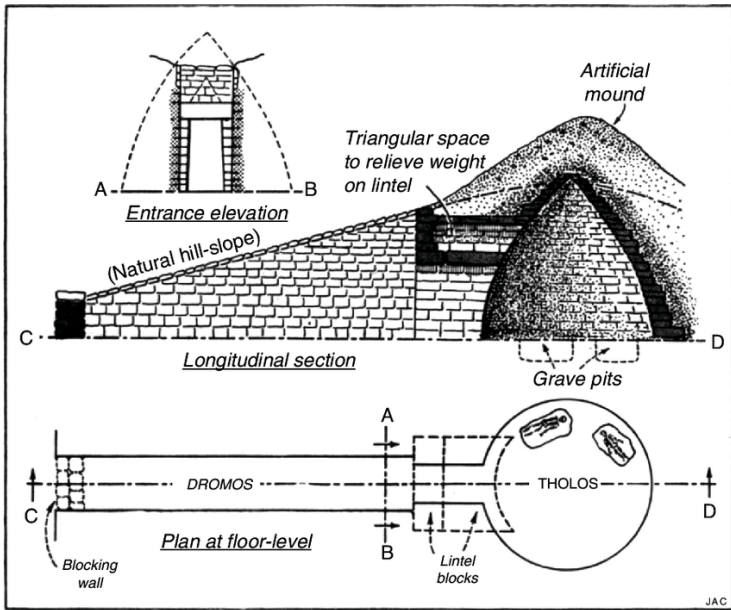


Fig. 2.1 – Plan and section of the Treasury of Atreus in Mycenae (From: *The archeologist, The Treasury of Atreus: A Masterpiece of Mycenaean Engineering*, https://www.thearchaeologist.org/blog/treasury-of-atreus-the-monumental-mycenaean-tomb#google_vignette).

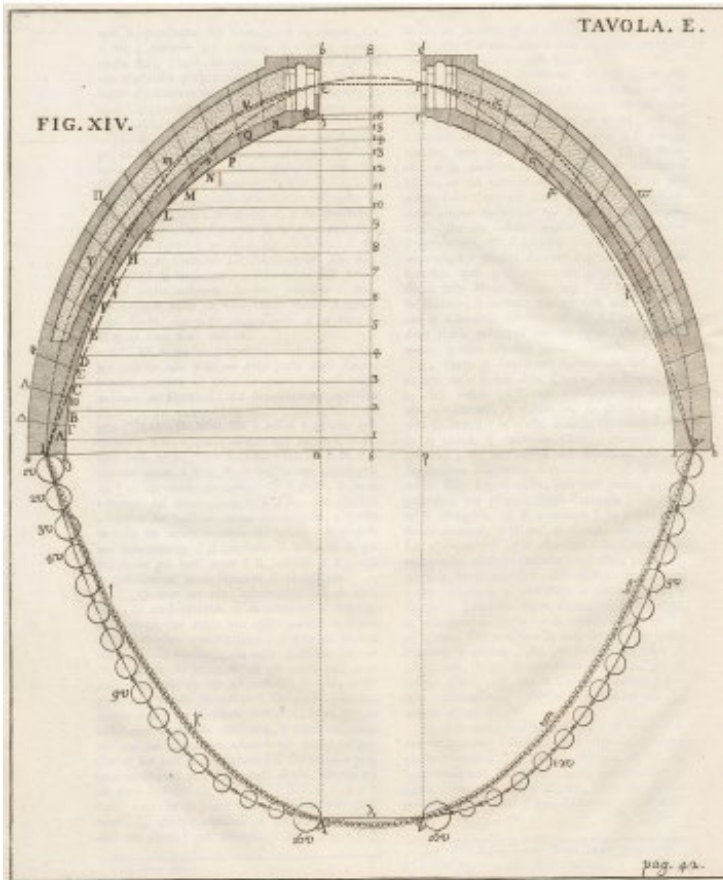


Fig. 2.2 – Giovanni Poleni thrust line studies on San Peter's dome (From: G. Poleni (1748), *ETH-Bibliothek Zürich, Rar 1229, Public Domain Mark*).



Fig. 2.3 – Tensile-only model of the Church of Colònia Güell (From: C. Karul (2015), The flexible Fourier form and panel stationary test with gradual shifts).

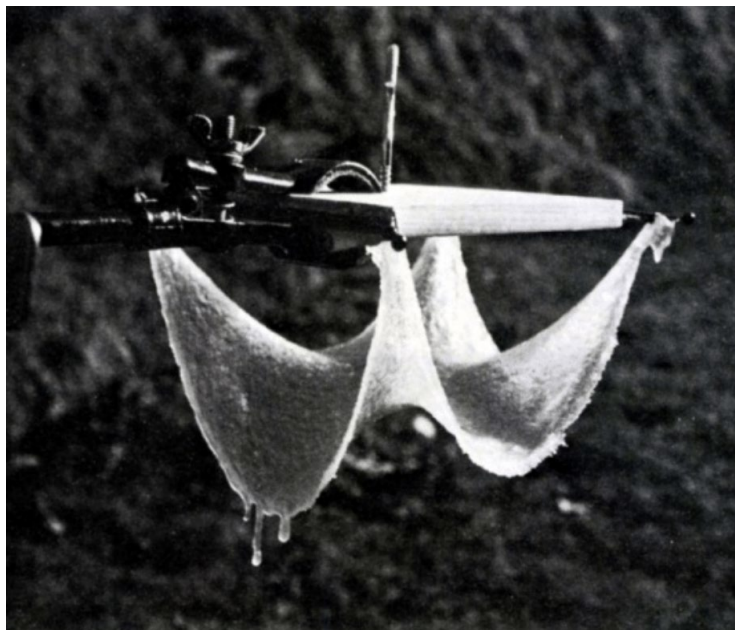


Fig. 2.4 – Tensile-only model of Isler's shells (From: H. Kloft (2011), Logic and form: From Isler shells to nonstandard structures).

2.1.2 Heyman scale law hypothesis

The use of reduced-scale models to simulate the structural behavior of masonry constructions is supported by Heyman's theory formulated in 1966 in the article "The Stone Skeleton" [9].

He developed three assumptions about the properties of arches and vaults material:

1. Stone has no tensile strength if we consider an arch made up of voussoirs laid either dry or with mortar. The joints do not have tensile strength, so only compressive forces can be transmitted from one portion of the structure to another.
2. The compressive strength of stone is effectively infinite due to the low general stress levels. In other words, the compressive stresses between the blocks do not come close to the crushing strength of the material.
3. Sliding one stone upon another cannot occur, therefore the friction between blocks must be high enough to ensure that they will not slide over each other.

Heyman's hypothesis imply that the stability of masonry structures relies on geometry rather than material properties. Consequently, the elastic calculation of stress is irrelevant and the elastic deformations may be omitted.

Even though arches and vaults' stability theoretically depends only on form, practically scaled models suffer from the effects of environmental vibrations and other altering factors.

To overcome this problem, some precautions should be taken. For example, high density models and a coherent angle of friction between blocks are suggested.

In the evaluation and better understanding of masonry structures, small-scale models are used as a suitable alternative. Building small-

scale models of vaults and arches is useful to validate previous numerical analysis as well as to deepen the knowledge on their structural behavior before designing and testing full-scale specimens.

In the present research, a small-scale model of a masonry cross-vault has been designed following Heyman's hypothesis.

Firstly, the geometric similarity requirements are respected. The vault's original geometry is scaled down by a factor of five so that the proportions remain unaltered. Even the interlocking blocks of the vault are scaled down by a factor of five from the regular dimensions of a solid brick (6x12x24 cm).

Then, sufficiently rigid material was chosen to address Heyman's rigidity assumption. The cross-vault's blocks are made of a 3D-printed nylon material with a density of 980 kg/m³.

To increase the mass of the vault, each brick was designed as a 2 mm thick envelope with an open intrados in order to be filled with lead pellets and epoxy resin. The choice of lead pellets was made to have a material heavier than the steel plates used by Rossi [4], but at the same time economic and readily available.

Finally, it was made sure that the bricks' material had a sufficiently high angle of friction to avoid sliding phenomena. Multiple tests were performed on various 3D-printed materials to achieve a friction coefficient closely matching that of masonry.

2.2 State of the art

As part of a larger research project, the present work directly derives from the case studies analyzed by researchers worldwide in the past. Therefore, to clarify the context of this work, it is necessary to summarize the state of the art regarding the topic of experimental campaigns on masonry vaults. Subsequently, the main connections between this research and previous studies will be highlighted, then an exploration of the direction that this thesis intends to take and deepen will follow.

2.2.1 The use of physical models in architecture

The use of physical models can be traced back to the earliest historical records of engineering and construction and addresses different purposes such as testing mechanisms and designs, checking mechanical functioning and structural behavior and demonstrating new ideas to the client. [10]

A significant advancement of architectural model practices occurred during the Renaissance, where physical models served both as representation and design tools. The purpose of models at this point in history was dual: being an operative object with which to explore specific construction details and being an object to be presented to clients.

A beautiful example of the first case is given by Filippo Brunelleschi who typically designed wooden models as a guide for the craftsmen (Fig. 2.5).

This said, another usage of physical models in architectural and engineering practice is here presented. A kind of modelling that aims at the observation and evaluation of structural behavior.

The earliest documented instances of scale-model testing can be traced back to the experiments conducted by Danyzy in 1732, who employed plaster models to study the failure mechanisms of masonry arches and buttresses [11].

From the Age of Enlightenment to the first decades of the nineteenth century the use of models in the structural field increased and the documentation about their use improved alongside the progression of technologies.

A broader adoption of physical structural models began at the end of the 19th century, involving the design of spatial structures to assess their overall behavior. We can find examples of this phase in the work of designers such as R. Buckminster Fuller, E. Torroja, F. Candela, R. Le Ricolais [12] and L. Mies Van der Rohe (Fig. 2.6) [13].

To conclude the historical development of small-scale models, the use of measurement models in structural engineering has declined since the Seventies due to the development of advanced computer model technologies. Nowadays, however, structural models are coming back due to different limitations in digital modelling and analysis.

Moreover, the behavior of theoretical models is often not sufficient when the analyzed physical phenomena are too complex to be modeled precisely. These cases include the movement of fluids, seismic effects and the interaction between structure and soil [14].

A more specific field of research where the results of digital models need to be cross-referenced with those coming from physical models is the analysis of masonry vaults and arches due to the complexity of the mechanical interlocking of voussoirs (wedge-shaped blocks) and its overall geometry [14].

In addition to the issue of simplifying real-world problems, numerous research cases have encountered the opposite problem. Specifically, modeling and software testing can be excessively precise, leading to an overestimation of the actual capabilities of masonry structures. As a result, some studies have discussed how to incorporate defects into digital models [15].

In conclusion, the use of physical models has long been vital in architecture for gaining an empirical understanding of how structures behave. Data gathering during physical model testing can be employed to define and validate numerical and analytical models by comparing their predictions with the outcomes of the experimental tests.



Fig. 2.5 – Brunelleschi, wooden model of the lantern displayed at the Museo dell’Opera del Duomo (From: Opera magazine, L’11 agosto 1446 Michelozzo avviava la costruzione della lanterna della Cupola).



Fig. 2.6 - Ludwig Mies van der Rohe, structural model of the Chicago Convention Hall, 1953 (From: A. Cabanillas Cuesta 2019).

2.2.2 Comparison table on small-scale masonry vaults testing campaigns

Although the interest in the topics of conservative restoration and the reinforcement of historical architecture has grown in recent years, there are still too few studies focusing on this area. As Elisa Bertolesi identified in her research [16], only 54 references were found with the keywords “masonry cross-vault” between 1960 to 2018.

Because of this observation, it became necessary to study and catalog the case studies from the past in order to identify the progressive development of research regarding the topic of small-scale masonry vaults and to highlight the analyzed recurring themes. A comparison table was chosen to be the most effective tool to express the comparison between studies focusing on small-scale masonry vaults.

A first comparison table, “Comparison table 1: small-scale masonry vaults testing campaigns“, summarizes in chronological order, starting from 2002, a series of small-scale masonry vaults testing campaigns. The chosen table’s parameters are as follows: the case study reference with an image of the small-scale model, the analyzed vault type, the model’s scale, its dimensions, the block’s material, their density, the joints type between blocks, the friction angle between adjacent blocks, the type of investigation (experimental/numerical), the conducted tests and the type of action.

A second comparison table, “Comparison table 2: centering systems used in the vaults testing campaigns“, addresses the different centering systems used in the vaults testing campaigns. The included parameters are: the reference case study with significant centering images, the vault type, the centering material and its removal mechanism.

While filling out the table, it was observed that since 2018, research on the topic of masonry vaults has intensified and deepened.

Some research takes its origin from real case studies of damaged historical masonry vaults and arches [17, 18, 19], others investigate and test ideal geometries [20, 21, 22, 23]. Furthermore, some studies revisit previously constructed small-scale models to conduct different types of tests [24, 25, 26, 27, 28], while others originate from numerical analysis [29, 15, 30, 31].

It was also observed that some studies focus on the experimentation of full-scale masonry vaults as a way of experimentation that allows for the direct observation of the hypotheses formulated through digital simulations and small-scale models [32, 33]. It was decided not to include such cases within the comparative tables, as the thesis focuses on scaled-down models. However, it is important to mention them to highlight how research is simultaneously evolving in the context of full-scale model testing.

2.3 Considerations on the selected case studies

To begin with, all the case studies listed in the “Comparison table 1” take scaling laws into account, but each adheres to them only partially, depending on the project’s objective. It is important to state from the beginning which scaling laws are being followed in order to better clarify the scalability of the results.

Another recurring factor concerns inaccuracies of the physical model. Sometimes, these inaccuracies come from the 3D-printing techniques used for the interlocking blocks, arranged like a puzzle, which can result in improper friction and contact between their faces, thus compromising the structural tests [23]. Other times, inaccuracies are related to assembly errors caused by human error. Those kinds of imperfections can be very slight dislocations that generate minor hinges and offsets between blocks which affect the initial vault’s geometry [20].

A third important factor to consider when designing a small-scale model is the mass of the vaulted masonry structure. Several research cases have encountered issues related to the influence of

environmental vibrations on the model, which were disproportionately large compared to the displacement values obtained [1, 20].

To prevent this factor from compromising the experimental tests and the model stability under accidental actions [27], it is recommended to work with average densities compatible with the one observed in solid brick masonry.

A fourth factor to analyze is the minimum friction angle between blocks. As previously mentioned regarding density, in this case as well, since it is a non-scalable property, the friction angle of the small-scale model's blocks must closely match that of the masonry vaults [4]. Working with too low friction angle would cause sliding phenomena between adjacent blocks even before the crack pattern could develop.

Finally, a few tests on a small-scale model cannot be reliable to draw accurate conclusions. Therefore, using a dry joints small-scale model can be a more effective choice for repeating structural tests multiple times without physical alterations to the initial state of the model [34].

With reference to the scaled-down examples presented in the "Comparison table 2", the cases where the centering system and its removal are described are limited and, at the same time, quite different from one another.

Starting with Rossi's case study [4], four mirror-image plywood webs were made, along with a complex formwork removal system using inclined rails. This solution was made possible thanks to the four free sides of the vault. One of the limitations encountered in this solution was the infinitesimal thickness of the plywood webs' apex, a too weak point to perform multiple assemble and disassemble operations.

In a second case study [1], the centering of a pavilion vault was made by interlocking simple sheets of wood board and it was lowered just enough to carry out the tests without compromising the collapse mechanisms. This solution is impossible to replicate in our case study, due to the presence of chains beneath the head arches.

In a third case study [23], only a polystyrene centering structure

is mentioned, with no further details provided about the removal process. From the images presented in the research, this scaffolding system seems to be rudimentary and difficult to control precisely during the assembly and disassembly maneuvers.

In Roselli's case study [28], instead, significant attention was given to the description of the plywood centering used to build a barrel vault and the subsequent lowering operations using a manual system with wedges. The main issue with this centering system concerns the slender and weak vault supports on the horizontal plane. Since the manual lowering system was placed below the plane of the vault, it was necessary to elevate the entire system on supports to access the knobs. Raising the plane on which the tests were conducted led to undesirable vibration errors.

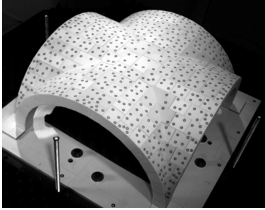
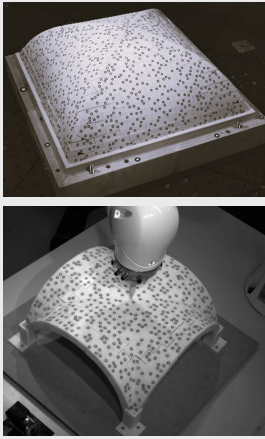
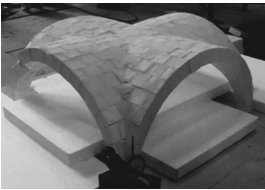
As previously mentioned, this thesis fits in the broader *REVHEAL* research which has the purpose to validate experimentally and numerically, through a 1:5 small-scale cross-vault model and a full-scale cross-vault model, the results found by Alforno's numerical analysis on full-scale cross-vault models [30].

The area of experimentation that this thesis concerns is the initial part of the *REVHEAL* project and aims to address the design and construction of a first scale prototype of a cross-vault testing set up. More precisely, a plywood centering and a manual maneuvering system will be designed and realized.

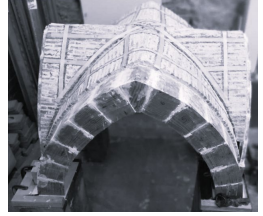
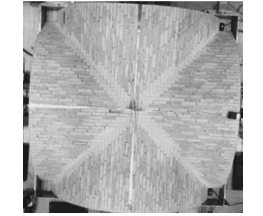
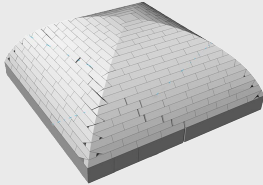
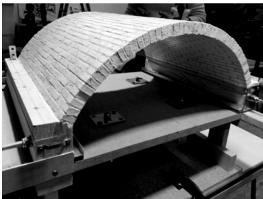
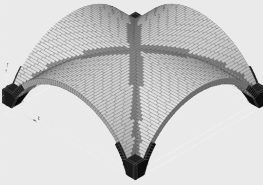
The idea of exploring the topic of the centering arose from the need to create a sturdy support capable of bearing the total weight of the vault during the assembly of the bricks, while also being easy to handle during the testing phases. To use the centering as support for the construction of the cross-vault, it is necessary to design a metal system that allows the centering to be raised and lowered manually until the desired height is reached.

The ultimate purpose of the present work is to develop and build a centering system that is as simplified as possible, easy to assemble and maneuver, but at the same time resistant to heavy loads.

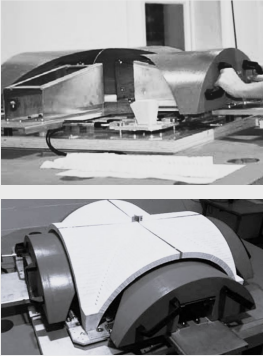
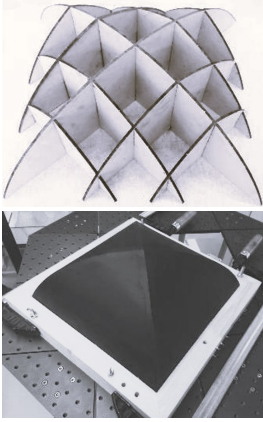
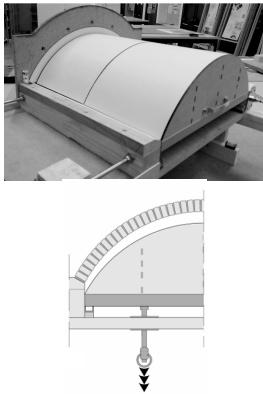
Comparison table 1: small-scale masonry vaults testing campaigns

Reference	Year	Image	Vault type	Model scale	Model dimensions	Blocks' material	Blocks' density	Joints' type	Friction angle	Type of investigation	Type of tests	Type of action
Theodossopoulos et al. [17]	2002		Ribbed radial pointed arch cross-vault	1:4	94,5 x 127,5 x 76 cm	Timber	n.a.	Lime mortar	n.a.	Experimental and numerical	Dead load Opening	Quasi-static
Van Mele et al. [20]	2012		Round arch cross-vault	n.a.	34,8 x 34,8 x 17,4 cm	Plastic powder (SLS)	$0,60 \pm 0,03 \text{ g/cm}^3$	Dry	$43^\circ \pm 3,5^\circ$	Experimental and numerical	Vertical disp. Opening	Quasi-static
Rossi et al. [21]	2016		Radial low rise cross-vault	1:5	66,8 x 66,8 x 24,9 cm	Plastic powder (SLS) + steel plate	$2,70 \text{ g/cm}^3$	Dry	$36^\circ \pm 2,5^\circ$	Experimental and numerical	Shear Opening	Quasi-static
Milani et al. [24]	2016		Radial low rise cross-vault	1:6	66,8 x 66,8 x 24,9 cm	Plastic powder (SLS) + steel plate	$2,70 \text{ g/cm}^3$	Dry	$37^\circ \pm 2,5^\circ$	Experimental and numerical	Tilting Simple shear Pure shear	Quasi-static - DSA Quasi-static - ISA
Rossi et al. [22]	2017		Pavilion vault - Round arch cross-vault	1:10	36,7 x 36,7 x 12,3 cm 35 x 35 x 17,5 cm	Plastic powder (SLS)	$0,60 \text{ g/cm}^3$ $1,41 \pm 0,06 \text{ g/cm}^3$	Dry	$38^\circ \pm 4^\circ$	Experimental and numerical	Opening Point load	Quasi-static
Foti et al. [23]	2018		Orthogonal and parallel round arch cross-vault	n.a.	100 x 100 x 57 cm	Thermoplastic filament (FDM) + cement	$6,50 \pm 0,37 \text{ g/cm}^3$	Dry	18°	Experimental and numerical	Vertical disp. Opening	Quasi-static

Continue in the next page ↓

Carfagnini et al. [25]	2018		Ribbed radial pointed arch cross-vault	1:4	88 x 110 x 76 cm	Timber	7,00 g/cm ³	Lime mortar	n.a.	Experimental and numerical	Shear	Quasi-static
Baraccani et al. [26]	2020		Ribbed radial pointed arch cross vault	1:4	89 x 110 x 76 cm	Timber	n.a.	Lime mortar	n.a.	Experimental and numerical	Shear	Quasi-static
Gaetani et al. [27]	2020		Radial low rise cross vault	1:5	66,8 x 66,8 x 24,9 cm	Plastic powder (SLS) + steel plate	2,70 g/cm ³	Dry	36° ± 2,5°	Experimental and numerical	Shear Tilting	Quasi-static
Bianchini et al. [34]	2021		Radial low rise cross vault	1:5	66,8 x 66,8 x 24,9 cm	Plastic powder (SLS) + steel plate	2,70 g/cm ³	Dry	36° ± 2,5°	Experimental and numerical	Shear Shake-table	Quasi-static Dynamic
Dell'Endice et al. [15]	2021		Pavilion vault	1:10	36,7 x 36,7 x 12,3 cm	n.a.	1,46 g/cm ³	Dry	45° ± 9°	Numerical	Opening	Quasi-static
Roselli [28]	2023		Radial and vertical barrel vault	1:5	40 x 40 x 12 cm	Cement	n.a.	Lime mortar	n.a.	Experimental	Shear	Quasi-static
Bianchini et al. [31]	2023		Radial low rise cross vault	1:5	66,8 x 66,8 x 24,9 cm	Plastic powder (SLS) + steel plate	2,70 g/cm ³	Dry	36° ± 2,5°	Numerical	Shake table	Dynamic
Caceres-Vilca et al. [19]	2024		Barrel vault	1:10	118,7x84x113,3 cm	Sillar	n.a.	Lime mortar	n.a.	Experimental and numerical	Lateral disp.	Quasi-static

Comparison table 2: centering systems used in the vaults testing campaigns

Reference	Year	Centering images	Vault type	Centering material	Removal mechanism
Rossi [4]	2015		Radial low rise cross vault	Plywood	Manual removal Four webs sliding on four inclined metal supports
Rossi et al. [1]	2017		Pavilion vault	Cardboard frames and cardboard sheets	The scaffolding is only lowered sufficiently to not interfere with the collapse mechanism
Foti et al. [23]	2018		Orthogonal and parallel round arch cross vault	Polystyrene	Manual removal
Roselli [28]	2023		Radial and vertical barrel vault	Plywood and MDF	Manual removal The centering is lowered on rails, then extracted from the front

3. *Design of the testing setup*

The case study addressed by the present work consists of a testing setup for a 1:5 scale model of a cross-vault.

The parts that constitute the testing rig are the following:

1. a low-rise cross-vault, with head arches, made of 3D-printed, dry-assembled blocks and its four abutments;
2. a centering system for the vault, made of plywood and cardboard shells;
3. elements that allow for the centering placement and removal;
4. elements that allow structural testing to be performed.

This thesis focuses on the design and modelling of the entire testing setup, following the developments of the decision-making process. It also aims to build the centering system and those fundamental elements, such as the support base, the reaction wall and the vault's abutments, to enable the assembly of the cross-vault.

3.1 Design of the cross-vault

3.1.1 The cross-vault's geometry and its boundary conditions

Addressing how the cross-vault has been designed, both the vault geometry and the blocks' shape are scaled down by a factor of five from a full-scale prototype. This means that the model respects the concept of geometric similarity.

Unlike many cases in the literature where only the vault's geometry is scaled while the dimensions of the blocks are approximated according to different criteria [20, 1], in the present case, working with scaled blocks allows for the evaluation of how the masonry texture influences the propagation of collapse mechanisms.

The vault has a squared base and it is generated by the intersection of two low-rise barrel vaults with a span of 570 mm and rise of 167 mm. The cross-vault is confined by three head arches, while on the fourth side, a rigid wall. The arches have the same span and rise as the cross-vault. The total footprint of the vault measures 892 x 796 mm. The cross-vault's thickness is 24 mm, whereas that of the arches is 48 mm (Fig. 3.1).

The head arches are added to the cross-vault's geometry as a consequence of numerical research conducted on the influence of constructive aspects on the structural behavior of masonry cross-vaults. After testing different types of confinements and bricks pattern was concluded that deformable head arches are needed to make the vault with a diagonal pattern able to find equilibrium under self-weight [29].

Addressing the blocks' geometry, the blocks have been designed in stereotomy. This means that their shape is slightly trapezoidal to compensate for the absence of mortar between them. Special care was given to the diagonal blocks of the cross-vault to guarantee a perfect voussoirs interlocking between adjacent webs [4, 35].

The present study analyses a cross-vault with a radial pattern. The vault's pattern refers to the arrangement of brick courses. Based on historical construction manuals, three main arrangements are suggested according to the generatrix of the web and, consequently, the position of the blocks' bed joints. To specify, the term bed joint refers to the longer side of a brick. When the arrangement of blocks' bed joints is orthogonal to the head arch plane the pattern is radial, when it is parallel to the head arch plane the pattern is vertical and when it is oblique to the head arch plane the pattern is diagonal [26] (Fig. 3.3).

For the research's final set up, also a diagonal cross-vault will be designed and tested. Indeed, it is necessary to study both patterns

to be able to compare the experimental results with the numerical ones obtained by Alforno et al. [29]. It is also fundamental to make a comparison between patterns, since the structural behavior of a masonry vault, its cracks and collapse mechanism propagation, is strongly influenced by the vault's pattern [36].

The vaults' geometry is completed by its supports on the horizontal plane. Moreover, the vault rests on four rigid 3D-printed plastic abutments. The ones against the back wall have a fixed condition of constraint, whereas the ones in the front can be classified as rollers (simple supports) since they rest on a steel platform which can move on the horizontal plane.

To clarify, during the assembly process of the cross-vault, all four abutments are fixed in place. Only during the testing phase, the frontal abutments can move in the direction imposed by the actuators (in-plane shear displacement or opening test) (Fig. 3.2).

3.1.3 Design of the 3D-printed blocks

The geometric model of the vault was previously created in Rhinoceros, with all intersections between blocks defined in earlier studies.

The radial vault pattern is composed of a total of 1221 solid blocks, 92 of them belong to head arches, 632 are regular blocks, 496 are special blocks (Fig. 3.4) due to their position between adjacent webs or alongside the border with head arches.

The head arches' blocks are ideal trapezoidal blocks measuring 96,0x24,0($\pm 1,6$)x47,8 mm, while the vault's regular blocks (code: U0) are scaled by a factor of 5 from real bricks and measure 48,0x11,6($\pm 0,4$)x24,0 mm.

Because of the choice to work with dry joints, all the model's blocks have a slightly trapezoidal shape. Thanks to the opportunity of

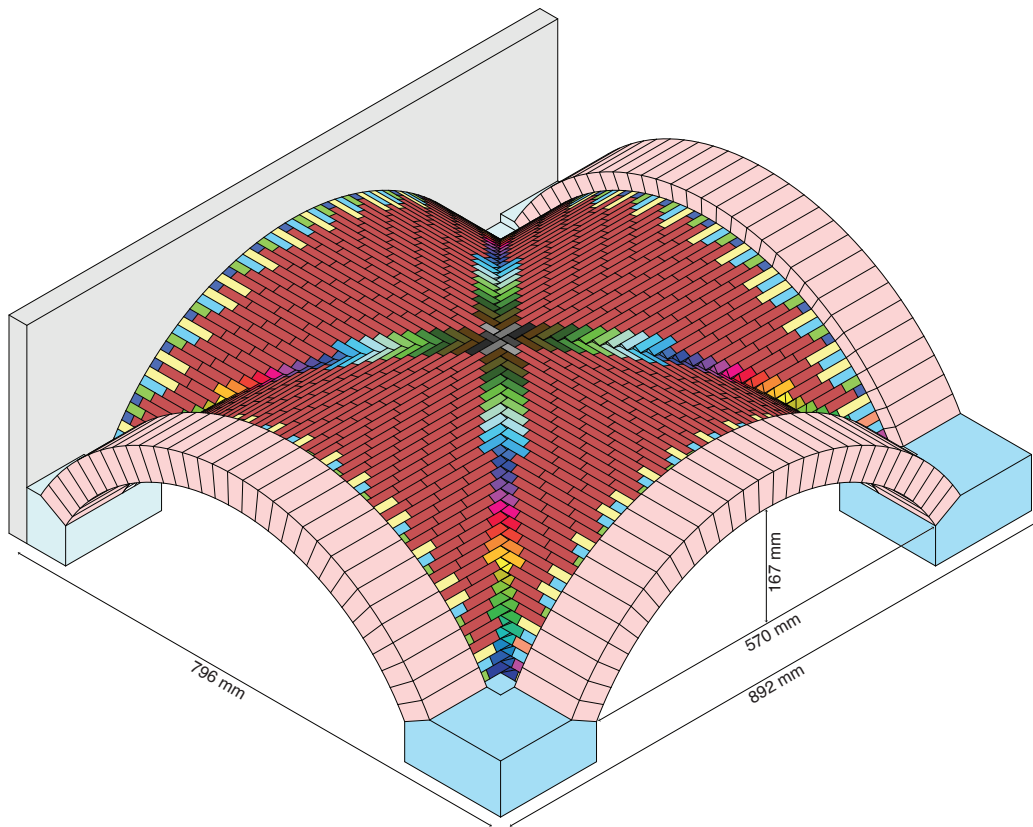


Fig. 3.1 – Radial cross-vault geometry, starting point of the design process. Each group color identifies blocks with equal dimensions (pink: head arches blocks, red: regular blocks (U0), other colors: special blocks).

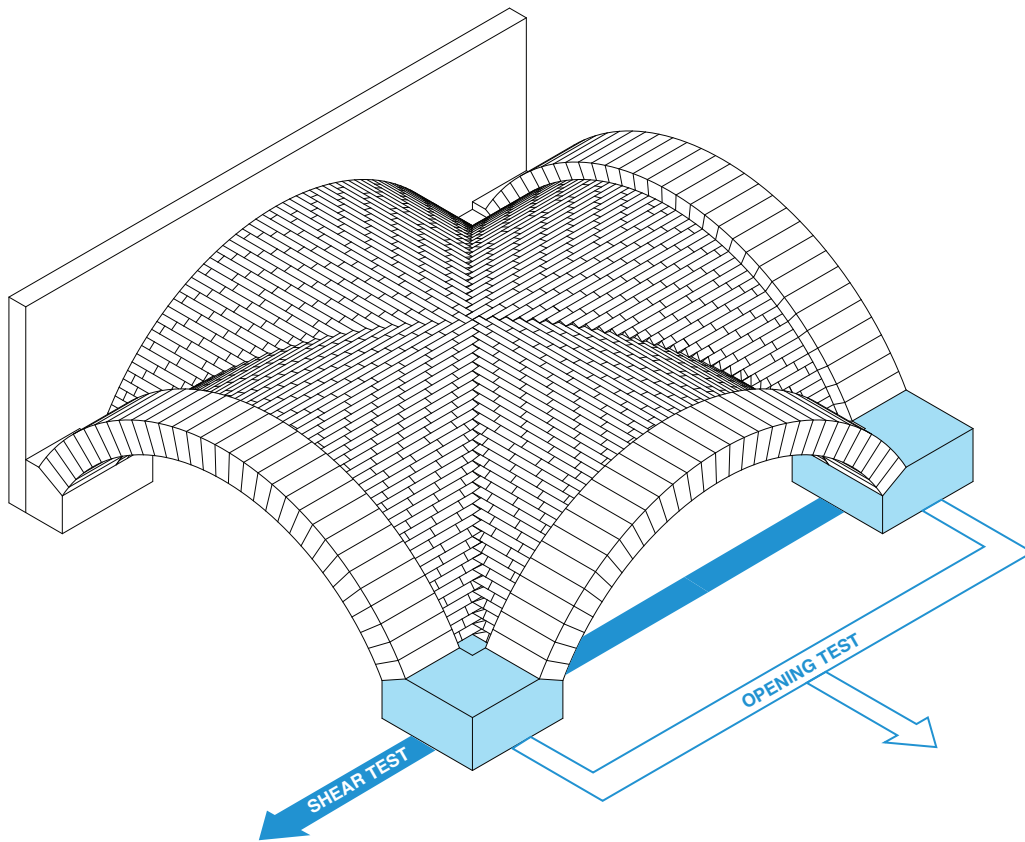


Fig. 3.2 – Cross-vault imposed displacements: shear test and opening test. The displacement is imposed to the frontal abutments.

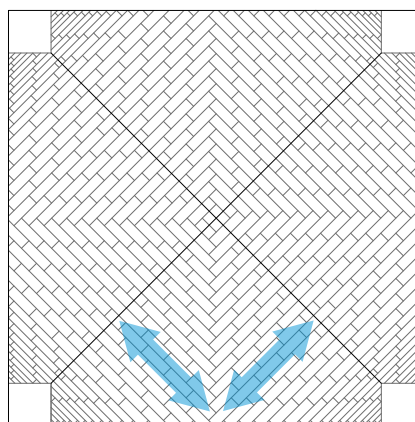
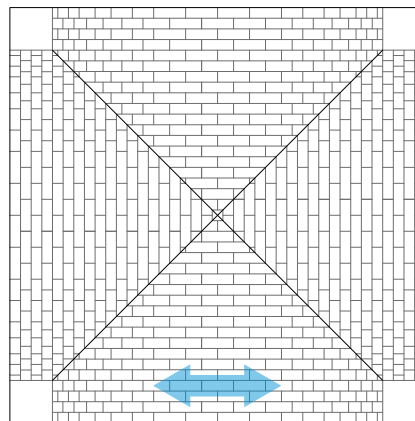
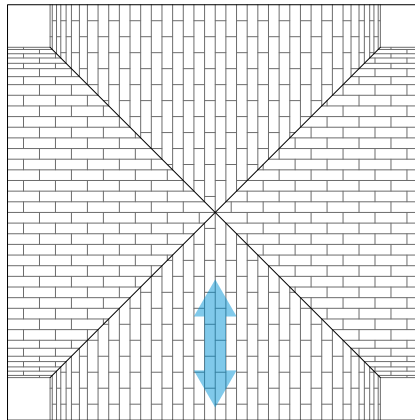


Fig. 3.3 - Brick patterns of a cross-vault. From the top: radial, vertical and diagonal.

designing a dry joints small-scale specimen, several tests can be easily performed without changing the initial conditions. Moreover, dry joint models can represent both actual dry joint masonry structures and ancient mortar joint constructions, in which the mortar has degraded over time, further diminishing their already limited tensile strength [34].

3.1.3.1 The issue of blocks' density

Following previous studies in the literature, such as Rossi's research on the seismic response of masonry cross-vaults [4], the need arises to increase the vault's mass to avoid the instability caused by accidental actions. Therefore, a study was conducted on how to design and fabricate blocks with an internal cavity that would be filled with heavy material.

An alternative to Rossi's solution was sought to achieve a better result in terms of mass, while also providing an economical and easily accessible solution. The ideal filling material was found to be lead pellets and a resin to keep them in position.

Moreover, each block of the cross-vault has a pocket. The thickness of each hollow block is 2 mm as a compromise between reducing to the minimum the external shell while keeping it sturdy and inflexible.

Firstly, it was decided that the open brick face would be the one at the intrados, so that the extrados surface of the entire vault would have turned out more even. In doing so, the contact faces between the blocks remained solid, thus avoiding issues of adhesion and friction. This choice also proved effective in relation to the creation of cavities in the diagonal blocks. These blocks, being smaller and irregular in shape, had been difficult to manage in Rossi's research and were therefore left solid. In this case, however, by utilizing their wider intrados-facing surface, it was possible to provide a filling for them as well.

Consequently, the only way to identify each block with a designated

code will be printing it on a laminated sheet and then place it on top of the filling of lead pellets and secured with a thin layer of resin. The code could not be printed on the extrados of each block nor on contacting surfaces.

Regarding the average of blocks' empty to full ratio is 0,51, for both radial and diagonal cross-vault.

All the blocks need to be of the same density; therefore, the thickness of the head arches' blocks was designed considering an equivalent void volume. This resulted in 4 mm thick perimeter walls and a 2 mm thick median stiffening wall, given the large size of these blocks.

Considering that the density of the 3D-printed nylon pa12 blocks is 980 kg/m^3 and the lead pellets' is 10800 kg/m^3 and knowing that the total volume of the cross-vault is $0,023 \text{ m}^3$, head arches included, the resulting vault's mass is approximately 86 kg.

This calculation considers that the volume occupied by lead pellets spheres is independent from their diameter and is equal to $1-\pi/6$ and the remaining void volume is filled with epoxy resin with a density of 1100 kg/m^3 . If the weight of the four PLA abutments, which are also hollow volumes filled with resin, is added, the mass reaches 160 kg.

Compared to the scaled vault model tested by Rossi [4], which has a total mass of 35,6 kg, this model, with dimensions similar to the previously mentioned one, will therefore have a mass that is quadrupled. Such a significant increase in mass is justified by the need to ensure that accidental loads have minimal impact during the structural tests that will be conducted on the vault.

3.1.3.2 Rhinoceros "pockets" modelling

Each block's cavity was created with Rhinoceros 7 using few different sequences of commands depending on the block's typology. This process was repeated 72 times for the radial vault and 119 for the

diagonal vault.

For webs' blocks, and in general for blocks whose shape was close to a right parallelepiped, the used sequence was *Explode*, *Delete* intrados face, *Join* the remaining faces and *OffsetSrf* to offset the joined surface inward.

When the block's geometry was characterized by an inclined face creating a convex angle on the intrados, the used sequence of commands was *OffsetSrf* to offset the solid surface inward, then the intrados perimeter was highlighted using *DupFaceBorder* and offsetted of the desired thickness using *Offset*, therefore a solid was created between the external intrados and the corresponding internal intrados using *Loft*. Finally, *BooleanDifference* was used to subtract the internal solid to the external solid.

This process became more complicated in the diagonal vault where the blocks' intrados face was not planar. In this third case scenario, before proceeding with the *OffsetSrf* command, a geometrical simplification of these blocks was needed. A similar solid with flat faces was created using the same vertices as the curved solid and, from there, the *OffsetSrf* was applied. Once the internal subtraction solid was identified, it was placed within the original geometry, and finally, the internal face corresponding to the intrados was extruded using *ExtrudeSrf*. Finally, the *BooleanDifference* command was used to create the cavity.

It is important to note that, since these solids were generated through approximation, the wall thickness is not exactly 2 mm. However, this error is uniformly distributed and therefore considered acceptable.

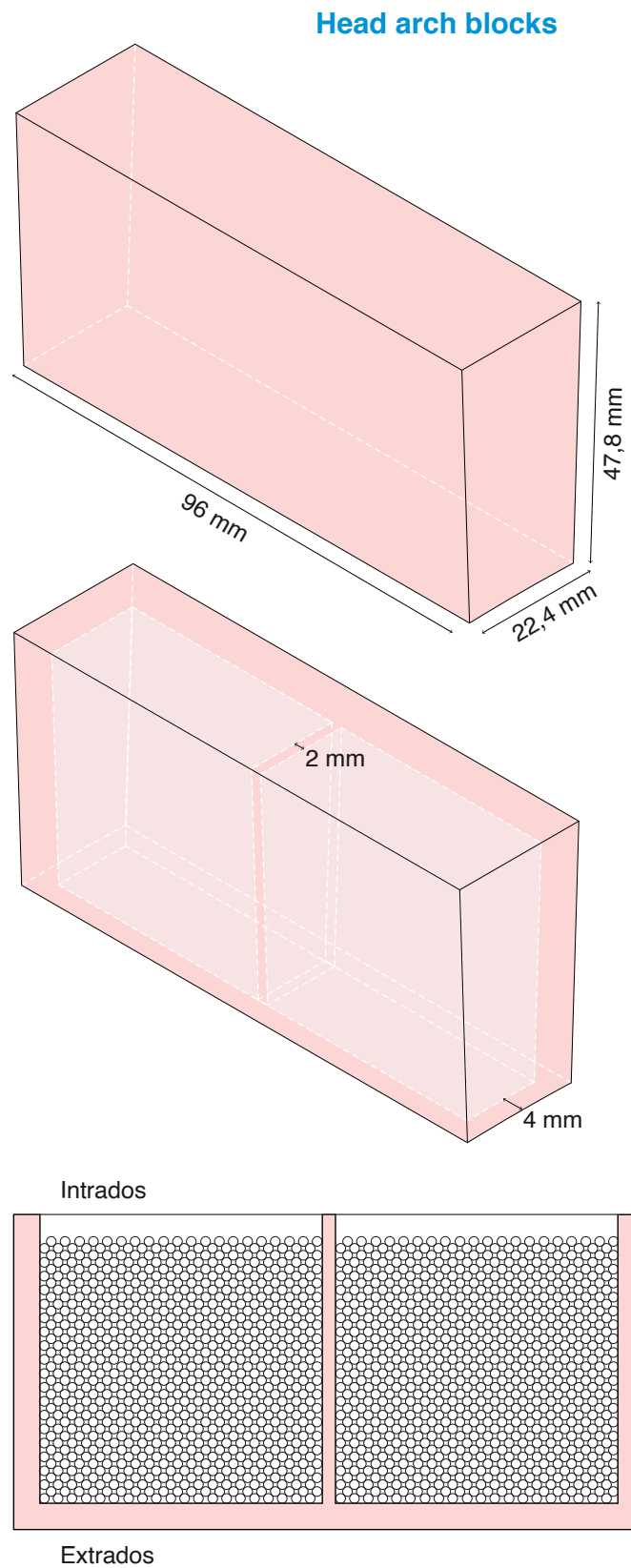
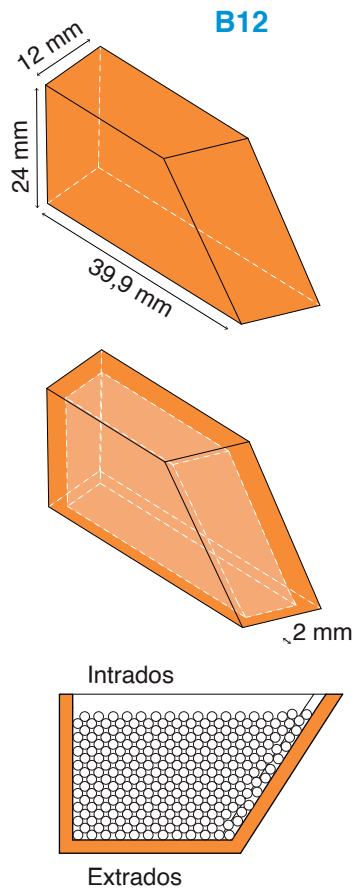
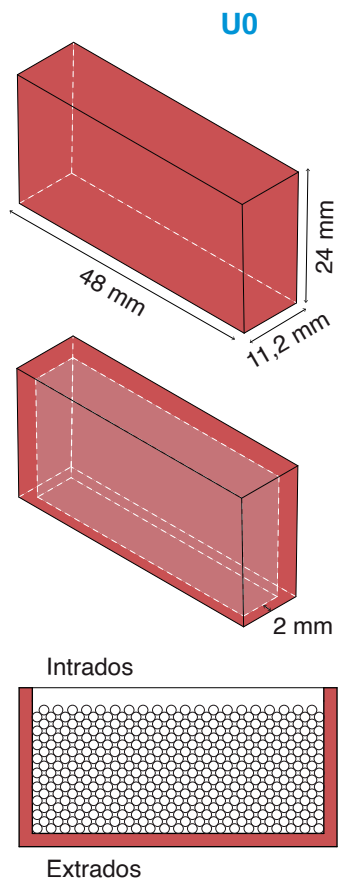


Fig. 3.4 - Radial cross-vault blocks: U0 regular blocks, B12 example of a special block and head arches' blocks. Solid block geometry, design of the pocket, lead pellets and epoxy resin filling.

3.2 Evolution of the conceptual design of the testing setup

As mentioned in chapter 2.3, not many studies in the field of vaults' small-scale models have thoroughly explored the topic of centering. Hence the importance of developing an easy assembly system that is also capable of withstanding the high loads of the cross-vault.

From the very beginning of the design process, it became evident that a modular centering needed to be constructed, due to the presence of the reaction wall at the back of the vault. This, in fact, prevents the possibility to replicate a centering system divided into four removable, like the one developed by Rossi [4]. With only three exit directions available, the decision was made to design a centering that could be divided into three separate pieces. The central portion, comparable to a barrel vault, would be extracted from the front, while the side webs would be removed from their respective sides.

The design process of the centering system and its lifting and lowering mechanism will be illustrated through the identification of three consecutive steps. Each of the three steps analyzes two different setups, one for the shear test and the other for the opening test. The plywood centering will be functional for both setups.

The general concept for the lifting and lowering system of the plywood centering is as follows.

Designing a mobile system that can reach the required height where the plywood centering will then be assembled. Subsequently, the centering is secured in such a way that allows for the precise placement of all the blocks of the vault. Once this step is completed, the previously mentioned mechanical system will enable the centering to be lowered enough to allow for its removal.

Finally, divided into three components, the centering will be extracted from beneath the cross-vault.

3.2.1 Step 1: first approach to the problem

Firstly, a main base (b_1), on which the entire testing system rests, is inserted and the rear containment wall (w) is reinforced with a series of triangular supports. Then, the vault's abutments are raised on a second level of bases (b_2) to create a maneuvering space below the centering. Therefore, a third level of bases (b_3) is required, placed at a higher elevation than the chains (ch), on which metal supports are installed to facilitate the removal of the centering.

Specifically, in this first step, two central tracks (r) were included to slide out the barrel portion of the centering (c_1), referencing Roselli, and two inclined metal supports (s_2) were designed to extract the side webs (c_2), following Rossi's centering model.

Addressing the topic of structural testing, two plates are inserted beneath the vault's abutments. The rear plate (p_2) is fixed to the main base (b_1), while the front plate (p_1) can move. Moreover, two actuators will allow the testing of the structural capacity of the vault through a shear test (a_{sh}), with load applied on the horizontal plane tangential to the movable plate, and an opening test (a_{op}), with load applied on the horizontal plane perpendicular to the movable plate.

The chains connect the plates only during the shear test, whereas they will be removed to perform the opening test.

This first phase is shown in Figure 3.5 and 3.6.

In this first step, no further considerations were developed regarding the centering lowering system before reaching the central rails and the inclined metal supports. The geometry of the cross-vault and its abutments are the one described in chapter 3.1.

Step 1

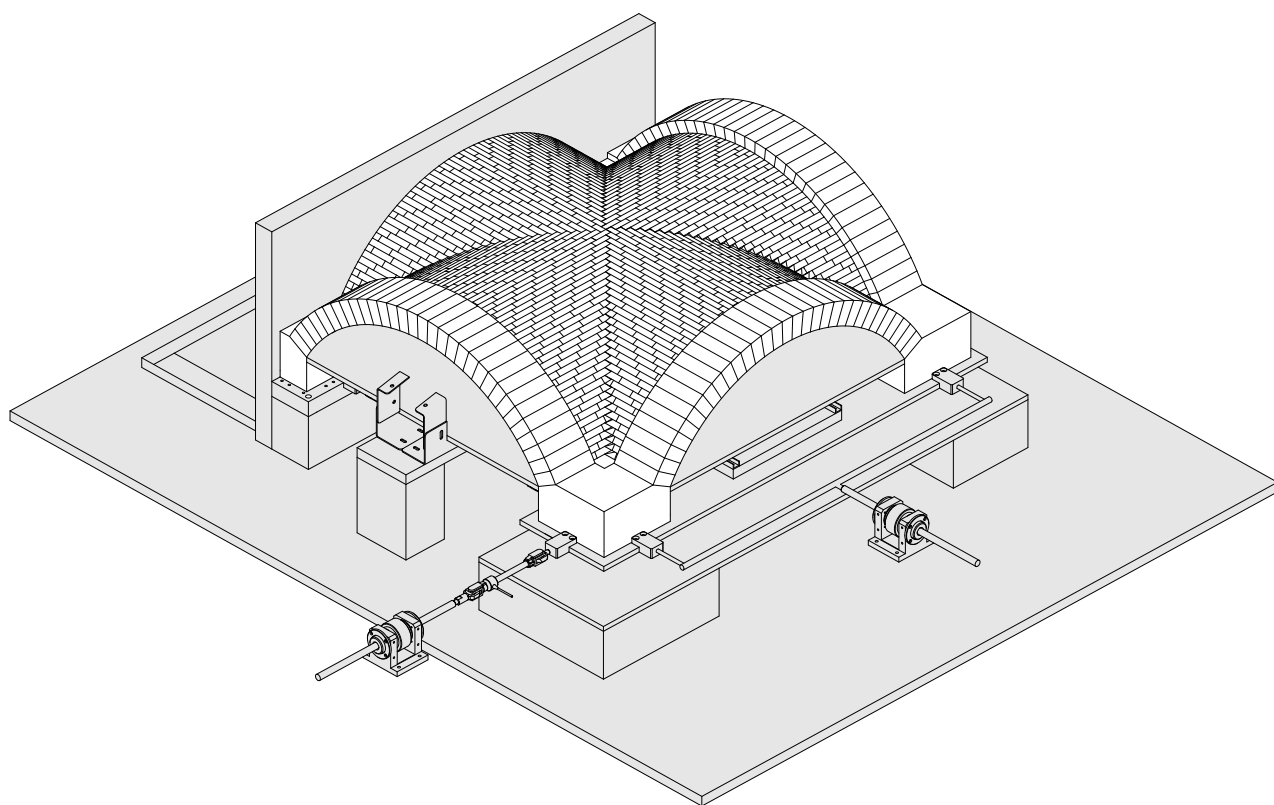


Fig. 3.5 - Step 1: general view of the testing setup with centering in place and vault assembled. Designed components in gray.

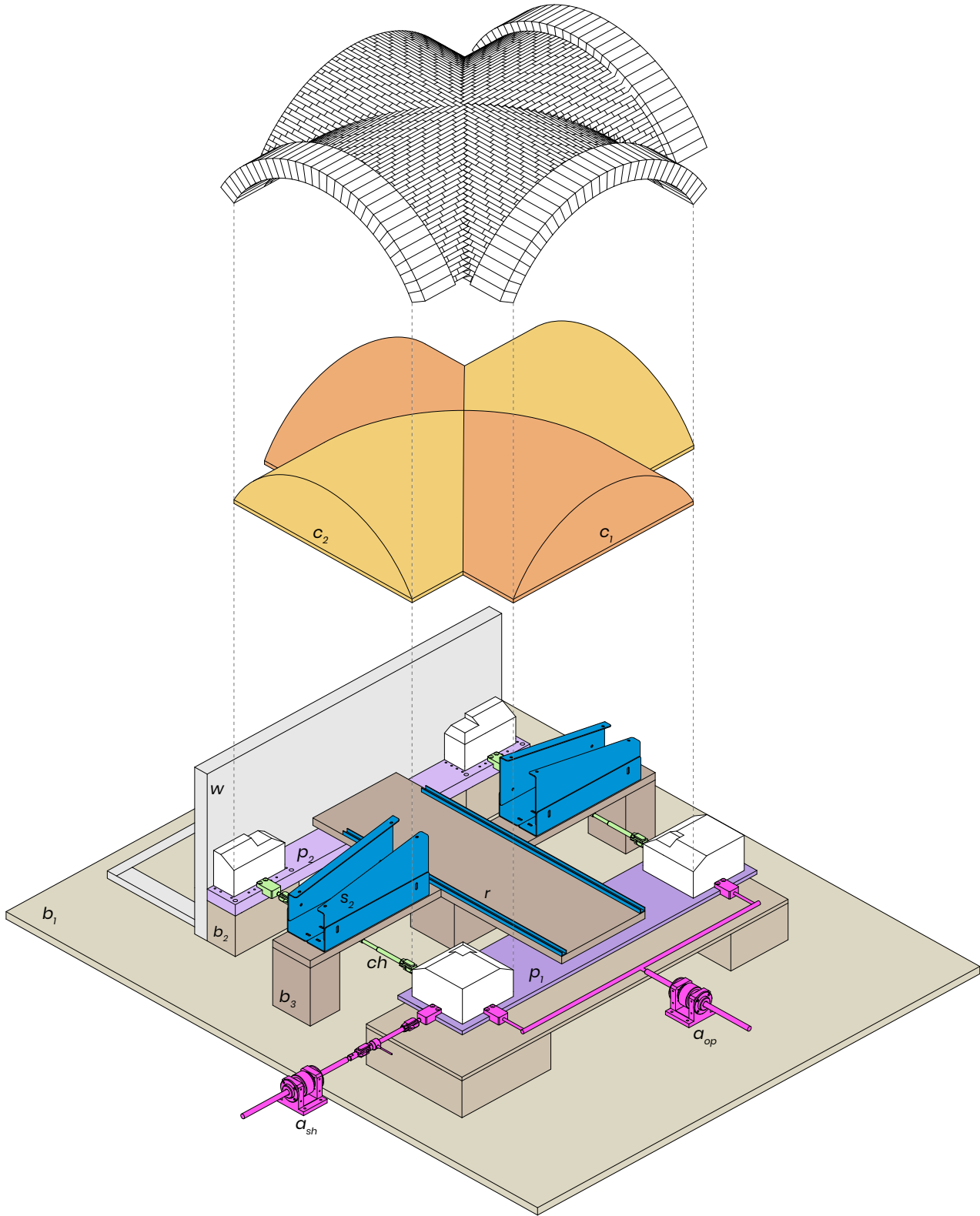


Fig. 3.6 - Step 1: exploded version of the testing setup with its components. Shear and opening test.

3.2.2 Step 2: prototype with an internal lowering mechanism

In the second step, the extraction mechanism of the centering was further developed (Fig. 3.7, 3.8, 3.9, 3.10).

Its three components are simultaneously lowered by 35 mm using a six-support mechanism (m_{int}) built inside the barrel portion of the centering (c_1). Four supports are located under the central portion of the centering, while the other two, outside the rails, intersect the geometry of the lateral webs (c_2). It was considered that the mechanism could be operated using a knob located on the front surface of the barrel.

Then, the central portion of the centering leans on the rails (r), and the side webs, fastened to the central body with three cylindrical threaded bars (tb), are supported by external wooden blocks (s_1) and removed using these bars as guiding supports. When the vault rests on the rails and the lowering mechanism is relieved of the weight of the centering, the six supports rise 40 mm upward into the geometry of the barrel vault, thus moving out along with it.

Once the central body is also extracted from beneath the vault, the rails can be removed to avoid interference during testing.

The entire testing rig rests on a 1200 x 1200 x 20 mm plywood base (b_1), while a secondary base measuring 1200 x 300 x 20 mm is added either at the front or the side, depending on the type of test performed (b_2).

Unlike step 1, the barrel portion now slides along the C-shaped rails (r) on two rows of spherical bearings (sb) positioned underneath its base. These spheres were arranged to prevent the barrel from tipping during removal once it reaches the rail's end. In other words, once the first pair of wheels exit the rails, the remaining two pairs keep the barrel horizontal, being positioned around its center of gravity. The wooden supports on which the rails rest are designed to be functional for both placements of the additional base (s_2).

Regarding the PLA abutments of the cross-vault, they have been raised a couple of centimeters to align with the centering height. Those volumes have been hollowed to be filled with denser material. To prevent deformation issues when supporting the vault's weight, a series of 4 mm thick diaphragms have been designed to stiffen these empty volumes. The front abutments (a_f) are attached to the mobile plate with three bolt pins, while the rear ones (a_r) are fixed with a slot system to the fixed base and secured with two bolts to the retaining wall.

The retaining wall, with a thickness of 30 mm, has a central recess, a few millimeters deep. A plate (pl), made of the same material as the vault, will be here inserted to prevent slippage between the two elements during the test phase.

For the structural testing elements, the mobile plate (p_1) has a rounded shape to ensure that the system's rotation is not hindered during the opening test. To restrict movement to a single direction during this test, two L-shaped lateral guides (g) are added.

Finally, the systems for conducting the tests are detailed. In both actuators, load cells are included. Those are electronic components used to measure a force applied to an object by detecting an electrical signal that varies based on the deformation caused by the force. The mechanism for the opening test (a_{op}) features two anchor points on the mobile plate, a transversal rigid element connecting them and a single central actuator applying the force. The one for the shear test (a_{sh}) features a single anchor point on the rounded part of the mobile plate. Both actuators allow the rotational movement of the cross-vault system.

Step 2

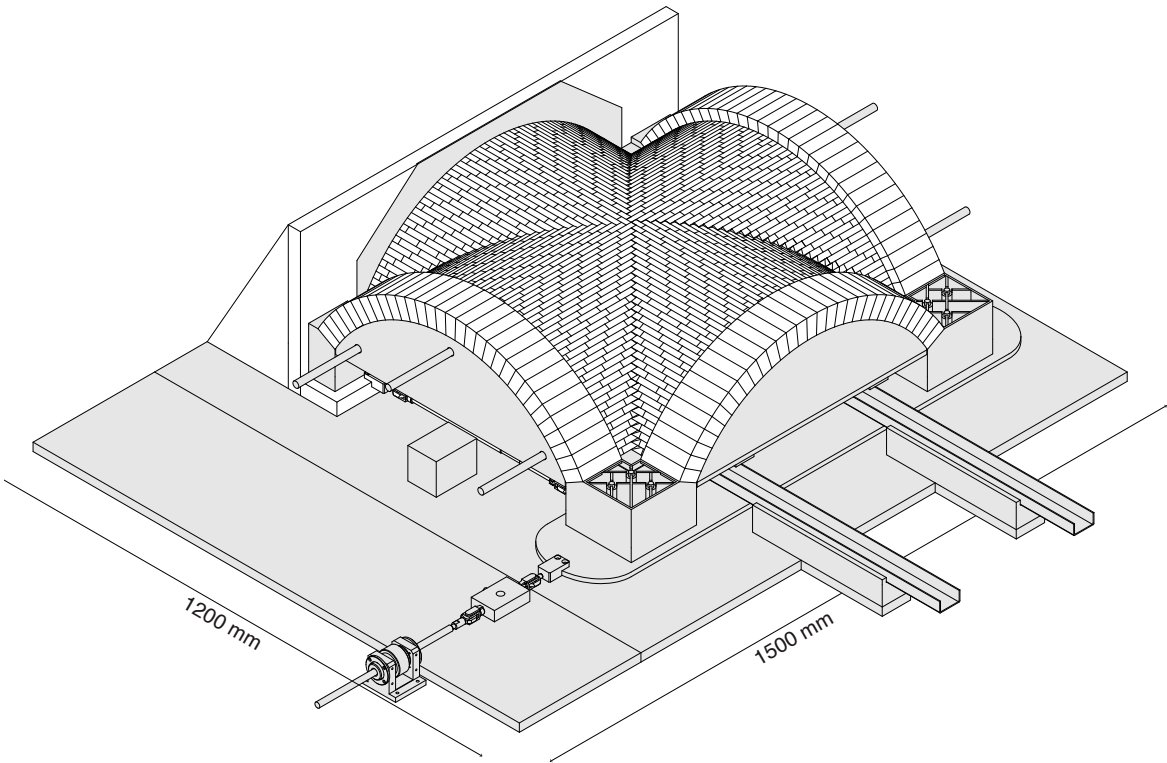


Fig. 3.7 - Step 2: general view of the shear testing setup with centering in place and vault assembled. Designed components in gray.

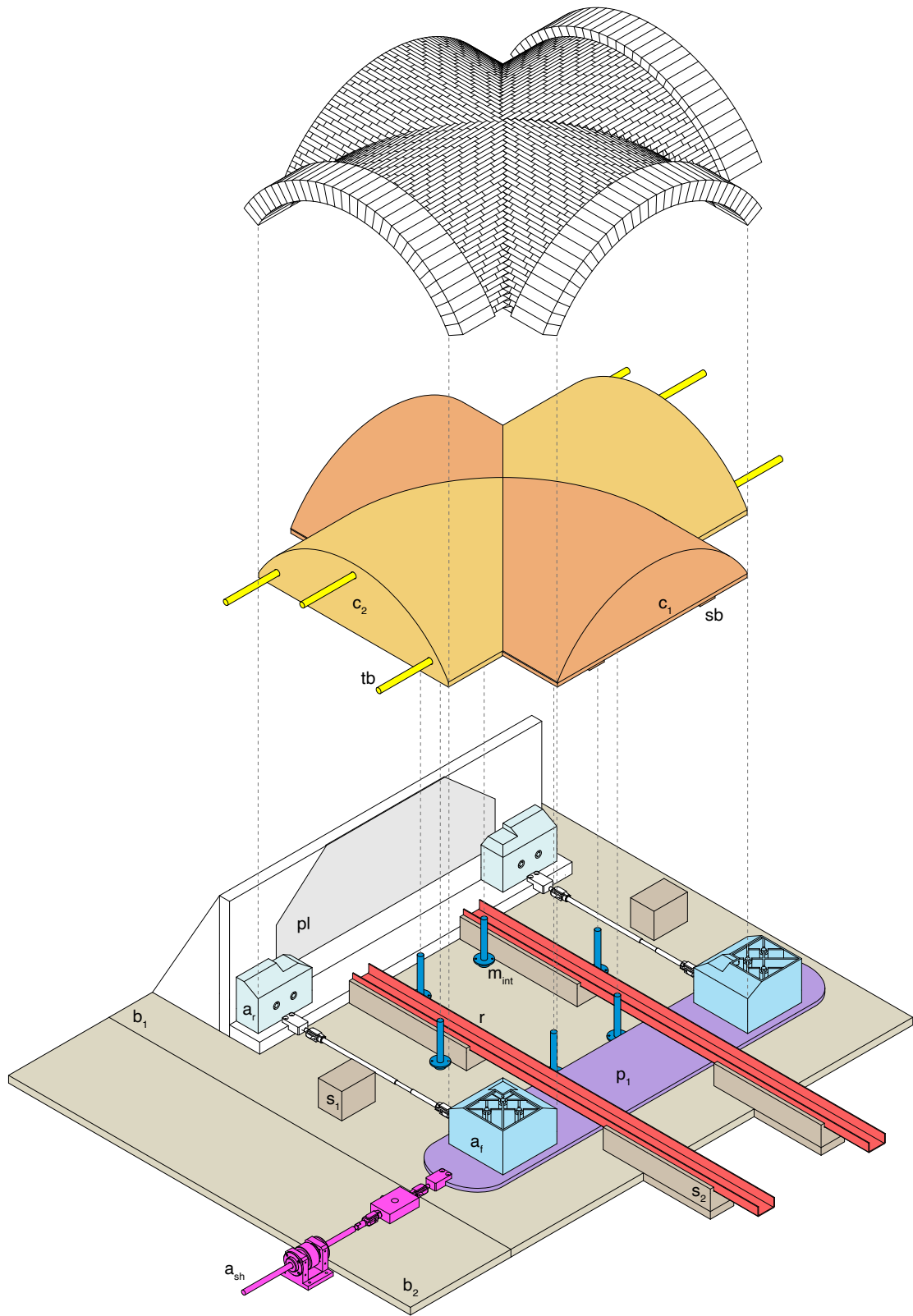


Fig. 3.8 - Step 2: exploded version of the testing setup with its components, shear test.

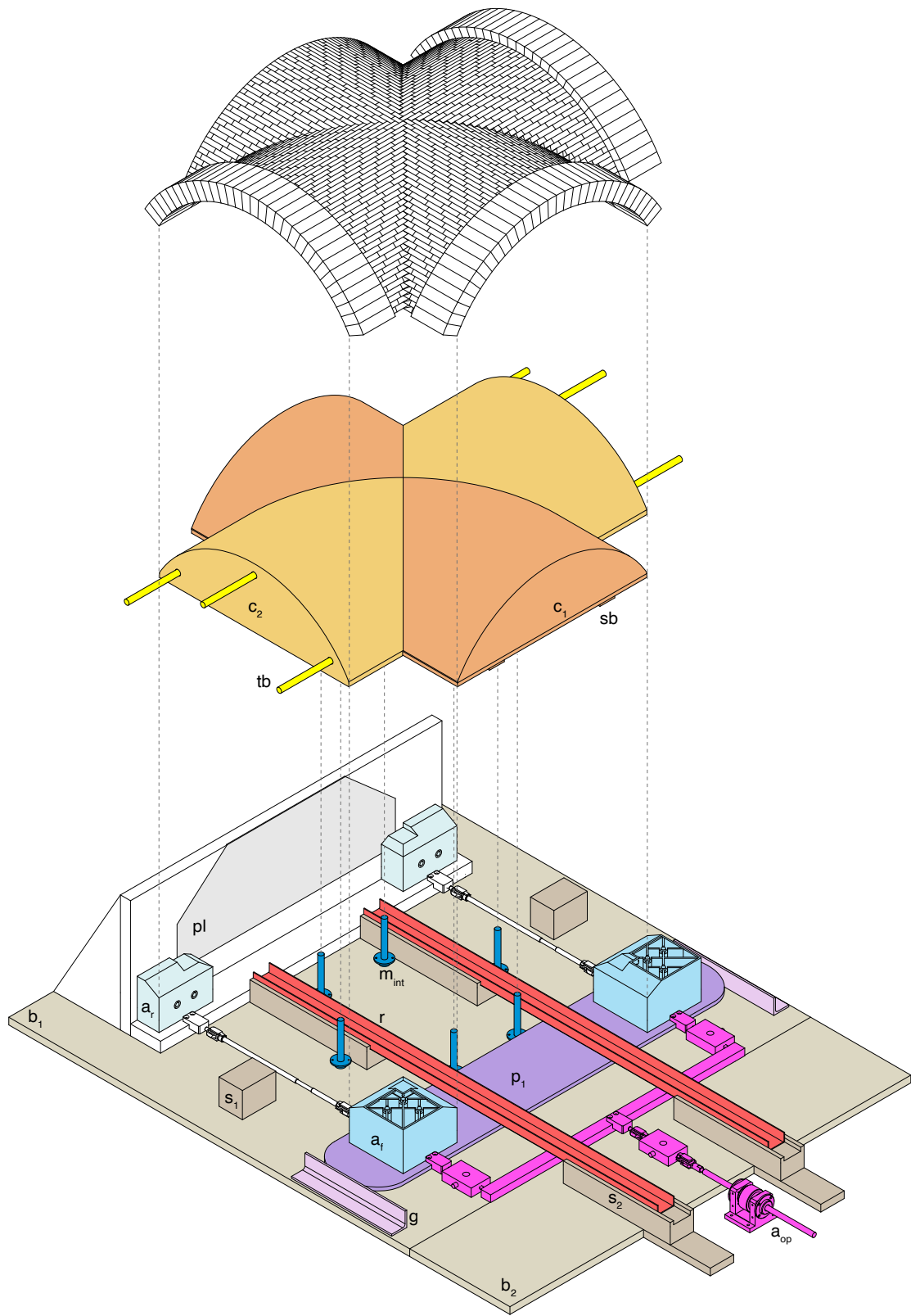


Fig. 3.9 - Step 2: exploded version of the testing mock-up with its components, opening test.

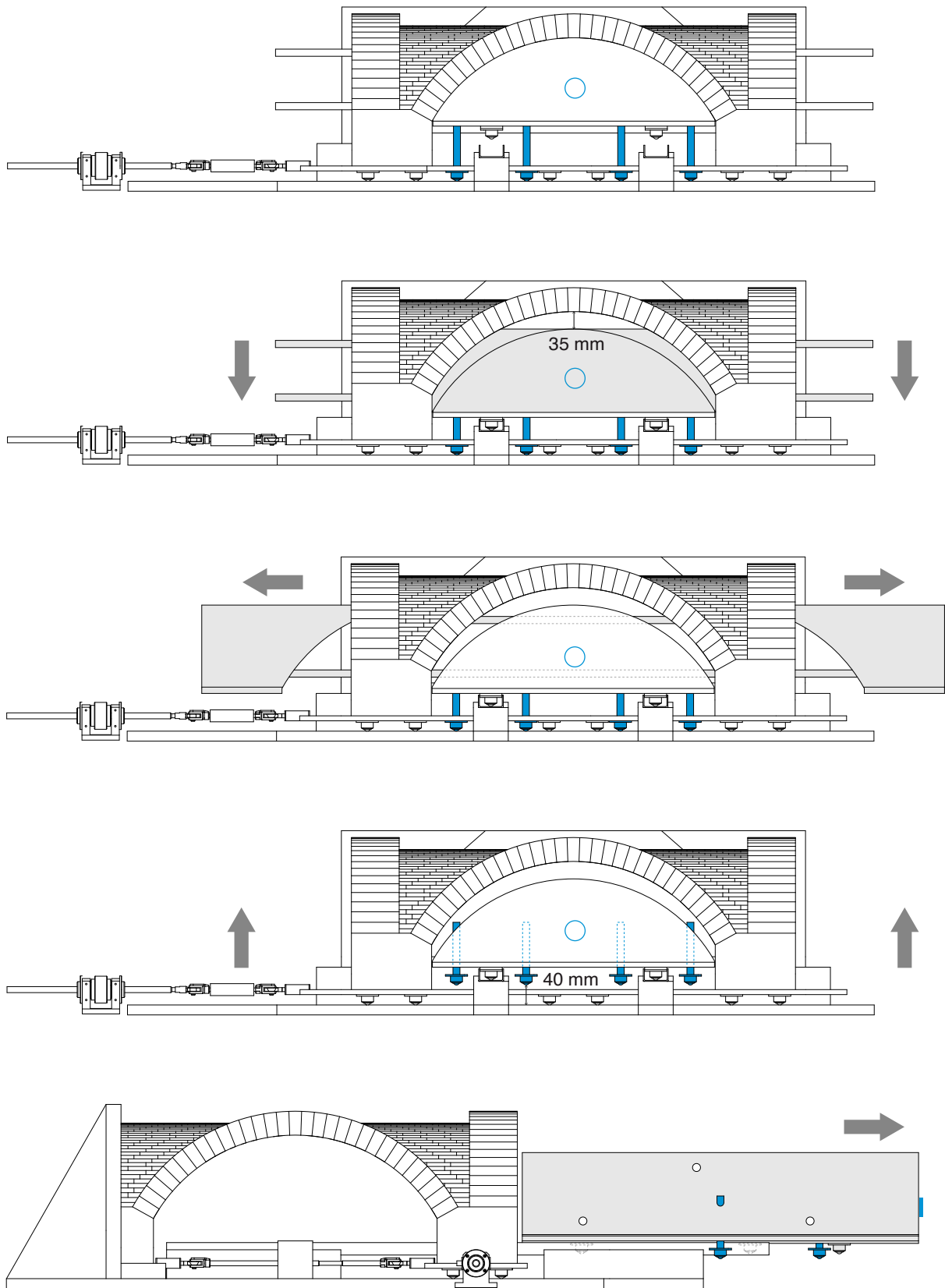


Fig. 3.10 - Step 2, detailed maneuvering and extraction process of the centering. In blue, the lowering mechanism. From the top: extended mechanism; the system lowers by 35 mm and rests on the rails; the lateral webs are removed using the threaded bars as guides; the six supports rise 40 mm upward into the geometry of the barrel vault; the barrel portion of the centering can exit from the front sliding on the rails.

3.2.3 Step 3: prototype with an external lowering mechanism

The third step marks the final evolution of the testing setup design (Fig. 3.12, 3.13, 3.14, 3.15).

Following the second step's design and an increasingly detailed characterization of the centering, certain challenges emerged regarding the feasibility of the maneuvering system developed in the previous step. For instance, the requirement for this internal mechanism to fit within the volume of the centering, combined with the need for the barrel to be internally divided by a series of diaphragms, led to the adoption of an alternative solution that would be easier to design and implement.

Thus, the new prototype involves the incorporation of an external metal frame (m_{ext}) that supports the plywood centering during maneuvering operations. This frame also proves to be useful in the subsequent testing phase as a support element for a soft material to cushion the fall of the vault's bricks.

The centering removal concept is similar to the one described in step two.

The centering-frame system, manually operated through four knobs located on top of the endless (es) screws, descends by 30 mm. The centering's base leans on one-way sliding wheels (sw) fixed on top of wooden supports. The frame is lowered by 15 mm, allowing the centering, divided into its three components, to be removed (Fig. 3.15). Three handles are added to the centering base (b_c) to facilitate the removal of its components.

Being a bulky system, with square profiles measuring 40 x 40 mm, it was necessary to raise the vault's abutments (a_r , a_t). Their height has been adjusted to allow for the insertion of the metal frame as well as to incorporate a base layer for the centering (b_c), measuring 36 mm in thickness. This substantial thickness was chosen not only for strength reasons, considering the weight of the vault being around 86 kg, but also to facilitate the practical removal of the centering's webs (c_2). To allow their removal, the height of the endless screws need to be considered, as they protrude upwards once the frame

system is lowered. Therefore, a thick base was needed to raise the centering and overcome these obstacles. Consequently, removable knobs on the endless screws are also required to manage precisely the system's lowering.

Another modification to the abutments involves the insertion of 3 mm thick plates at the contact surfaces with the cross-vault. They are made of the same material as the vault's blocks (Fig. 3.11).

In this third step, all connections between the different elements of the testing rig have been detailed. These include screw connections, interlocking joints, bolts and bushings.

The thickness of the wooden elements has also been detailed, sometimes modified, depending on the available materials on the market. The main plywood base (b_1 , b_2) is now 30 mm thick to improve its resistance.

The wall's plate (p) has been divided into a series of interlocking elements to facilitate its manufacturing process and prevent breaking issues during transportation.

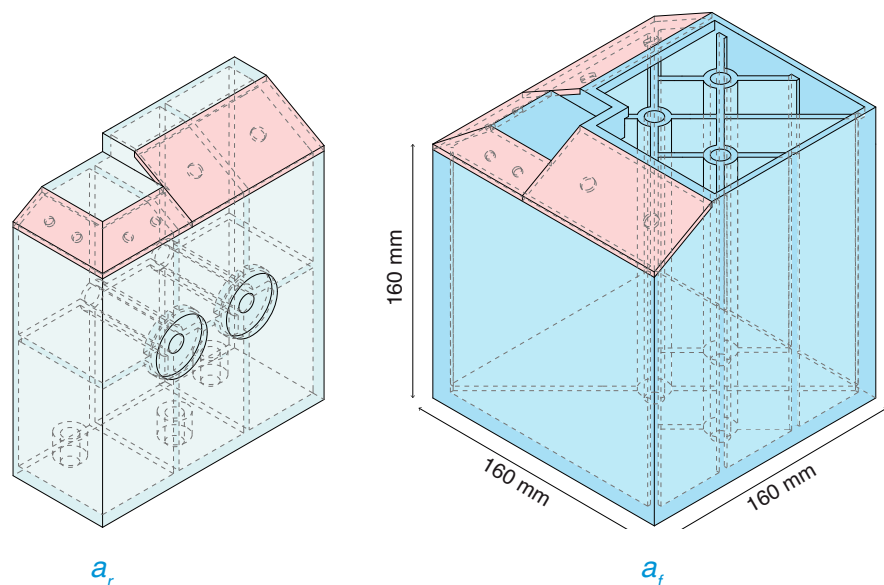


Fig. 3.11 - Cross-vault's abutments. From left: rear abutments (a_r) and frontal abutments (a_f). They are designed as PLA volumes with internal diaphragms to be weighed down with resin. In pink the 3 mm plates.

Step 3

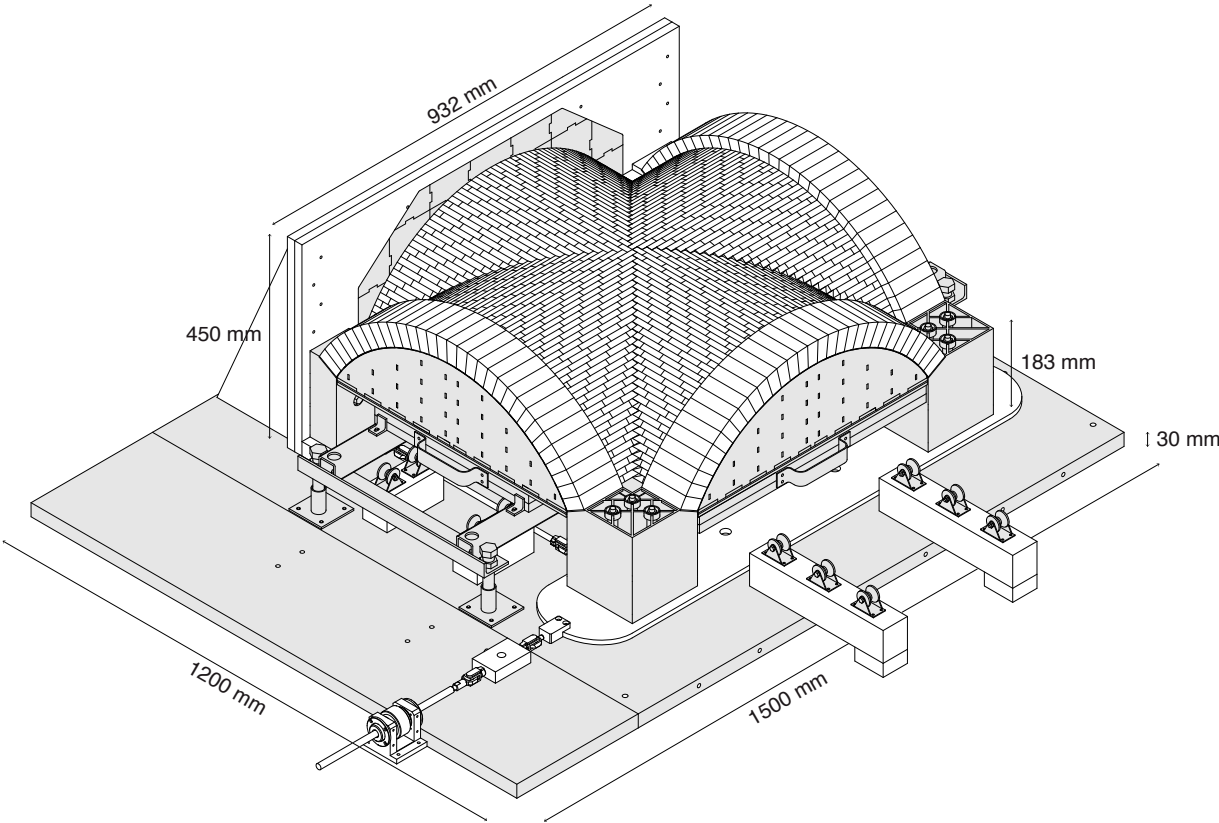


Fig. 3.12 - Step 3: general view of the shear testing setup with centering in place and vault assembled. Designed components in gray.

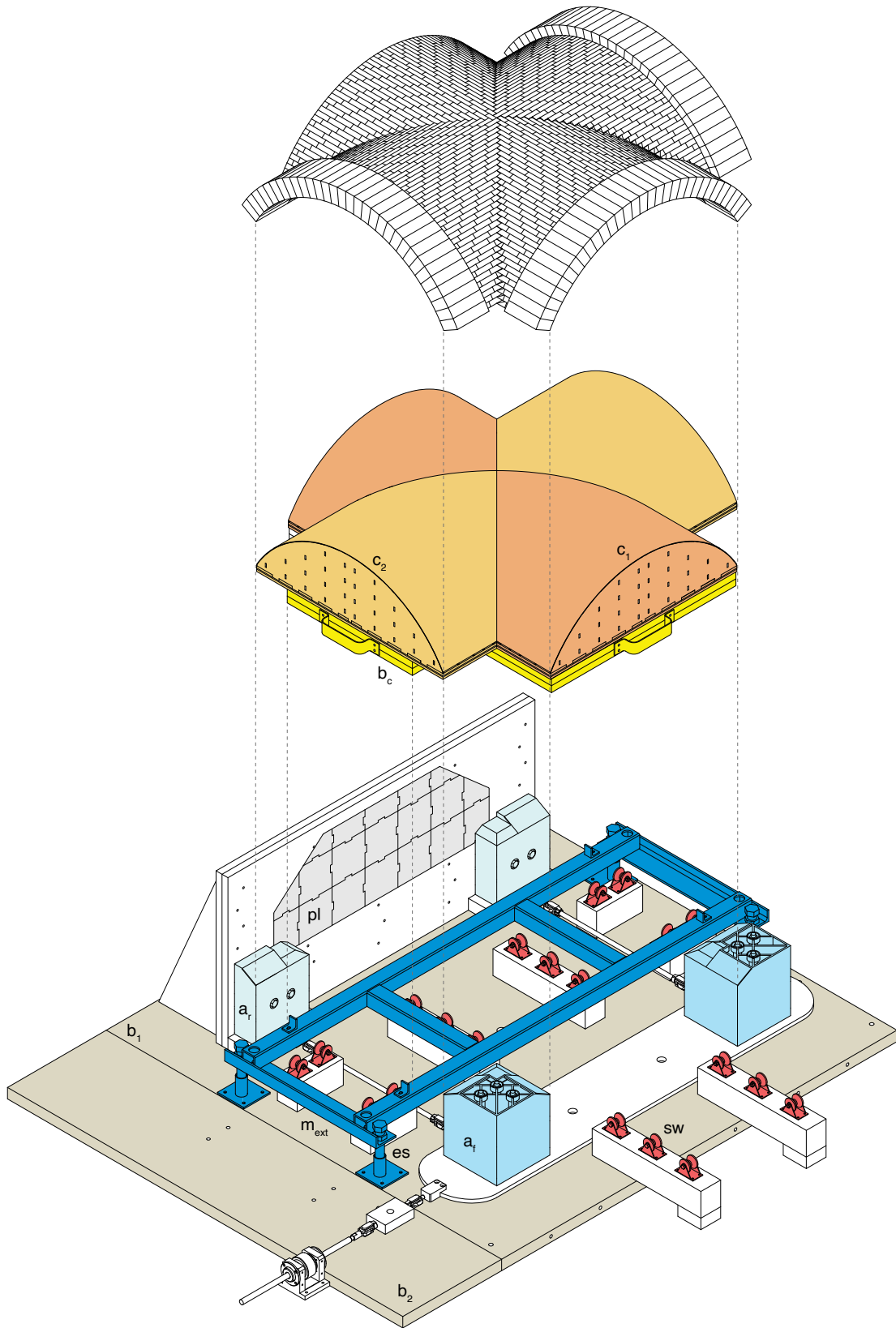


Fig. 3.13 - Step 3: exploded version of the testing setup with its components, shear test.

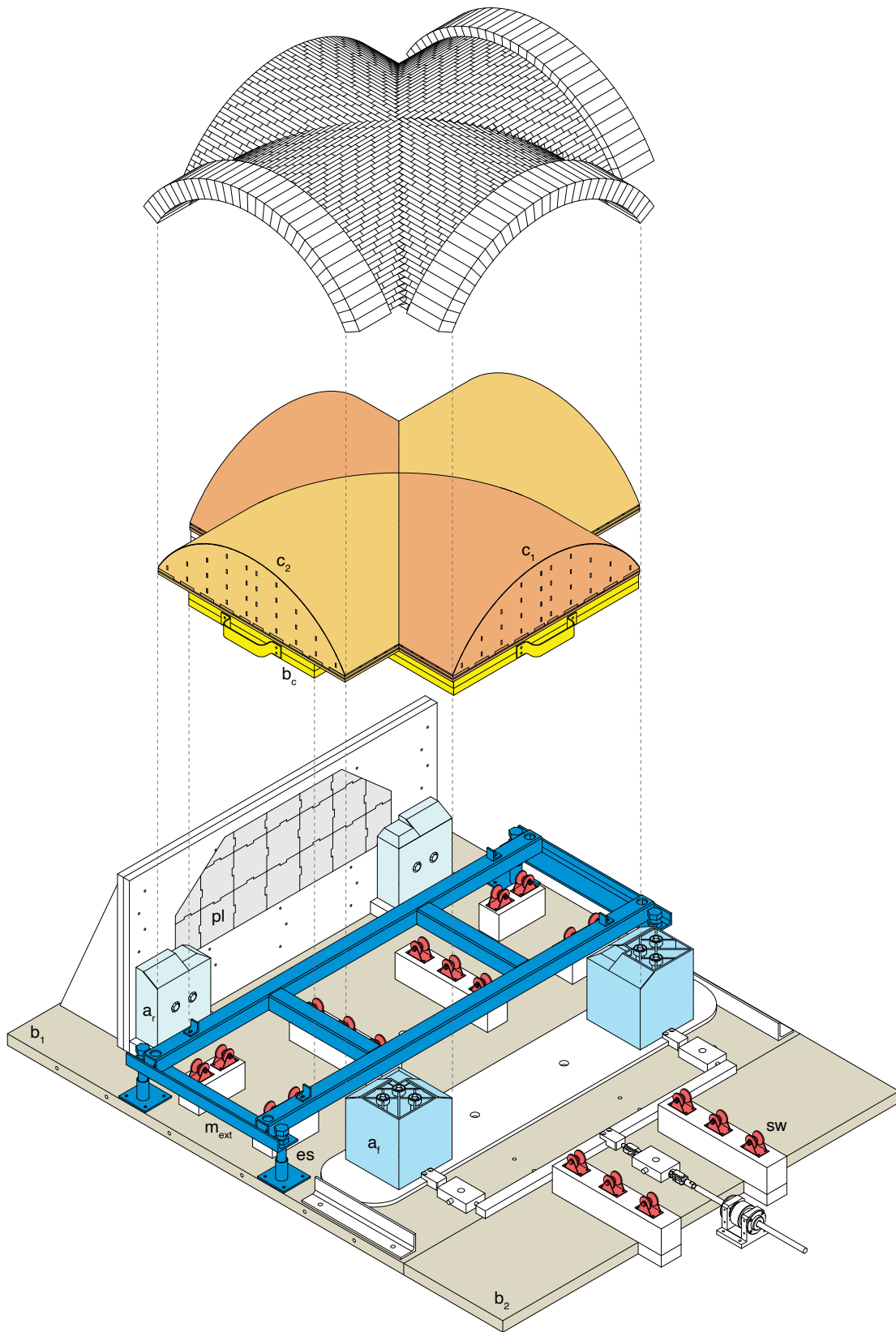


Fig. 3.14 - Step 3: exploded version of the testing setup with its components, opening test.

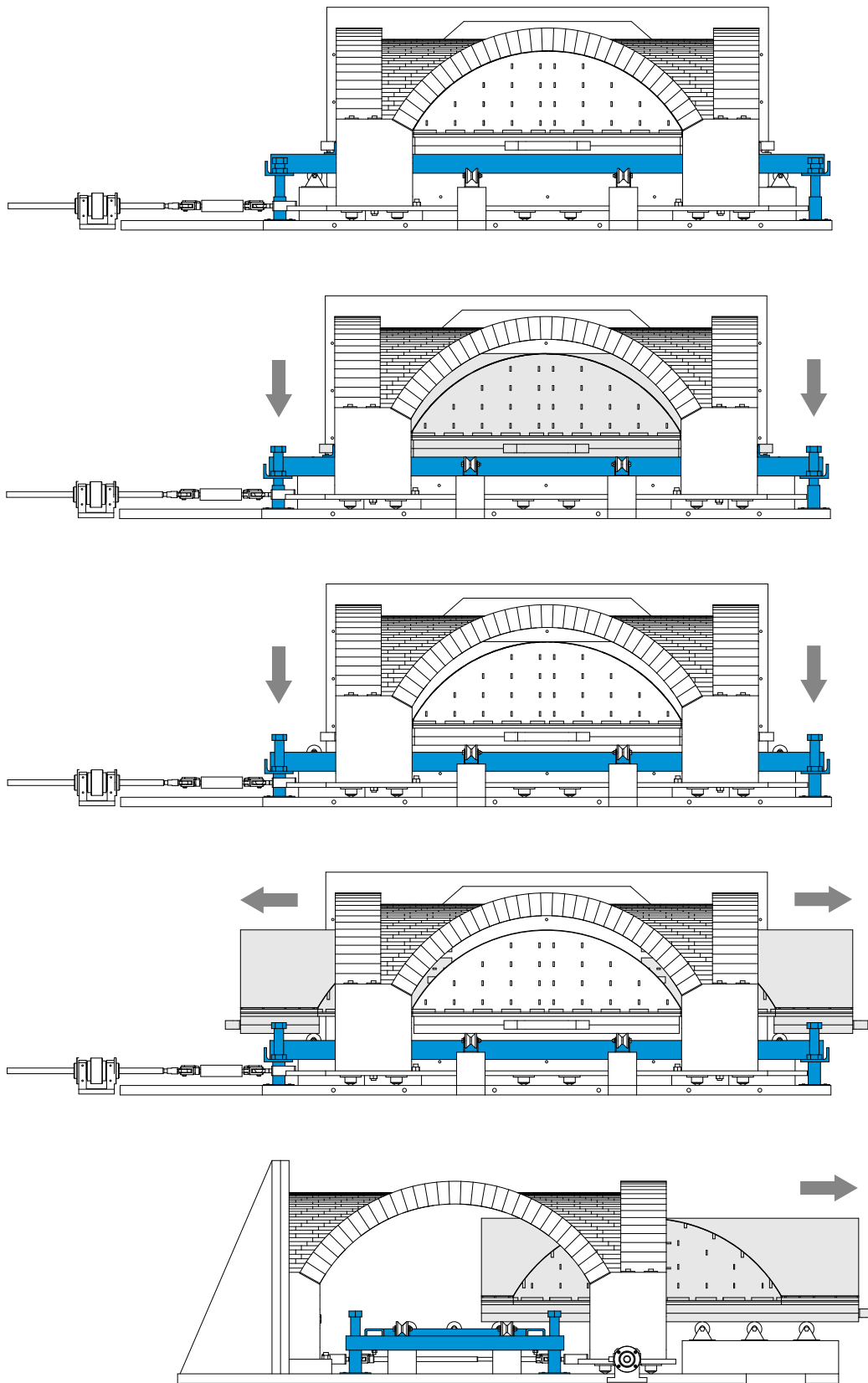


Fig. 3.15 - Step 3, detailed maneuvering and extraction process of the centering. In blue, the external lowering mechanism. From the top: extended mechanism; rotating the endless screws, the system lowers by 30 mm and centering rests on the wheels; the metal frame lowers by 15 mm; lateral webs are removed, overstepping the endless screws; the barrel portion of the centering can exit from the front sliding on wheels.

3.3 Design of a plywood centering

As mentioned in chapter 3.2, the centering used for constructing the cross-vault was conceived from the beginning as a modular wooden system made up of three main geometries: a central barrel vault and two lateral webs.

The subdivision in three separate geometries is necessary to allow the centering to be removed once the cross-vault construction is completed, enabling structural testing. With only three sides accessible because of the containment wall, this approach emerged as the only feasible solution.

From the initial design phases to the final project of the centering, various aspects have been thoroughly investigated and refined:

- The overall geometry of the three elements.
- The centering's support plane.
- The interlocking methods between the elements.
- The geometry of the inner partitions of the centering.

3.3.1 Excursus on the centering's design

To clarify the development of the centering geometry's, different models will be categorized and described according to the three steps outlined in chapter 3.2.

In the first step, the centering is characterized by three simple solid volumes: a central barrel vault (bv) and two side webs (sw) with an infinitesimally thin edge at their apex (Fig. 3.16). Each volume rests on its own base. At this stage, no further details were developed regarding the internal geometry of the centering nor the connection methods between the different volumes.

Proceeding with the second step, the one with an internal lowering

mechanism and six central supports, three horizontal threaded bars (tb) are added to serve as connecting elements between the centering volumes, keeping the webs anchored to the barrel, as well as guides for the removal of the side webs (Fig. 3.17). This tie-rod system was designed to secure the overhanging side webs in the correct position, anchoring them to the central structure of the centering.

Subsequently, the internal geometry of the centering was analyzed. A series of longitudinal and transverse diaphragms with a thickness of 3 mm, as well as a shell covering (sh) of 1 mm for each volume, were designed.

The modelling process begins with the lateral webs by placing a pair of diaphragms ($d_{l,sw}$) aligned with the threaded bars to stiffen the structure around these tie-rods. The remaining partitions are then positioned leaving sufficiently wide spaces for the six-support maneuvering mechanism.

The intersection between the webs and the central barrel is ensured not only by the threaded bars, but also by two interlocking “step” joints (sj). This acute-angled intersection was designed to prevent unwanted vertical movement of the webs during the building process of the cross-vault as well as during maneuvering operations of the centering.

Four diagonal diaphragms (dd) were added to ensure optimal adherence between the shell coverings and the underlying structure. At this point, it was clear that the most critical point of this centering system was the diagonals, corresponding to the groins of the cross-vault. Even a slight misalignment between the three geometries of the centering can impact the intersection of the vault’s blocks, resulting in unwanted imperfections and therefore errors in the subsequent testing phase.

PVC tubes (t) were added to insert the threaded bars and wooden blocks with tapered joints were used to ensure the precise positioning of the tubes.

As in the previous step, the three centering’s volumes rest on three separate bases (b_{sw} , b_{bv}), but semi-circular positive and negative shapes were added for better interlocking.

Continuing with this second phase, the connections between the transverse (d_t) and longitudinal diaphragms (d_l) were further detailed and initial considerations regarding the assembly process of the various elements were made.

First, the diagonals and longitudinal diaphragms are placed, fitted into recesses in the base, followed by the vertical insertion of the arched transverse diaphragms. The “stair-step” intersection is covered with a thin surface to facilitate the alignment of the geometries.

Among the critical issues of this model is the lack of support for the shells of the lateral webs. Their free edge, particularly at the central vertex, is a very fragile point, making it unsuitable for the numerous maneuvers that will be performed during the structural testing phase. A second issue concerns the clear incompatibility between the diaphragm-based internal partition of the centering and the intent to insert its maneuvering mechanism inside. Although space has been allocated for the vertical movement of the six supports, it is quite challenging to determine where to position their horizontal connections. Additionally, drilling the diaphragms to make room for this internal mechanism would mean weakening the entire structure (Fig. 3.17).

3.3.2 Final centering prototype

When it was decided to modify the centering maneuvering system, it became clear that the centering system itself needed to be rethought considering the new developments.

By eliminating the threaded rods and the six-support system, it became possible to simplify the external and internal geometry of the centering, creating a symmetrical model in both x and y directions (Fig. 3.18).

Firstly, the spacing between the diaphragms was regularized. A grid of 60 x 60 mm proved to be functional, except for the first span, which

measures 93 mm as it aligns with the arches above.

The second essential change involves the subdivision of the support bases. Now, the entire system is resting on a metal frame. A first base layer (fb), 36 mm thick, rests directly on the underlying metal frame, while the centering's diaphragms rest on a second base layer 15 mm thick (b_{sw} , b_{fw}). This arrangement allows the centering to be viewed as the composition of four equal webs: two side webs (sw) and two central webs, frontal (fw) and rear (rw). The rear one is shorter than the others due to the absence of the head arch in the vault portion adjacent to the containment wall.

This symmetrical design solves the issue related to the lack of lateral support for the webs. Each web has two diagonal elements (dd) anchored to the base that define their perimetral geometry. Those diagonals give support to the webs' apex and, at the same time, they become adhesion elements for the covering shells.

Regarding the connection method between the longitudinal diaphragms and the base, alternating intersections were chosen instead of placing the diaphragms within single grooves.

Another refinement of the geometry involved straightening all the oblique sides of the diaphragms, created by the geometric subtractions with the diagonal elements and the shell covering. This step was necessary to facilitate the cutting of the centering components using a laser cutting machine.

This chapter includes a preview of the latest centering prototype, designed after the creation of an initial *carton bois* model. It was necessary to make certain adjustments: refine the diaphragm intersections, give more strength to the system and adapt the thickness of the model components according to the availability of materials on the market (Fig. 3.19). A more detailed explanation of this latest prototype will be provided in the following chapter.

Step 1: first approach

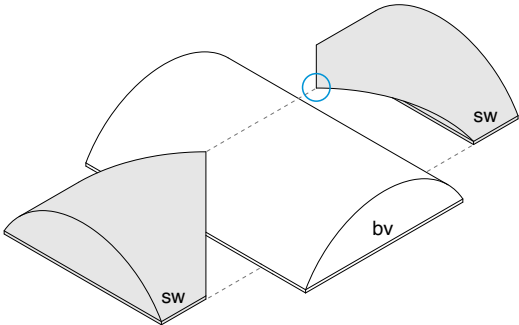
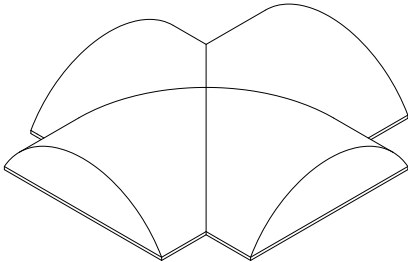
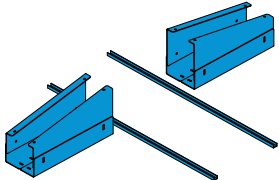


Fig. 3.16 – Centering design: step 1, first approach. In blue the model's issue: an infinitesimally thin edge of the lateral webs.

Step 2: internal mechanism

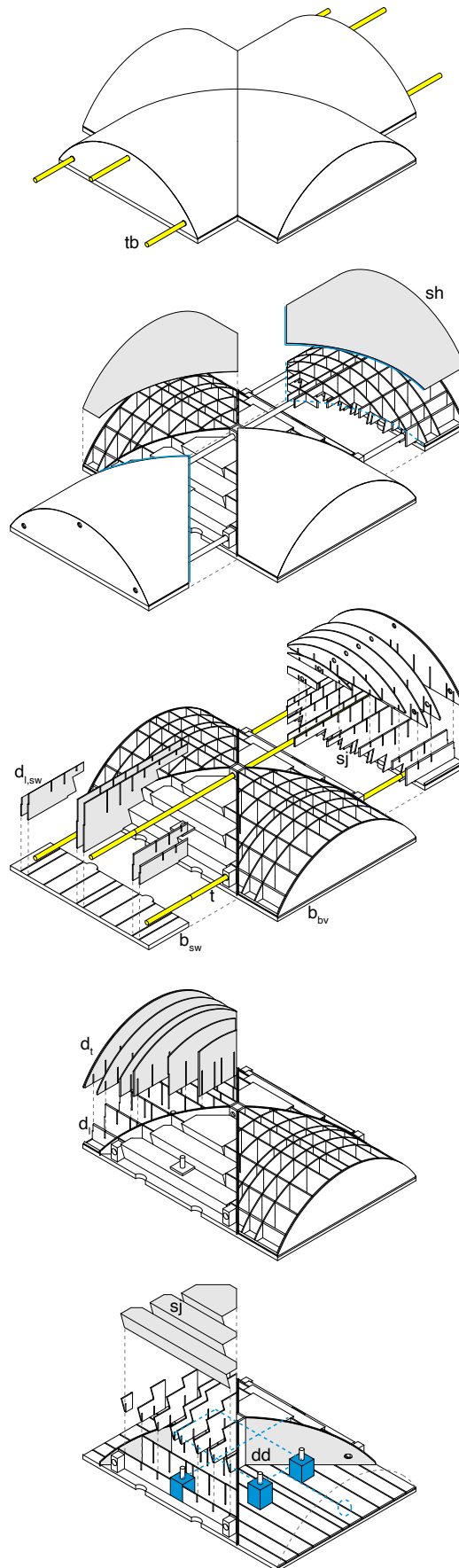
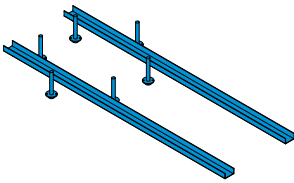


Fig. 3.17 - Centering design: step 2, internal mechanism. In blue the model's issues: lack of support for the shells of the lateral webs and incompatibility between the internal mechanism and the diaphragms partition. In yellow the threaded bars.

Step 3: external mechanism

First prototype

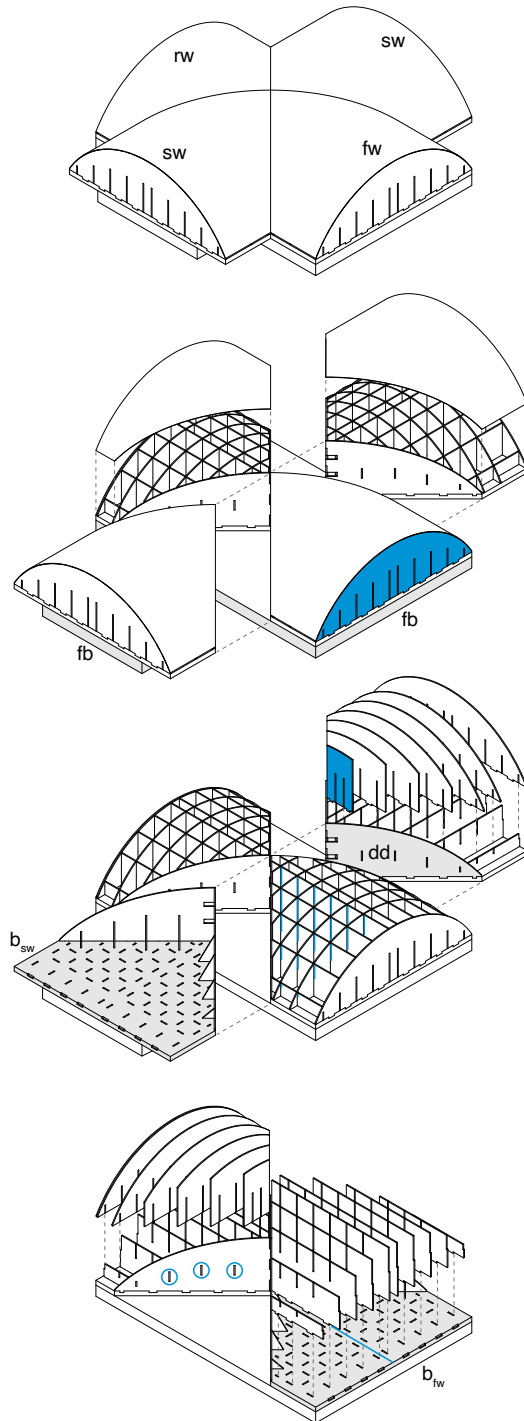
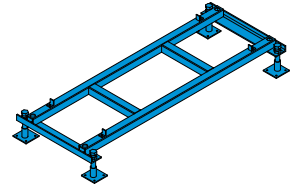
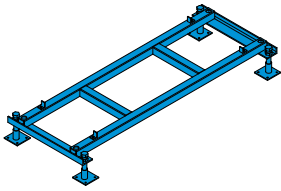


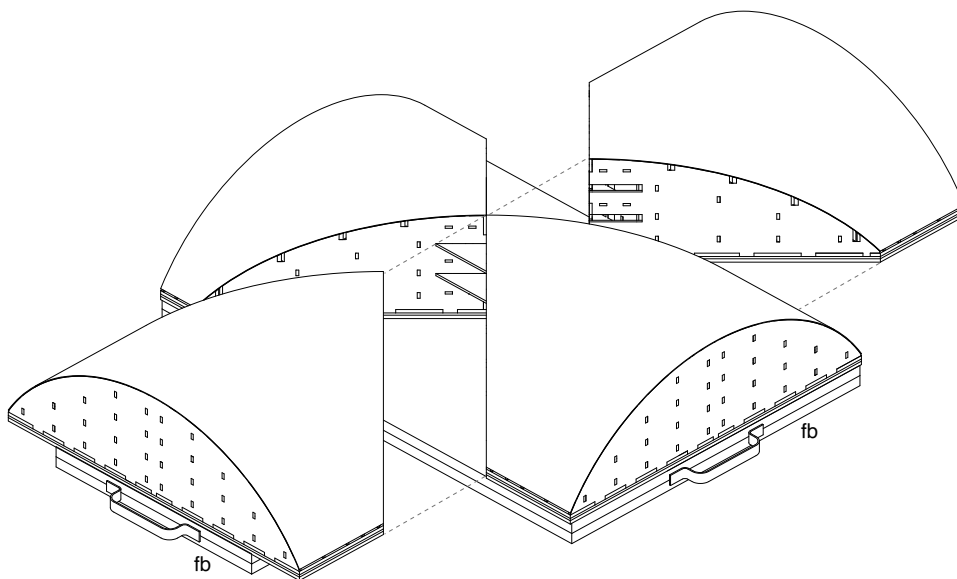
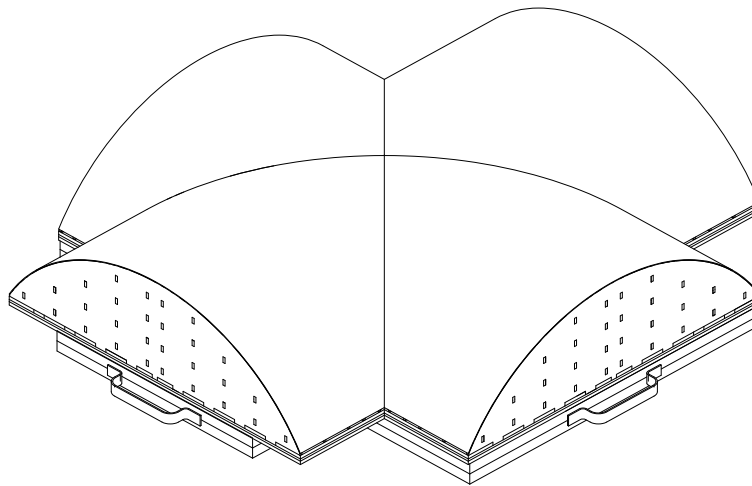
Fig. 3.18 – Centering design: step 3, external mechanism. First carton bois prototype, in blue the model's issues occurred during the building process.



Step 3: external mechanism

Final prototype

Fig. 3.19 – Centering design:
step 3, final prototype on which
the final assembly is based on.
Designed to solve the issues of
the lastest prototype.
a. Complete centering prototype
b. How side webs are extracted



a.

b.

Fig. 3.19 – Centering design:
step 3, final prototype on which
the final assembly is based on.
Designed to solve the issues of
the lastest prototype.
c. Small arches stiffening the
longitudinal diaphragms
d. The first arched diaphragm is
slotted from the front

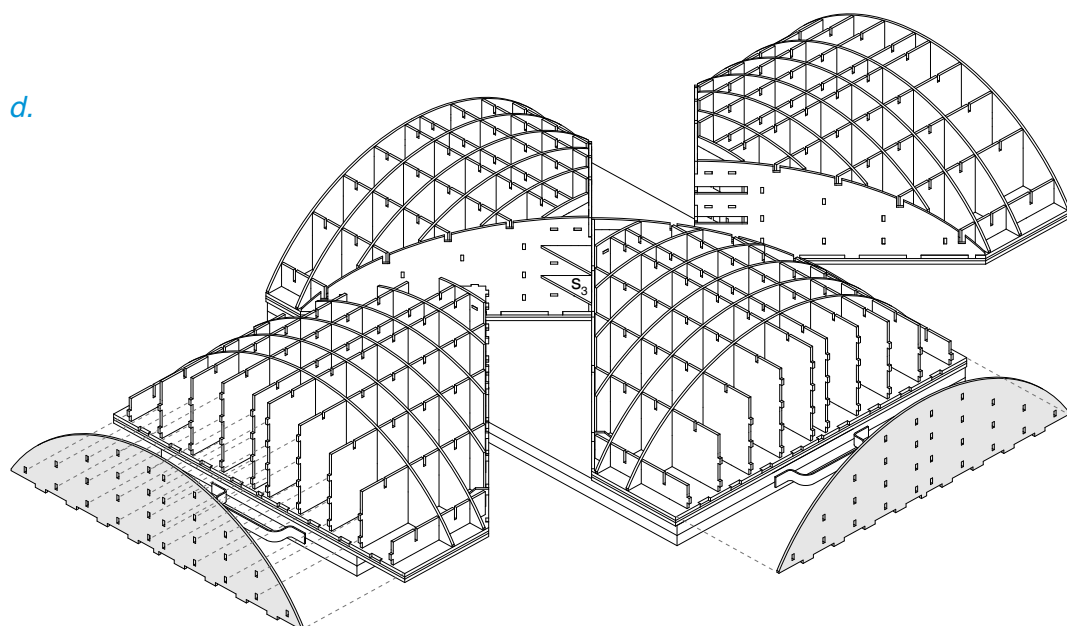
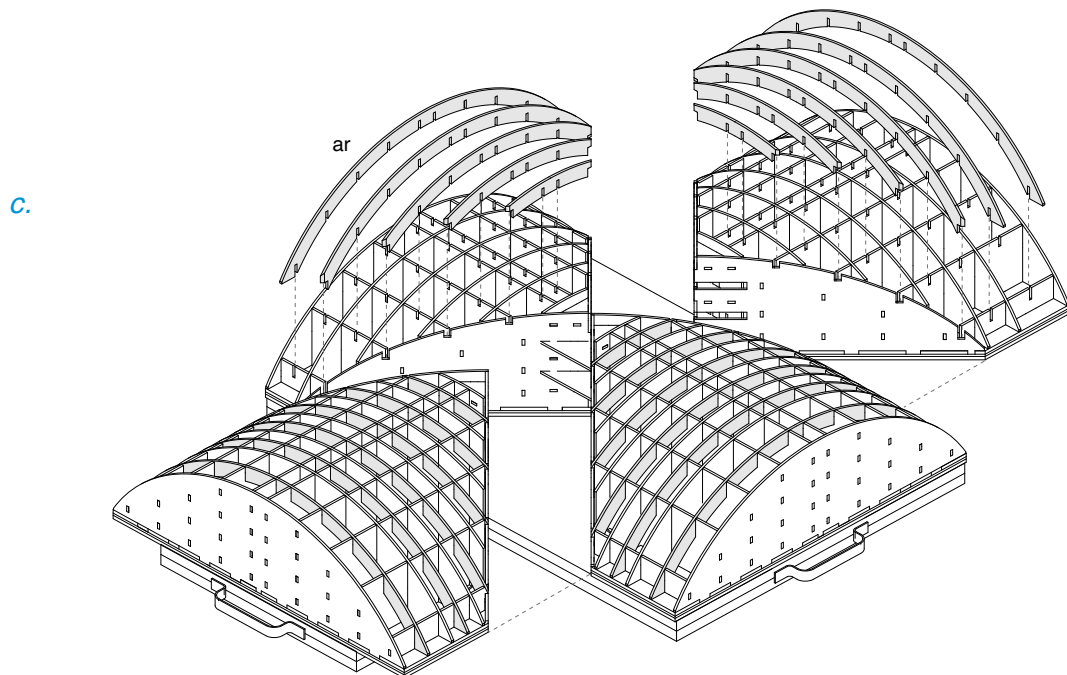
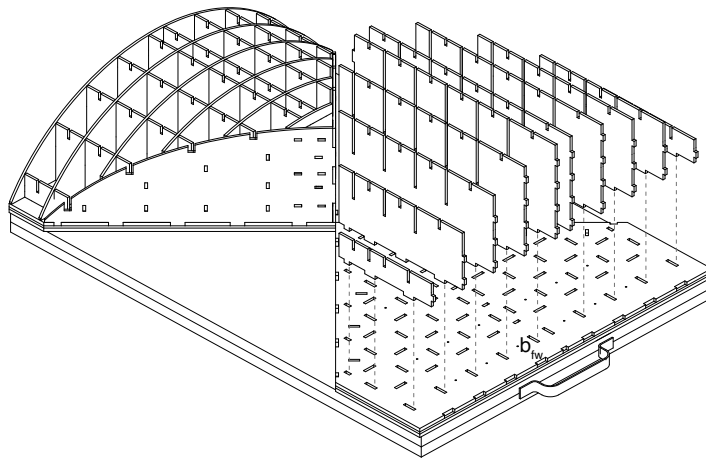


Fig. 3.19 – Centering design: step 3, final prototype on which the final assembly is based on. Designed to solve the issues of the lastest prototype.

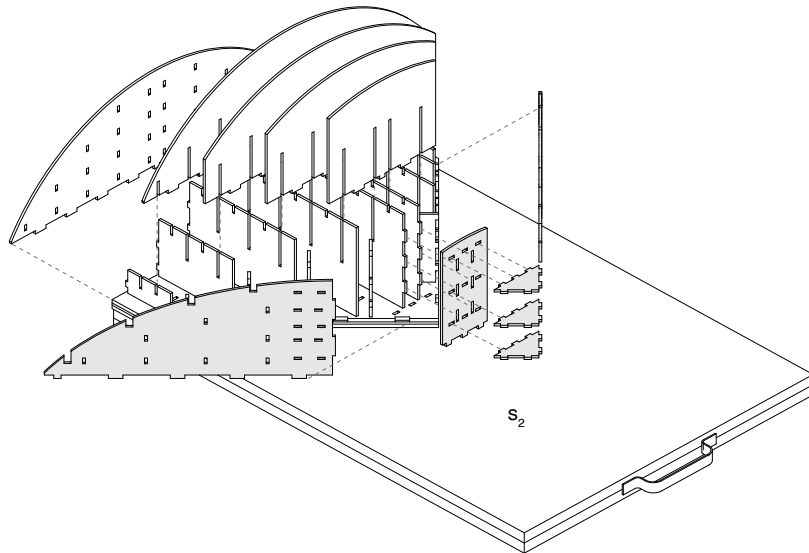
e. How longitudinal diaphragms vertically interlock with the base layer

f. The apex of each web is redesigned as a connection element for the diagonal diaphragms

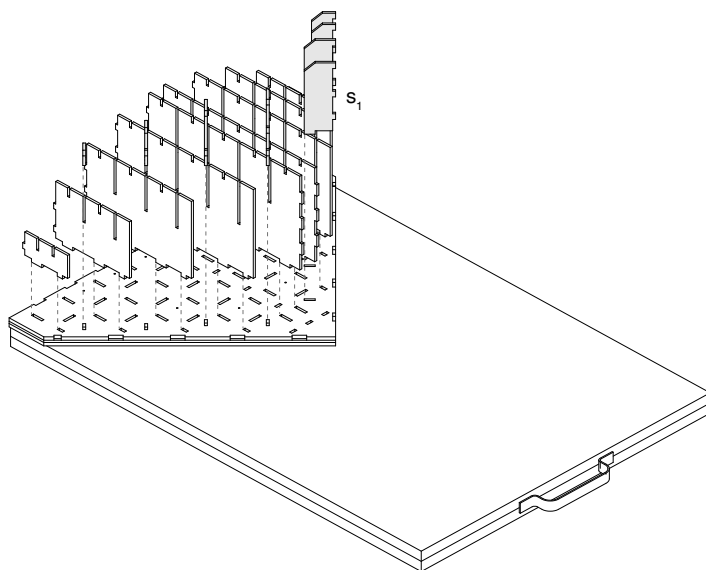
g. Other supports for the diagonal diaphragms



e.



f.



g.

3.4 Design of the centering moving system

The new mechanism for moving the wooden centering, introduced in Chapter 3.2.3, is here explored in all its aspects.

A key factor in choosing this system was the ability to position the structure outside the geometry of the centering, along with the decision to use a simple four-support system operated manually at four points.

Before describing the elements that make up this manual maneuvering system, it is necessary to discuss its positioning. Since this involves a fixed frame screwed to the main base and located beneath the cross-vault, it was essential to study the vault's geometrical movement during the testing phase to avoid collisions between the elements.

Knowing the displacement applied by the shear actuator along the x-axis, which is 10,00 cm, with the rear fixed abutment as the rotation center and knowing the radius of curvature, equal to the chain length, the aim was to calculate the movement of the frontal abutment along the y-axis. Moreover, it is essential to verify that the mobile plate, on which the front abutments are located, does not collide with the metal frame.

Through simple trigonometric calculations, it was determined that the front support of the vault shifts by 9,2 mm along the y-axis (Fig. 3.20).

From this point, allowing for a precautionary movement of 30 mm along the y-axis, the maximum space requirement for the maneuvering system was established. Along the x-axis, the maximum space is determined by the size of the base panel, measuring 1200 mm. The height requirement for the frame system, along the z-axis, was designed by considering several factors: the need to lower the centering structure by 30 mm for extraction plus an additional 15 mm as a safety margin, the constraint of maintaining a 10 mm distance from the chains, the space occupied by the frame itself and the infinite screws and the necessity to avoid excessive raising of the vault's abutments.

The frame system for moving the plywood centering consists of four support elements, endless screws with a diameter of 20 mm and height of 120 mm, two unequal-sided angle brackets connected to the endless screws via four welded bolts, two squared beams resting transversely on the angle brackets and a pair of additional squared beams to complete the frame (Fig. 3.21, 3.22).

The upward and downward movement of the metal frame system is controlled by endless screws. Specifically, these screws are rotated using four removable metal rings placed on their hexagonal heads. By applying simultaneous rotation, the four endless screws press against metal plates screwed to the wooden base, and, thanks to the bolts welded to the angle brackets, the frame moves in the desired direction.

Each endless screw is housed in a small cylinder welded to the base plate, which serves to physically prevent the frame from descending beyond the predetermined distance, thereby protecting the chains. Moreover, the endless screw features a fine threading to allow for precise, millimeter-level adjustments.

Four small 25x25 mm angle brackets are screwed onto the longitudinal squared beams as stops for the centering base. These elements will be unscrewed to allow for the removal of the centering structure.

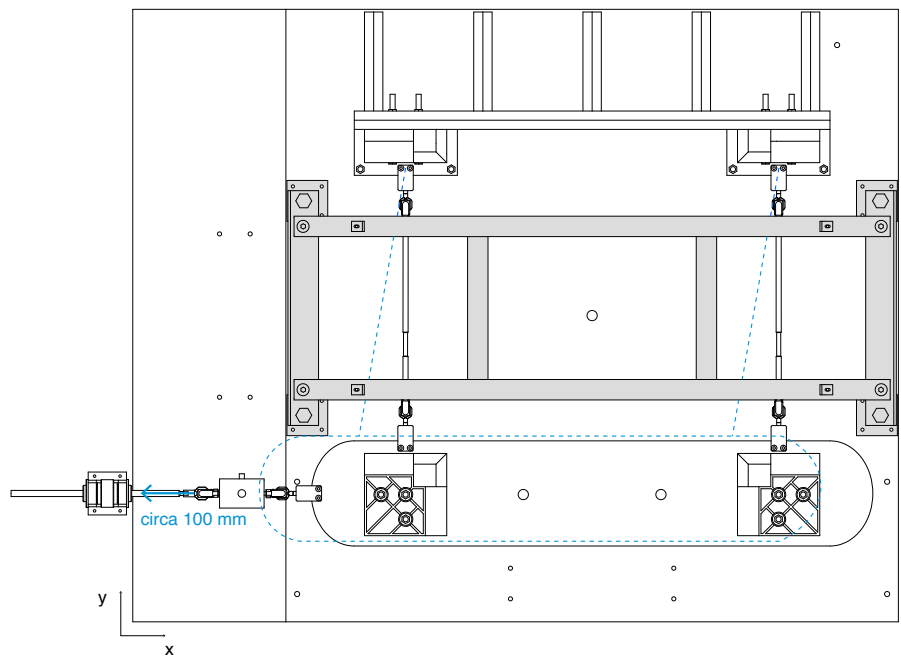
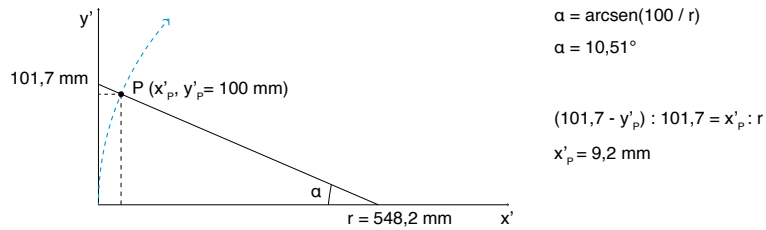
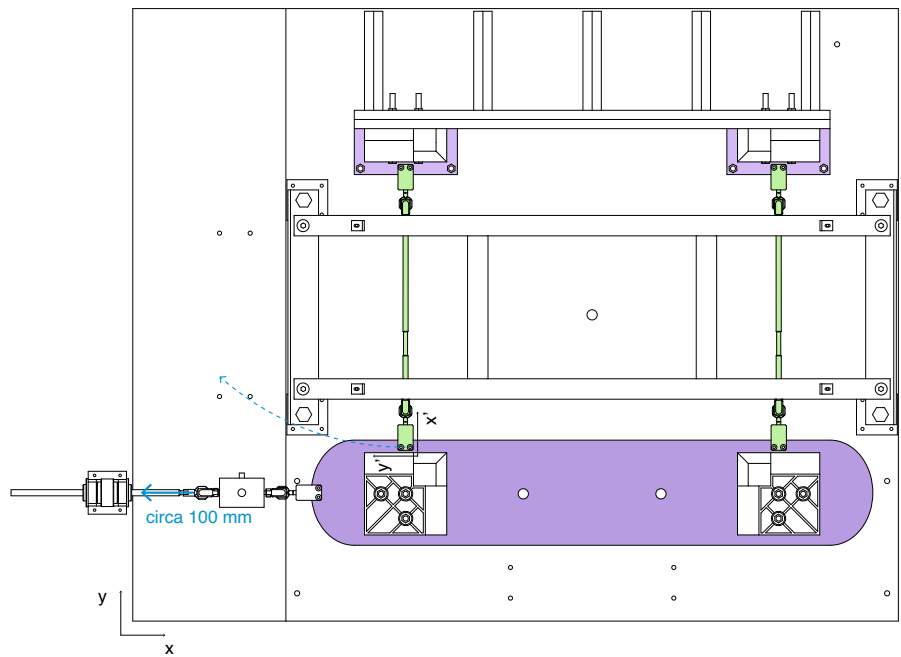


Fig. 3.20 - Geometrical movement of the cross-vault's abutments during the shear testing phase. From the top: system's direction of rotation; trigonometrical calculation of x and y displacements; frontal plate movement and the frame positioning.

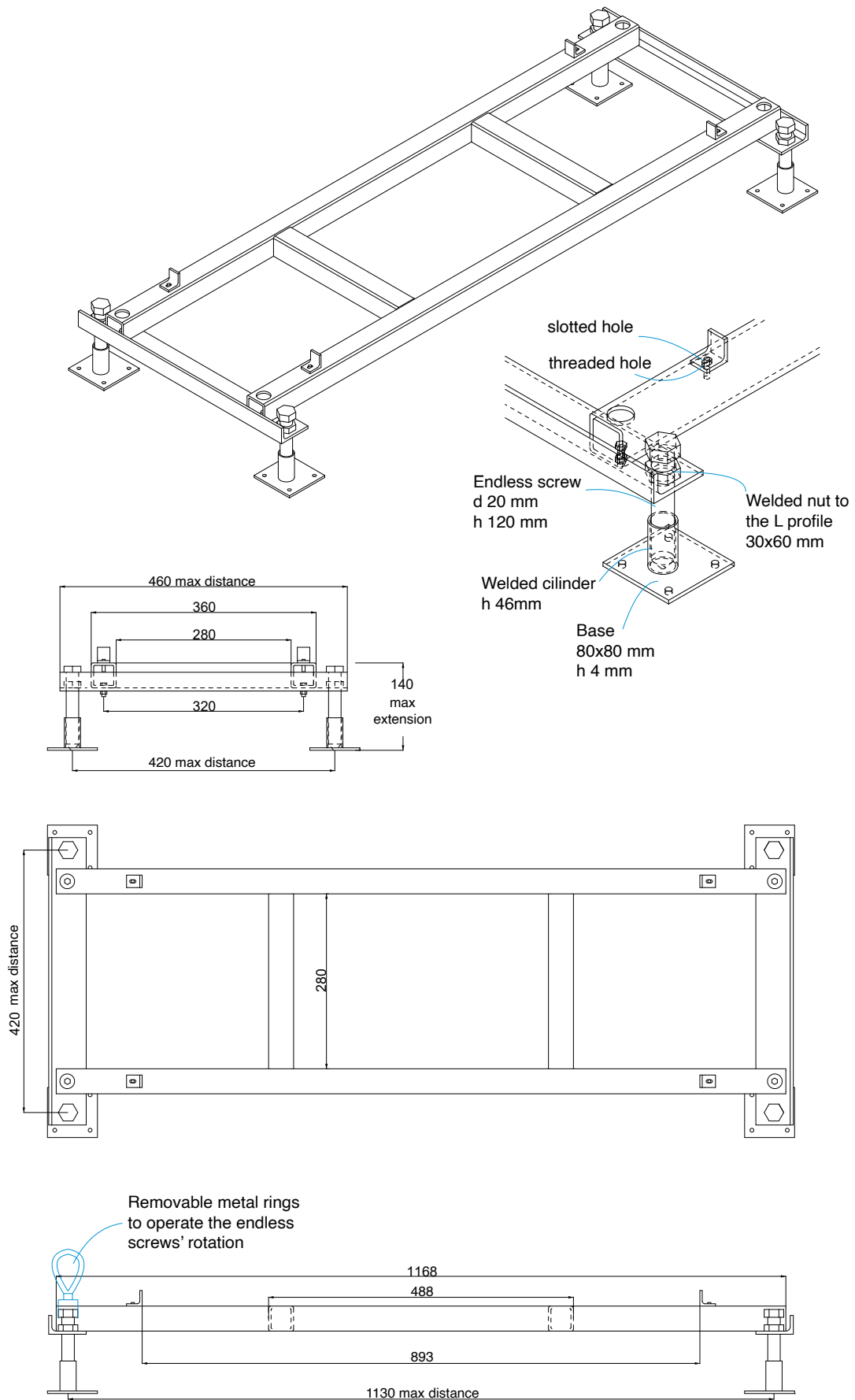


Fig. 3.21 – Details of the centering moving system. From the top: axonometric view; zoom on the endless screw system; side view; top view; front view

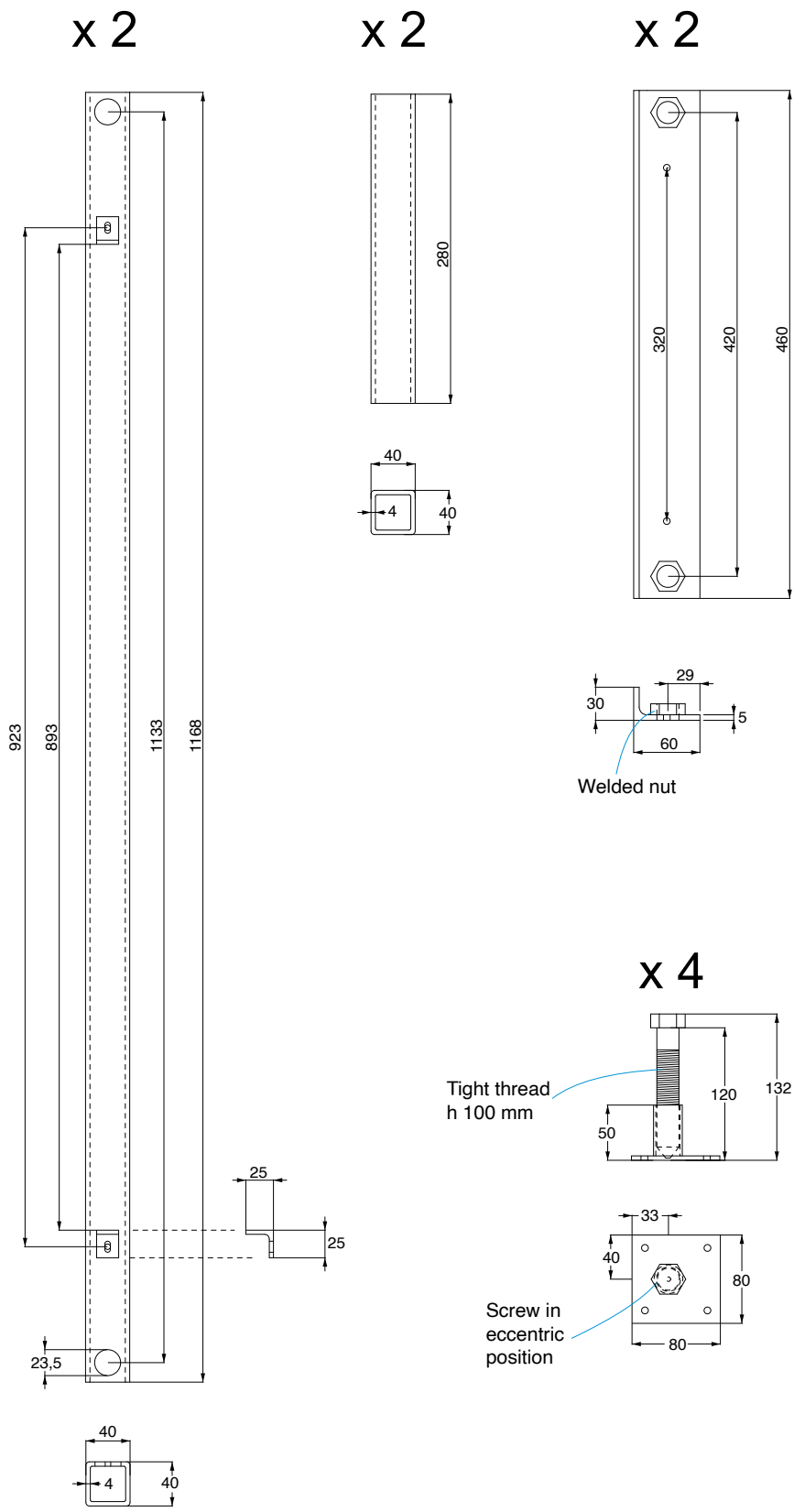


Fig. 3.22 – Catalog of the moving system's components.

4. *Building process of the testing setup*

The physical construction of the testing setup was developed based on the three-dimensional Rhino model described in chapter 3.2.3.

The building process of the testing setup took place in the laboratories of the Politecnico di Torino, specifically MOD Lab Arc, MOD Lab Design and LASTIN - Laboratorio Sistemi Tecnologici Innovativi.

The main machinery used for building the setup includes a laser cutter machine, for materials up to 1 cm thick; a CNC milling machine, for wood panels thicker than 1 cm; a PLA filament 3D-printer, which was used to create the cross-vault abutments and some test blocks for the vault.

To produce certain elements, including the 1200 x 1200 x 30 mm testing setup base, the MJF and MSLA-printed vault blocks and the centering maneuvering system, resources external to the Politecnico were required.

4.1 Manufacturing of 3D-printed components

Great attention was given to the creation of blocks that form the cross-vault. Numerous print tests were conducted to ensure that the friction angle of the blocks was satisfactory for the research purposes. In this regard, different materials, 3D-printing techniques and external finishes were tested.

Referring to the research conducted by Michela Rossi [4], an attempt was made to reproduce the friction coefficient of her model's blocks, equal to 35° . However, difficulties were immediately encountered in reproducing a similar prototype. As a matter of fact, with advancements in additive manufacturing techniques producing increasingly precise surface finishes, achieving a grooved finish similar to that of Rossi's blocks proved to be challenging.

Regarding the 3D-printing techniques explored, the first printing tests for the vault's blocks were conducted using Fused Deposition Modelling (FDM) with Poly Lactic Acid (PLA) filament (Fig. 4.1a).

However, the external finish of the blocks quickly proved to be too smooth for the friction research requirement, whereas the creation of structural supports along the blocks' inclined sides led to numerous geometric inaccuracies (Fig. 4.3).

A second test was done using a PLA wooden filament (Fig. 4.1b), but the material roughness did not improve from the previous test.

In parallel, a different 3D-printing technique, Multi Jet Fusion (MJF), was tested using both nylon PA12 and a composite filament as printing material (Fig. 4.1c, 4.1d). This technique offers improvements in terms of geometric precision and roughness compared to the previous printing method.

Ceramic resin was tested as a fourth option, using a different 3D-printing technique called Masked Stereolithography (MSLA) (Fig. 4.1e). The friction angle of this latest sample appears higher than in previous cases, though production costs are notably increased [37].

For each of these options, a filling test of the inner pocket with lead pellets and epoxy resin was conducted. It proved to be an effective technique even though it requires a lot of manual work. Each of the blocks shown in Figure 4.1, of type U0, weighs approximately 50 grams.

A printing and filling test was also conducted on one of the arch blocks. PLA was used, and once filled, its weight is around 400 grams (Fig.4.2).

Lastly, an external spray coating was tested on each type of block to increase its friction coefficient. This proved to be an unsuitable solution due to the evident potential for human error in applying the product evenly across all surfaces. Furthermore, with the intention of testing the vault multiple times, the coating appears unable to adhere firmly to the underlying material, thus ineffective.

Using the FDM technique and PLA filament, prototypes of the vault abutments were also created. To optimize printing success and reduce material usage, each volume was split into two pieces, which were then stacked and glued together (Fig. 4.4).

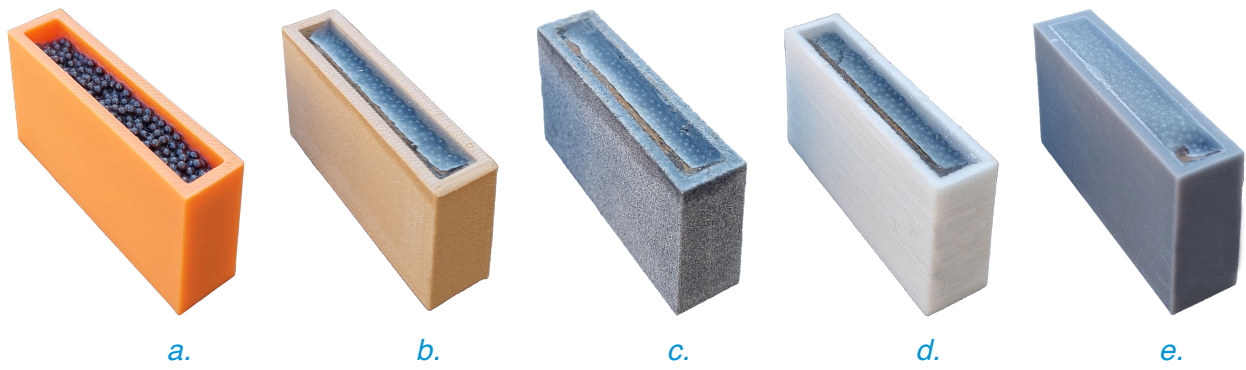


Fig. 4.1 – Blocks U0 manufactured using different materials and technologies. From left to right: a. PLA via FDM, b. wooden PLA via FDM, c. Nylon pa12 via MJF, d. composite filament via MJF, e. ceramic resin via MSLA.



Fig. 4.2 – Head arches blocks: 3D-printed via FDM and filled with led pellets and epoxy resin.



Fig. 4.3 – Example of PLA external supports created by the 3D-printing machine.

Frontal abutment



Rear abutment



Fig. 4.4 – 3D-printed prototypes of the cross-vault abutments. The green parts represents the plates described in Figure 3.11; although they will be printed using the same material as the vault blocks, they were printed at this stage to test the functionality of the interlocks with the underlying part.

4.2 Building process of the centering

It is important to start this chapter with a note on how the discrepancies between the digital and the physical model had been addressed.

Digital modeling in Rhino brings with it geometries, angles and details of intersections between solids that are either impossible or at least very costly to reproduce in a physical model. For example, consider that a laser cutting machine only makes straight cuts in the direction of the sheet's thickness. Therefore, diagonal cuts could have only been made manually. Moreover, it was necessary to adapt the model to the available tools and reduce to the minimum the manual work.

Firstly, it was necessary to approximate the geometry of the centering's diagonals (dd) to a uniform solid, then to square all the diaphragms in both the longitudinal and vertical directions. The only elements for which it was deemed necessary to perform manual finishing work were the small arches (ar). Their straight ends were made angled using a wood file and sandpaper so they could adhere more precisely to the diagonal elements (dd) (Fig. 4.10).

4.2.1 First prototype

As the first centering's prototype, a single side web was chosen to be reproduced using *carton bois* as construction material. The reference model is the one described at the end of chapter 3.3.2, Figure 3.18.

Starting with 100 x 60 cm *carton bois* panels, the individual pieces were cut using a laser cutting machine.

All the internal diaphragms have a thickness of 3 mm, while the base (b_{sw}) is made by stacking cardboard layers of 2 mm and 3 mm, totaling 15 mm. Regarding the outer shell (sh), several tests were conducted. The 2 mm cardboard proved to be too inflexible to adapt to the curvature of the vault, so three layers of thinner ribbed cardboard were used instead. They are more flexible yet still resistant.

Among the advantages observed in the building process of this first prototype was the high precision of joints between diaphragms, thanks to the accurate cuts made by the laser in a highly planar material like *carton bois* (Fig. 4.5).

Instead, a few elements needed further modification. The diagonal components (dd) required reinforcement through the addition of new supports (s_1), the first arched diaphragm should have frontal joints and the apex of each section needed to be reinforced with triangular elements that also connect to the diagonals (s_2) (Fig. 4.6). Additionally, new arched (ar) elements between transverse diaphragms are required to solve the instability issue of longitudinal diaphragms (Fig. 4.7). These new elements also intersect with the diagonals, making them even more stable. These latest modifications are shown in chapter 3.3.2, Figure 3.19.

This first phase was certainly useful for better understanding the assembly process of the interlocking pieces. The preferred sequence is as follows: longitudinal diaphragms, transverse diaphragms starting from the largest to the smallest, diagonal elements with their supports and finally the arched elements.

4.2.2 Final assembly

The reference model here described is the one presented in chapter 3.3.2, Figure 3.19.

The latest version of the centering structure was developed after the creation of the first physical prototype in *carton bois*. It was necessary to make certain adjustments to refine the diaphragm intersections, give more strength to the system and adapt the thickness of the model components according to the availability of materials on the market.

This final prototype is made of plywood to overcome fragility and deformability issues of *carton bois*. This modification required adjusting the model's thicknesses to match the one of purchasable

panels.

In this case as well, starting with 100x60 cm plywood panels, the individual pieces were cut using the laser cutter machine (Fig. 4.8).

The first base layer (fb) consists of two 18 mm plywood panels, while the secondary bases (b) are made up of three layers of plywood panels (6+4+6 mm). The top panel features slots for the longitudinal diaphragms, the diagonals and the external transverse diaphragms. All these elements are 4 mm thick.

The connection between the diagonals and the base has been reinforced with the addition of multiple interlocking supports (s_1). Additional support is also given by the triangular elements added to each web's central vertex (s_2).

A series of small arches (ar) has been added to the centering's internal geometry to secure the ends of the longitudinal diaphragms and minimize the possibility of flexion of the covering shell by reducing the span between adjacent diaphragms.

The only difference among the four webs lies in the diagonal elements, which are symmetrical in pairs: the central ones are externally secured by a pair of triangular supports (s_3), while the diagonals of the side webs are cut to align with these elements and achieve a perfect fit with the central webs.

In conclusion, three handles were added to the thicker base layer to facilitate the removal of the centering components.

The biggest issue encountered with plywood, especially for the thin thickness of 4-6 mm, is its lack of flatness (Fig. 4.9). For this reason, the laser cut machine was not as precise as in the previous model made of *carton bois* because it achieves millimeter-precise cuts as long as the starting panel is perfectly flat. The cut lines on slightly warped plywood panels were sometimes thicker, sometimes thinner, and in some cases, it was necessary to manually refine the cut (Fig. 4.11). Despite these inaccuracies and some millimetric misalignments, it was decided to continue using plywood as the assembly process was still effective and the pieces interlocked without any remarkable

difficulties. The web's misalignments were corrected by adding small paper layers before gluing the covering shells.

Using MDF panels would have likely resulted in more precise cuts but would have also significantly increased the weight of the centering. This choice would have caused greater load on the manual handling system, in addition to the substantial weight of the cross-vault.

Specifically discussing the construction process of the centering structure, assembly began with attaching the bases of the four webs to their respective underlying thicker bases using vinyl glue and 50 mm and 20 mm screws. Subsequently, the remaining pieces are glued in the following order: longitudinal diaphragms, transverse diaphragms starting from the largest to the smallest, diagonal elements with their supports and finally the arched elements. As the last step, three layers of ribbed cardboard are glued to the top of each web plywood structure to make the covering shell. The shells mainly adhere to the primary curvature of the vault, represented by the arched diaphragms, while the longitudinal diaphragms stiffen the centering structure remaining slightly lower than the transverse diaphragms.

Addressing the issues of plywood unevenness and further reinforcement of the centering structure, it was decided to secure the various components with small nails.

The assembly sequence of the centering system for a small-scale model of a cross-vault is illustrated in the following pages. First, the assembly sequence of a single web is shown, then follows the assembly of the entire centering structure. (Fig. 4.12, 4.13).

First prototype _ carton bois

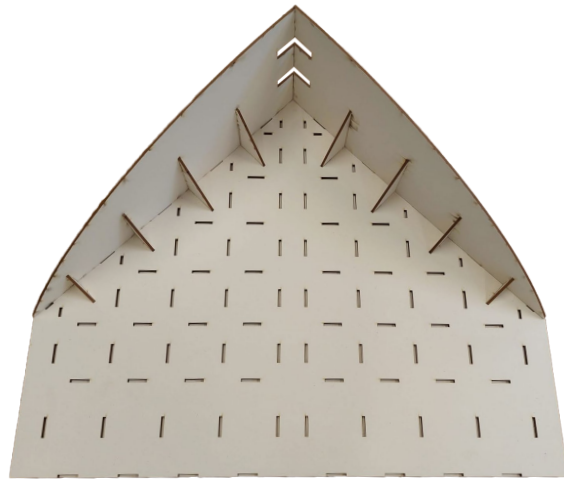


Fig. 4.5 – First prototype in carton bois, assembly test. From the top: diagonals; longitudinal diaphragms; transverse diaphragms; first arched diaphragm.

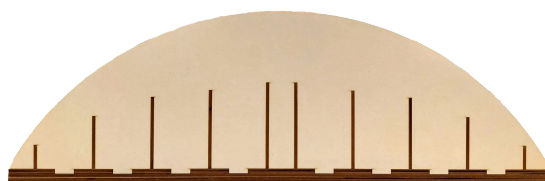




Fig. 4.6 - First prototype in carton bois, main issues. Instability of the apex, lack of support in relation to the diagonal diaphragms.

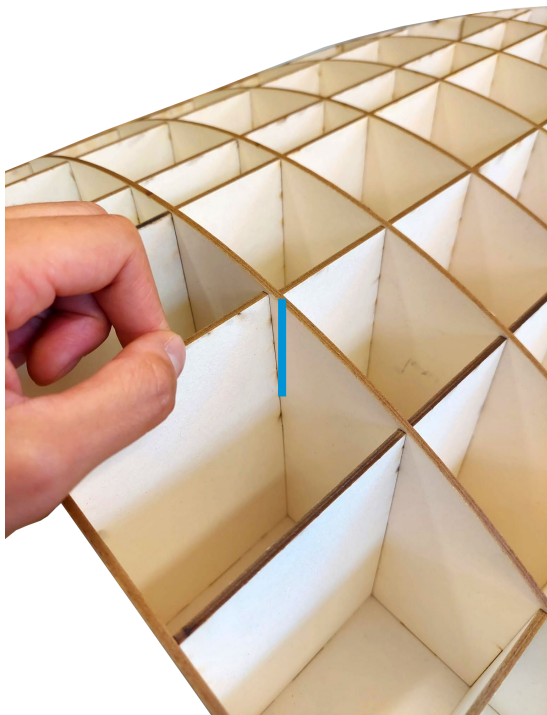


Fig. 4.7 - First prototype in carton bois, main issues. Instability issue of longitudinal diaphragms.

Final assembly _ plywood

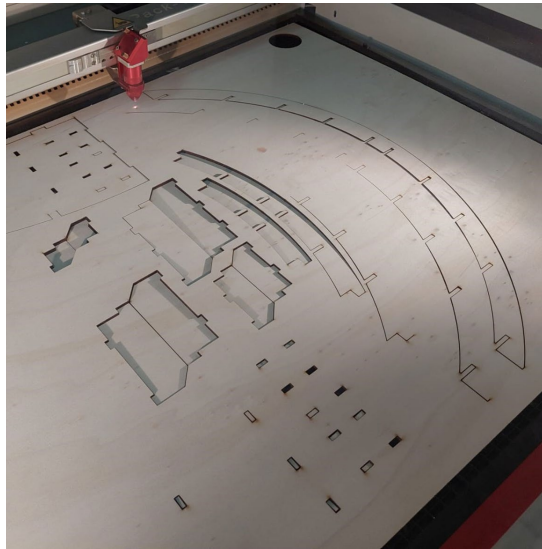


Fig. 4.8 – Final plywood prototype, laser cutting machine.

Fig. 4.9 – Final plywood prototype, flatness issues.



Fig. 4.10 – Final plywood prototype, manually sanding the ends of small arches.

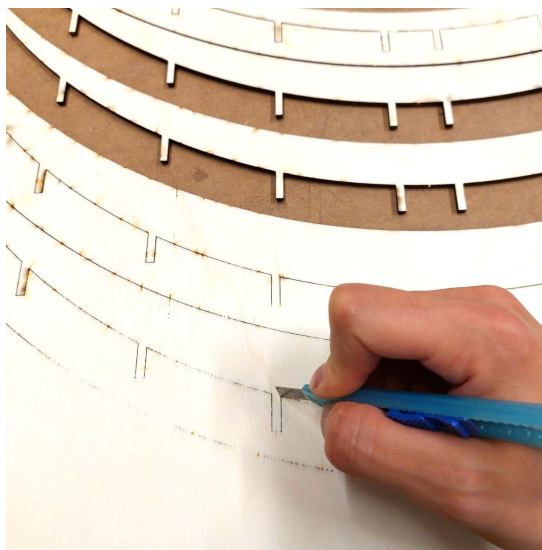
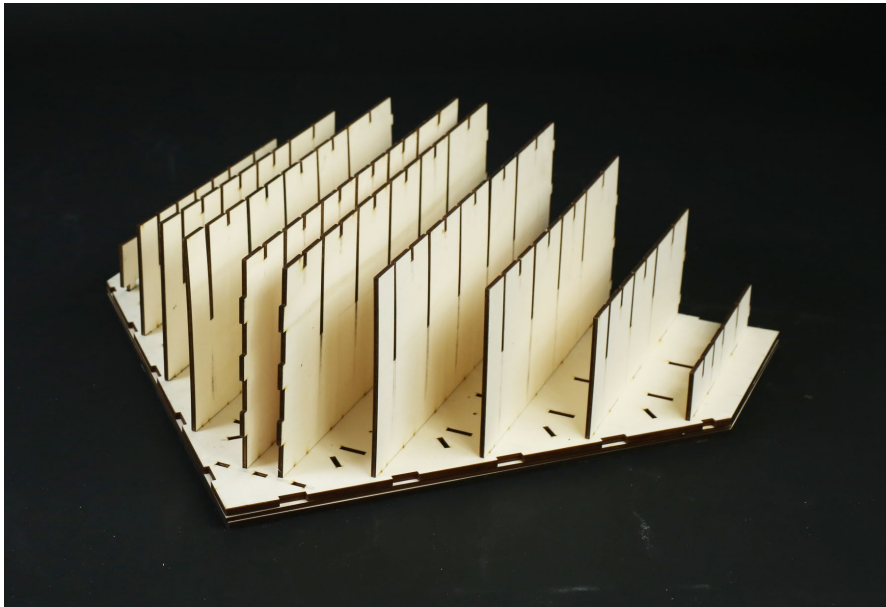


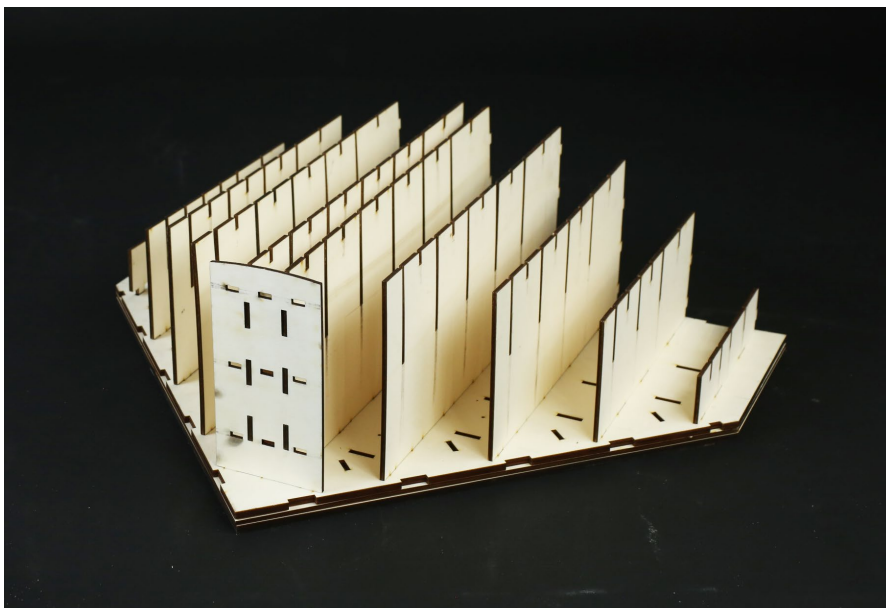
Fig. 4.11 – Final plywood prototype, manually refining some unsuccessful laser cuts.



a.



b.



c.

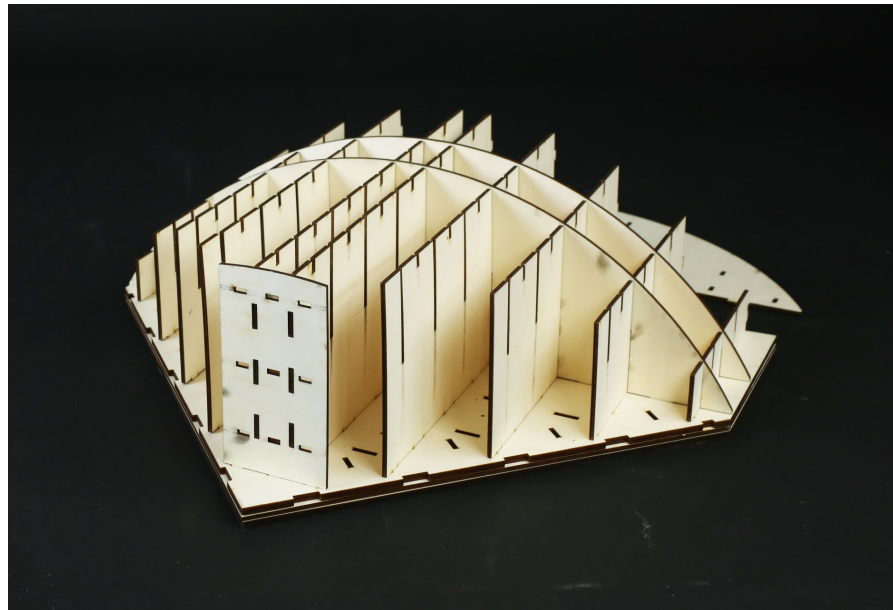
Fig. 4.12 – Final plywood prototype, assembly process of the centering system. Single web.

a. Base layer

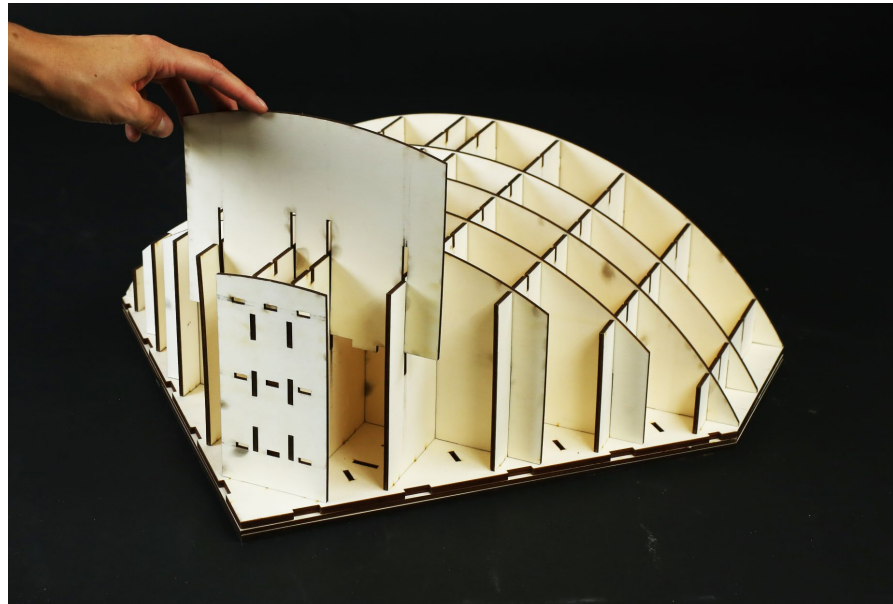
b. Longitudinal diaphragms

c. Apex piece

d.



e.



f.

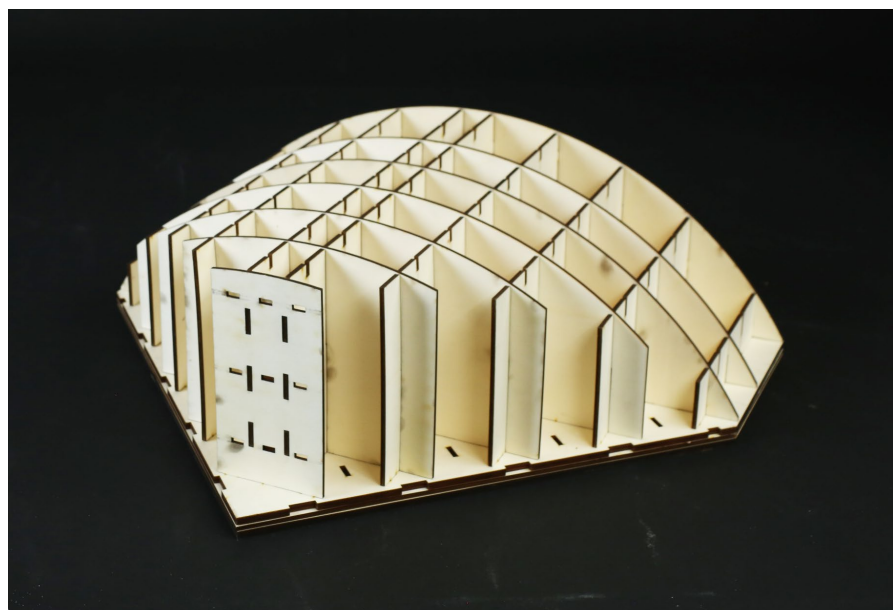
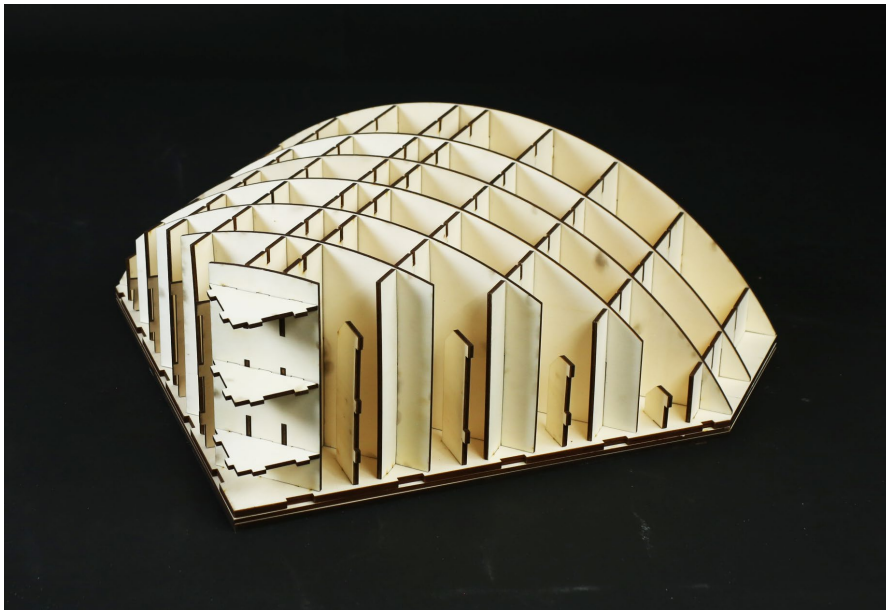
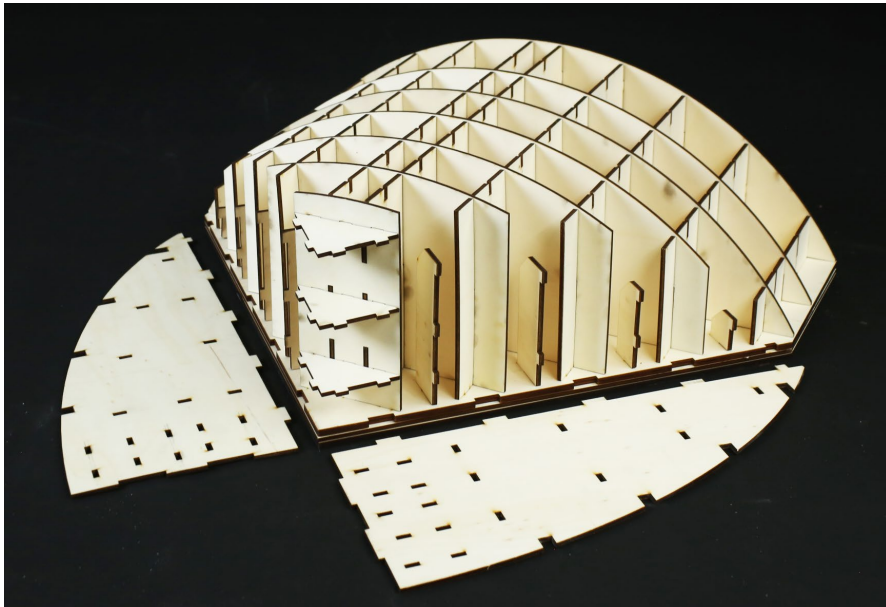


Fig. 4.12 – Final plywood prototype, assembly process of the centering system. Single web.
d. First arched diaphragm
e. Transverse diaphragms fitted from above
f. Complete longitudinal and transverse diaphragms



g.



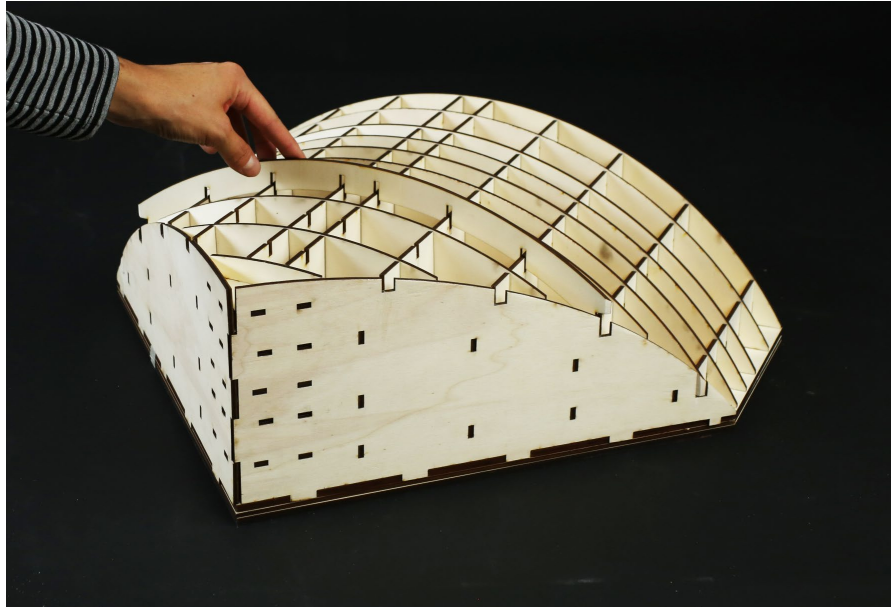
h.



i.

*Fig. 4.12 – Final plywood prototype, assembly process of the centering system. Single web.
g. Supports for the diagonals
h. Diagonal pieces
i. Diagonals in place*

j.



k.



l.



Fig. 4.12 – Final plywood prototype, assembly process of the centering system. Single web.

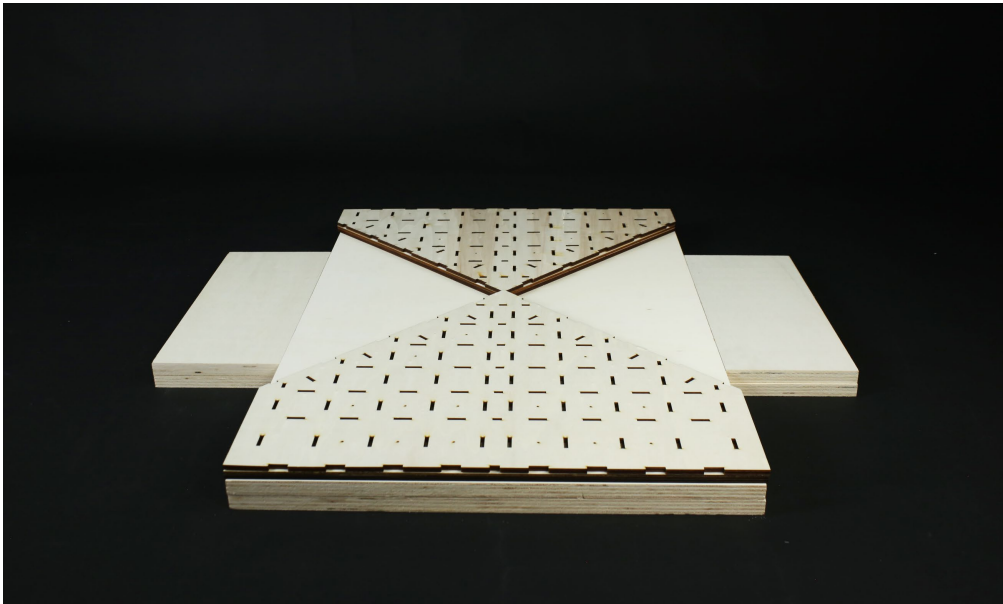
j. Positioning the small arches

k. Arches in place

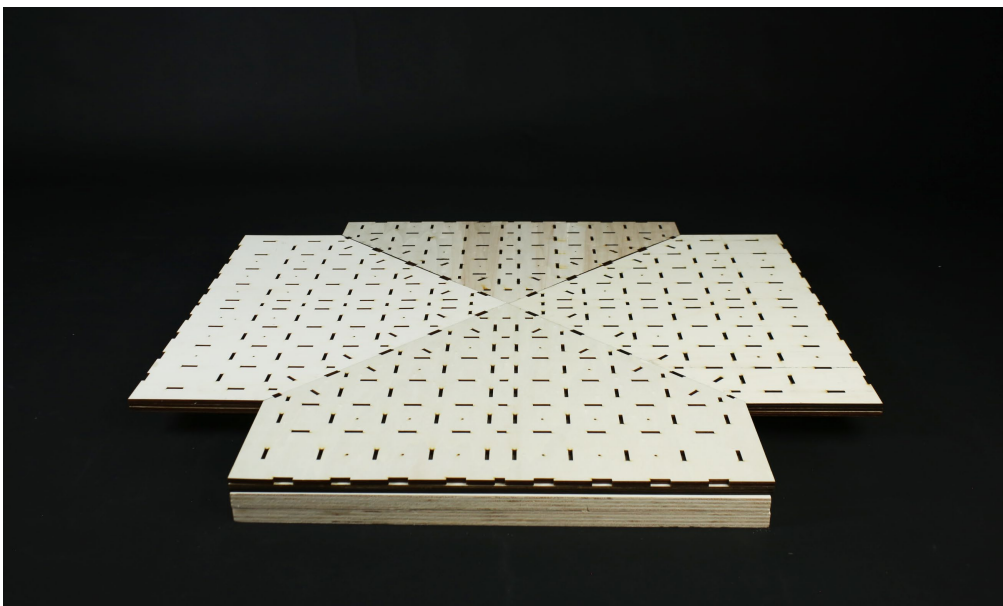
l. Cardboard shell



a.



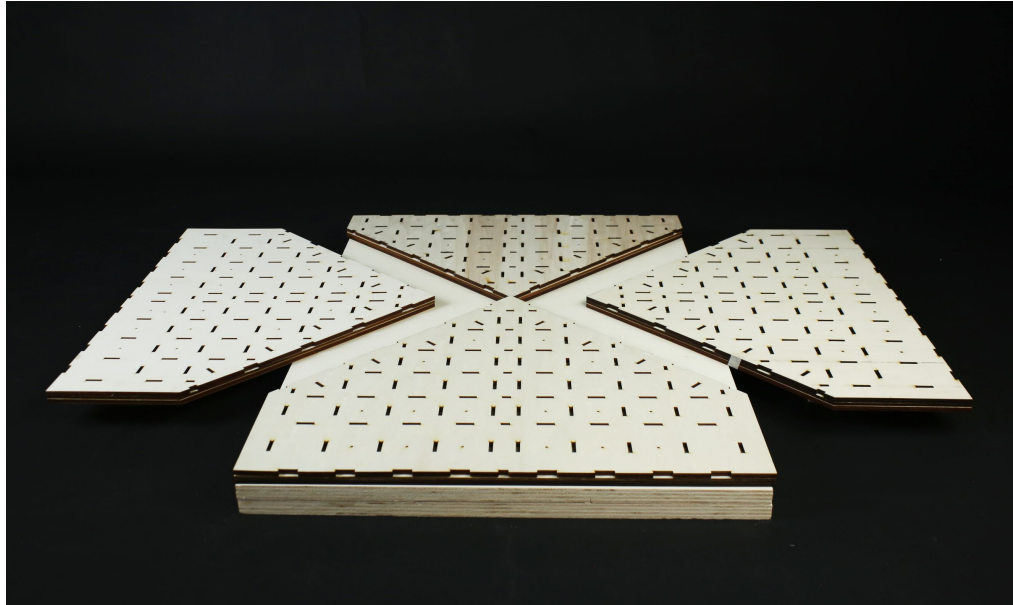
b.



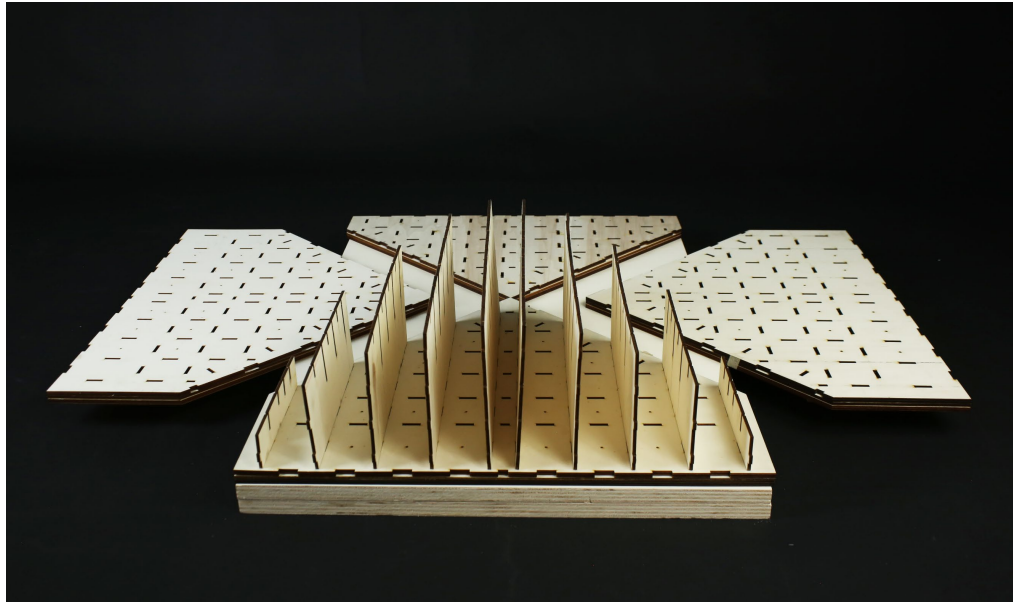
c.

*Fig. 4.13 – Final plywood prototype, assembly process of the centering system. Entire centering structure.
a. First base layer
b. Second base layer, central webs
c. Second base layer, lateral webs*

d.



e.



f.

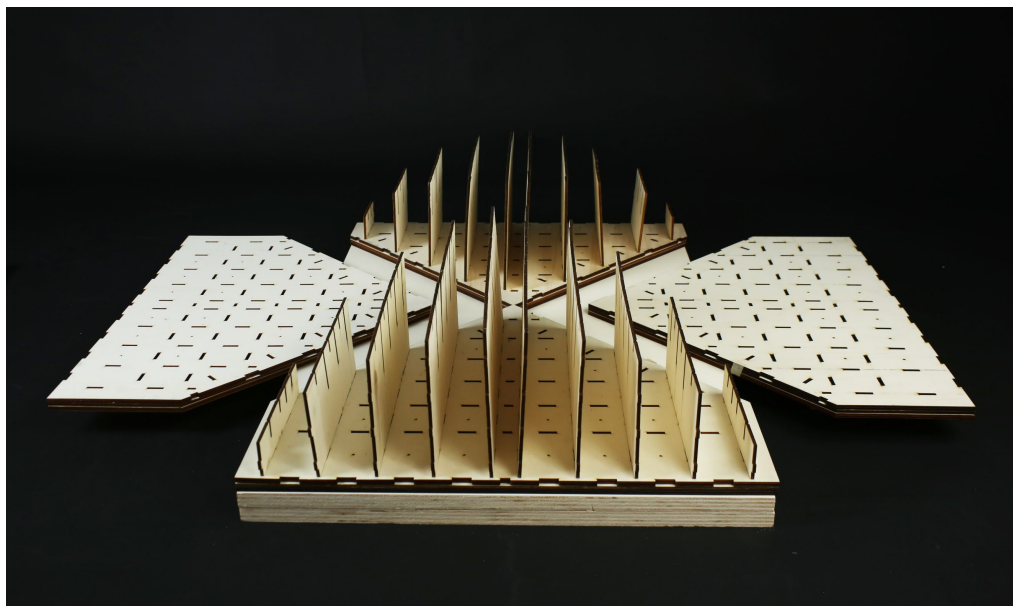
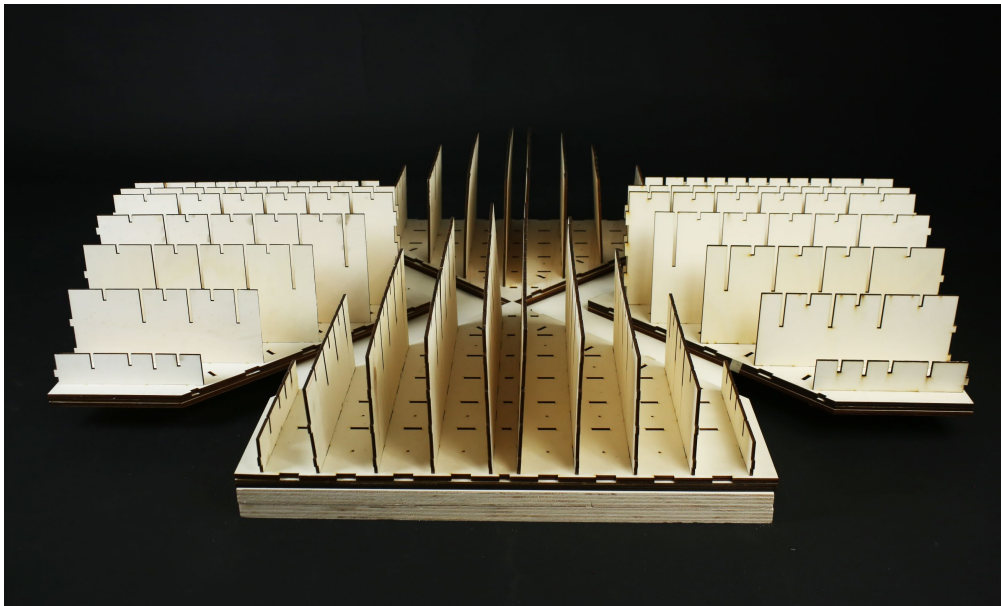
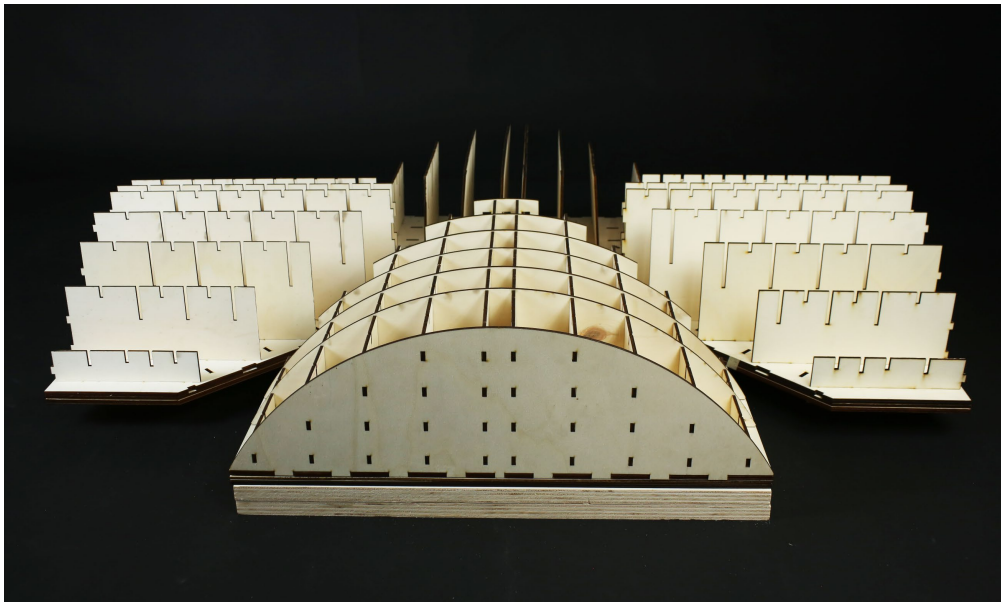


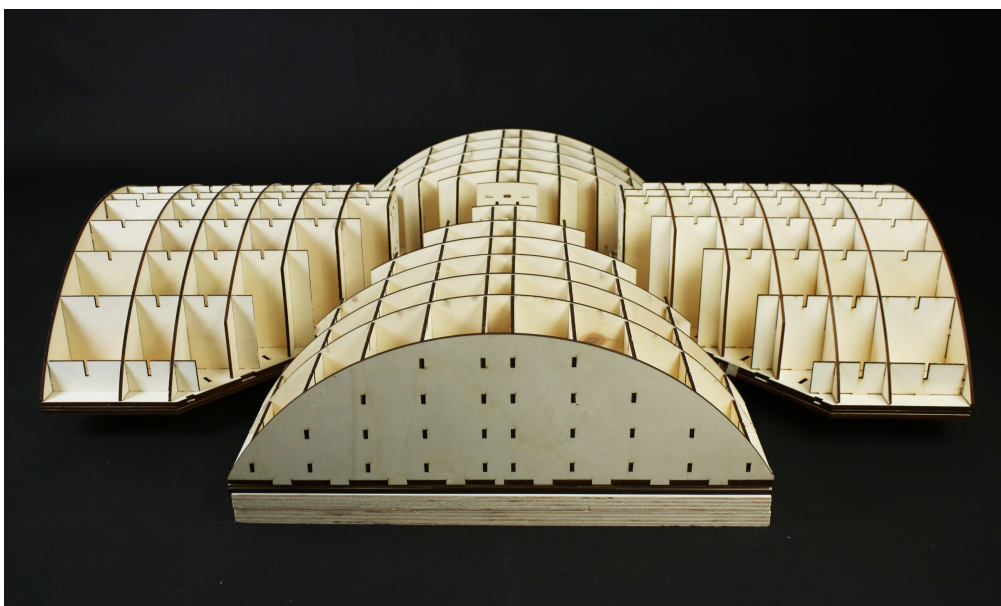
*Fig. 4.13 – Final plywood prototype, assembly process of the centering system. Entire centering structure.
d. Sliding the lateral bases
e. Frontal web longitudinal diaphragms
f. Rear web longitudinal diaphragms*



g.



h.



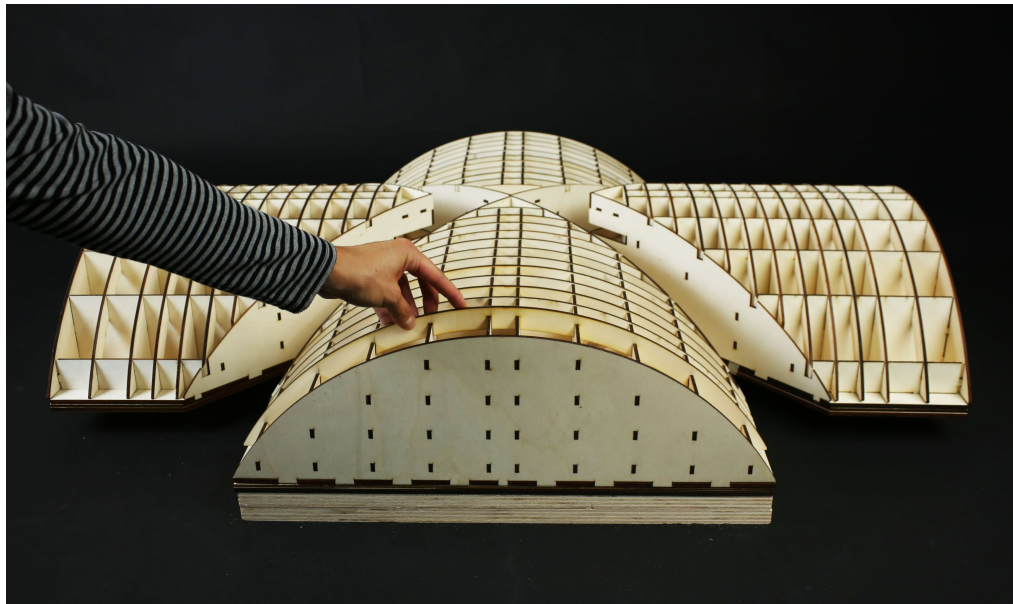
i.

*Fig. 4.13 – Final plywood prototype, assembly process of the centering system. Entire centering structure.
g. Lateral webs longitudinal diaphragms
h. Frontal web transverse diaphragms
i. Transverse diaphragms in place*

j.



k.



l.

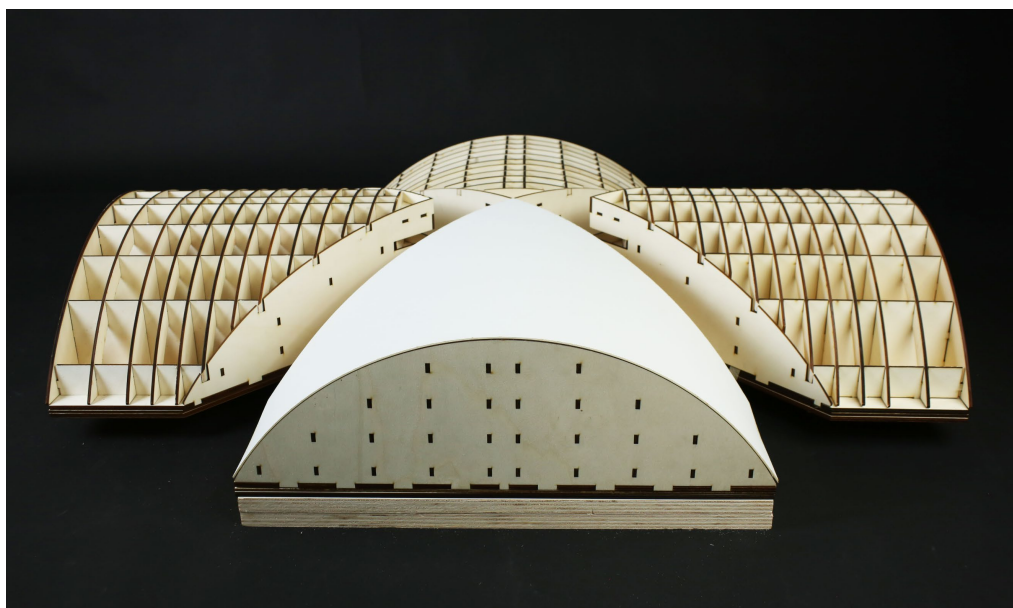
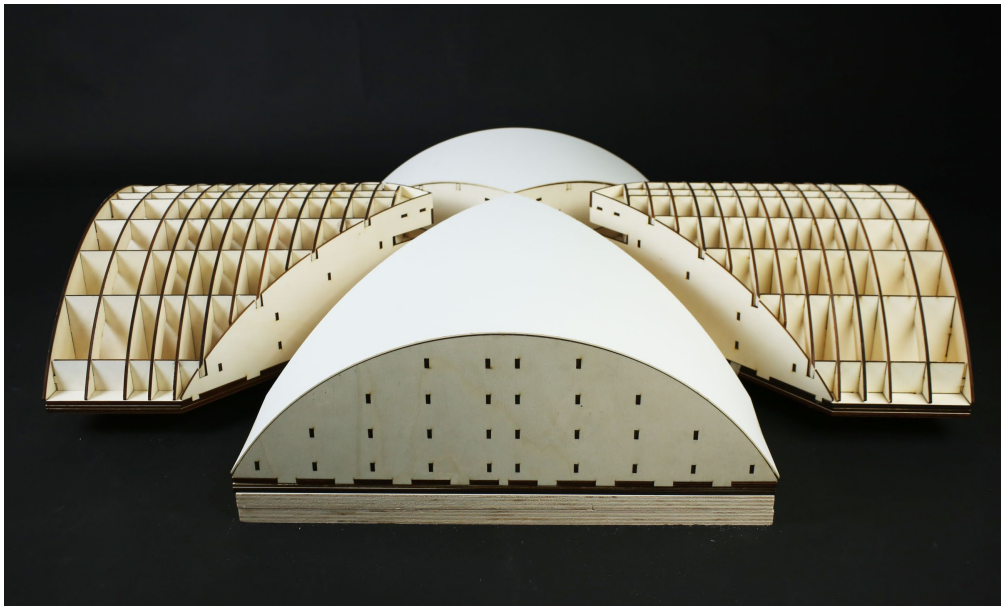


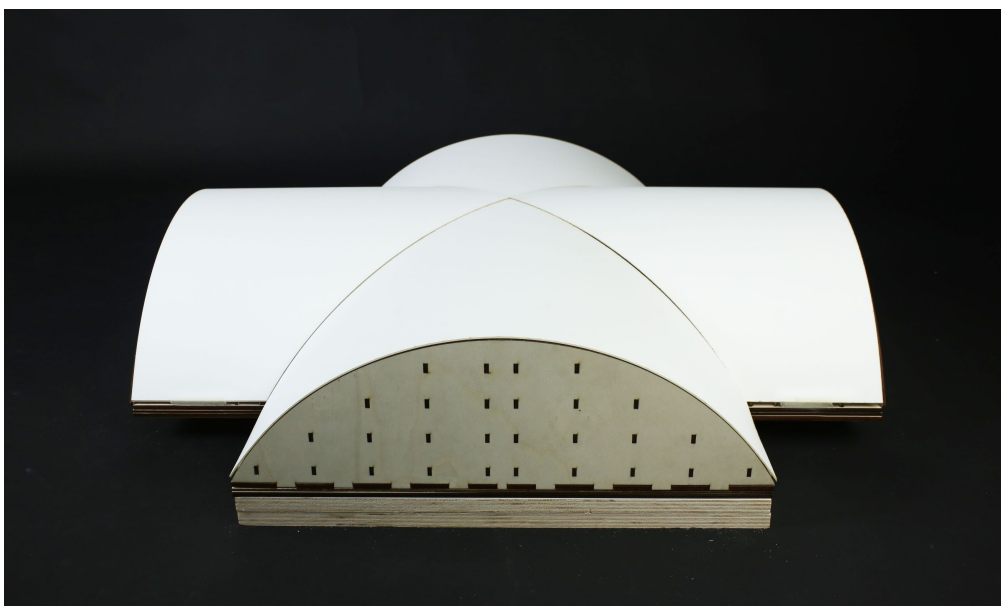
Fig. 4.13 – Final plywood prototype, assembly process of the centering system. Entire centering structure.
j. Diagonals in place
k. Arches in place
l. Frontal cardboard shell



m.



n.



o.

Fig. 4.13 – Final plywood prototype, assembly process of the centering system. Entire centering structure. m. Rear cardboard shell n. Lateral webs shell o. Complete prototype, sliding the lateral webs in place

5. *Conclusions*

The present work focused on the design and realization of a small-scale model for the analysis of vaulted structures. In particular, the research involved the conception and subsequent construction of a plywood and metal testing setup, intended for conducting structural tests on 1:5 scale models of cross-vaults.

The main objectives of the work are displayed in Chapter 1, while an excursus about small-scale models of arches and vaults is presented in Chapter 2. The compilation of comparison tables summarizing the state of the art in experimental campaigns on masonry vaults has proven to be an effective tool to chronologically organize the research studies, highlighting encountered key issues in the experimental phases and, consequently, clarifying the specific direction this thesis aims to further explore.

Not many literature cases thoroughly address the topic of centering, which is used as the support for the small-scale vault construction. However, this is not a minor issue. Indeed, poorly studied procedures for constructing, positioning and handling the centering can lead to assembly errors between vault's blocks. Moreover, imperfections during the initial assembly phases of the vault can result in more significant errors during the structural testing phase.

Therefore, the concept of a modular centering, positioned beneath the vault and removed prior to the testing phase, was developed alongside the other components of the testing setup.

The design phase of the testing setup model is explained in Chapter 3. First, the geometry of the vault, its boundary conditions and its interlocking blocks are introduced.

This first part is followed by a detailed description of the evolution of the testing setup design process. The numerous tests carried out were grouped into three consecutive steps.

From an initial approach to the problem, a first complete version of the

testing setup was developed, featuring centering movement through an integrated system within its geometry and a six supports system. Although conceptually functional, this system quickly proved to be too complex to be realized. Therefore, reconsidering the system in terms of feasibility and general simplification, the final version of the testing setup was designed. The final prototype is characterized by a frame-based centering maneuvering system.

Two subsections of Chapter 3 are dedicated to the detailed description of the design of the plywood centering and its manual maneuvering system.

Chapter 4 focuses on the realization of the elements that compose the testing setup.

It starts with printing tests of the vault blocks and abutments using additive manufacturing techniques, followed by the full assembly of the centering system. The images on the following page (Fig. 5.1, 5.2) have been included to conclude this work, showing which components of the setup have been designed (Fig. 5.1) and which ones have been prototyped (Fig. 5.2). With regard to Figure 5.2, the elements that have been realized are listed hereafter:

- a plywood centering system for the cross-vault
- the cross-vault PLA abutments
- the vault's contrast wall
- the steel frame system for moving the plywood centering

In this regard, it is important to highlight the delicate transition between the digital and the physical model. Too often, the focus is placed on digital models involving geometries, angles and details that are either impossible or highly costly to be physically reproduced. Therefore, one of the central experimental aspects of this thesis was managing this delicate transition: designing the setup's components, while thinking at the assembly process. For instance, designing the interlocking elements of the centering, the plywood back wall and the PLA abutments required tailoring the joints, cut lines and the surfaces

orientation specifically for the machinery that would have produced each piece.

In conclusion, the future developments of this thesis will include an experimental and numerical study on the structural behavior of cross-vaults under the effects of quasi-static displacements such as shear displacement, opening test and tilting test.

To achieve this goal, several intermediate steps need to be developed in detail. These include defining a mechanical frame system for moving the plywood centering, producing other mechanical parts to conduct the structural tests, 3D-printing and filling all the interlocking blocks of the cross-vault and finally ensuring that all the connections between the different elements are precise to guarantee an effective assembly of the testing setup.

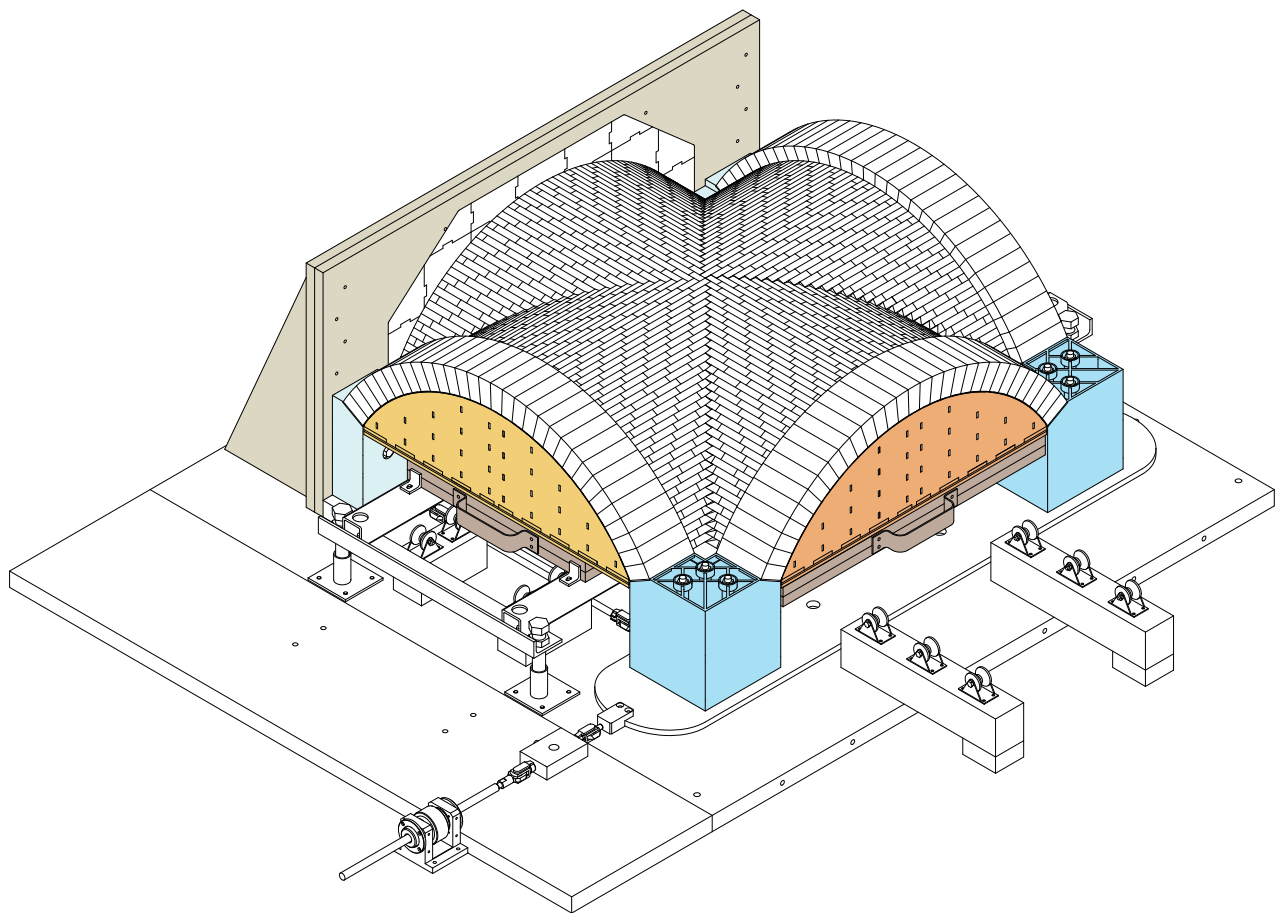


Fig. 5.1 - Designed components of the testing setup system. In color the built components.



Fig. 5.2 - Prototyped components of the testing setup system. From the top: plywood centering system, plywood back wall (932 x 450 x 18 mm) realized with a CNC milling machine, vault's 3D-printed abutments.



Fig. 5.2 - Prototyped components of the testing setup system. From the top: the steel frame system for moving the plywood centering, assembled components of the testing setup, lateral view and frontal view.

6. References

- [1] M. Rossi, C. Calvo Barentin, T. Van Mele, P. Block (2017), *Experimental study on the behavior of masonry pavilion vaults on spreading supports*, in «Structures», Vol. 11, pp. 110-120, DOI: 10.1016/j.istruc.2017.04.008
- [2] CHG Polito, *REVHEAL: Structural Rehabilitation of Vaults in Heritage Asset Learning*:
<https://constructionhistorygroup.polito.it/revheal-structural-rehabilitation-of-vaults-in-heritage-asset-learning-collapse-identification-and-design-of-compatible-strengthening-systems-supported-by-adaptive-3d-models-a-monaco-principal-in/> (last cons. 20/10/2024)
- [3] M. Alforno (2021), *Investigation of the Role of Constructive Aspects on the Structural Response of Masonry Vaults*, doctoral thesis, Politecnico di Torino
- [4] M. Rossi (2015), *Evaluation of the Seismic Response of Masonry Cross-Vaults*, doctoral thesis, Università degli studi di Genova
- [5] E. Buckingham (1914), *On physically similar systems; Illustrations of the use of dimensional equations*. *Physical Review*, Vol. 4, N° 4, pp. 345-376
- [6] S. G. Longo (2022), *Principles and Applications of Dimensional Analysis and Similarity*, Springer
- [7] B. Addis (2013), *Toys that save millions - A history of using physical models in structural design*, in «The structural engineer», Vol. 91, issue 4, pp. 12-27, DOI:10.56330/UUCG3306
- [8] B. Addis (2021), *Physical Models and Innovation in Architectural and Civil Engineering*, in «Nexus network journal», Vol. 23, pp. 833-854, DOI:10.1007/s00004-021-00560-1
- [9] J. Heyman (1995), *The Stone Skeleton*, Cambridge University Press, p. 249-279

- [10] B. Addis (2020), *Physical models: Their historical and current use in civil and building engineering design*, Ernst & sohn, Germany
- [11] A.A.H. Danyzy (1732), *Méthode générale pour déterminer la résistance qu'il faut opposer à la poussée des voûtes. Histoire de la Société Royale des Sciences établie à Montpellier*, pp. 40-56
- [12] N. Sardo (2004), *La figurazione plastica dell'architettura: modelli e rappresentazione*, Kappa, Roma
- [13] A. Cabanillas Cuesta (2019), *Convention Hall. Chicago 1953. Contexto e implantación urbana. Mies van der Rohe*, master thesis, Universitat Politècnica de València
- [14] B. Addis (2020), *Past, current and future use of physical models in civil engineering design*, ICE Proceedings Civil Engineering, DOI: 10.1680/jcien.20.00028
- [15] A.Dell'Endice, A. Iannuzzo, M. J. DeJong, T. Van Mele, P. Block (2021), *Modelling imperfections in unreinforced masonry structures: Discrete element simulations and scale model experiments of a pavilion vault*, in «Engineering structures», Vol. 228, DOI:10.1016/j.engstruct.2020.111499
- [16] E. Bertolesi, J. M. Adam, P. Rinaudo, P. A. Calderón (2019), *Research and practice on masonry cross vaults - A review*, in «Engineering structures», Vol. 180, pp. 67-88, DOI:10.1016/j.engstruct.2018.10.085
- [17] D. Theodossopoulos, B. P. Sinha, A. S. Usmani, A. J. Macdonald (2002), *Assessment of the Structural Response of Masonry Cross Vaults*, in «Strain», Vol. 38, pp. 119-127, DOI:10.1046/j.0039-2103.2002.00021.x
- [18] B. Torres, E. Bertolesi, P. A. Calderón, J. J. Moragues, J. M. Adam (2019), *A full-scale timber cross vault subjected to vertical cyclical displacements in one of its supports*, in «Engineering structures», Vol. 183, pp. 791-804, DOI:10.1016/j.conbuildmat.2019.06.015
- [19] G. Caceres-Vilca, J. Copa-Pineda, F. Copa-Pineda, C. Malaga-Chuquitaype (2024), *Experimental assessment of sillar masonry barrel vaults retrofitted with reinforced concrete elements*, in «Structures», Vol. 62, DOI:10.1016/j.istruc.2024.106145

- [20] T. Van Mele, J. McInerney, M. J. DeJong, P. Block (2012), *Physical and computational discrete modelling of masonry vault collapse*, Structural analysis of historical constructions, SAHC, Wroclaw, Poland
- [21] M. Rossi, C. Calderini, S. Lagomarsino (2016), *Experimental testing of the seismic in-plane displacement capacity of masonry cross vaults through a scale model*, in «Bulletin of Earthquake Engineering», Vol. 14, pp. 261-281, DOI 10.1007/s10518-015-9815-1
- [22] M. Rossi, C. C. Barentin, T. Van Mele, P. Block (2017), *Collapse Analysis of Unreinforced Masonry Vaults Using 3D-printed Scale-model Testing*, 7th International Conference on Advances in Experimental Structural Engineering, Pavia, Italy, DOI:10.7414/7aese.T2.130
- [23] D. Foti, V. Vacca, I. Facchini (2018), *DEM modeling and experimental analysis of the static behavior of a dry-joints masonry cross vaults*, in «Construction and building materials», Vol. 170, pp.111-120, DOI:10.1016/j.conbuildmat.2018.02.202
- [24] G. Milani, M. Rossi, C. Calderini, S. Lagomarsino (2016), *Tilting plane tests on a small-scale masonry cross vault: Experimental results and numerical simulations through a heterogeneous approach*, in «Engineering structures», Vol. 123, pp. 300-312, DOI:10.1016/j.engstruct.2016.05.017
- [25] C. Carfagnini, S. Baraccani, S. Silvestri, D. Theodossopoulos (2018), *The effects of in-plane shear displacements at the springings of Gothic cross vaults*, in «Construction and building materials», Vol. 186, pp.219-232, DOI:10.1016/j.conbuildmat.2018.07.055
- [26] S. Baraccani, L. Zauli, D. Theodossopoulos, S. Silvestri (2020), *Experimental test on a fibre-reinforced scaled cross vault subjected to in-plane shear displacements at the springings*, in «Construction and building materials», Vol. 265, DOI:10.1016/j.conbuildmat.2020.120305
- [27] A. Gaetani, N. Bianchini, P. B. Lourenço (2020), *Simplified micro-modelling of masonry cross vaults: stereotomy and interface issues*, in «International Journal of masonry research and innovation», Vol. 6, N° 1, DOI:10.1504/IJMRI.2021.112076

- [28] F. Roselli (2021), *Use of physical models in the structural analysis of spatial structures: an application to masonry arches and vaults*, master thesis, Politecnico di Torino
- [29] N. Bianchini, P. B. Lourenço, N. Mendes, C. Calderini (2019), *Seismic assessment of masonry cross vaults through numerical nonlinear static and dynamic analysis*, 7th International Conference on Computational Methods in Structural Dynamics and Earthquake Engineering, Crete, Greece, DOI:10.7712/120119.6942.18709
- [30] M. Alforno, F. Venuti, A. Monaco, C. Calderini (2023), *Numerical Investigation of the Influence of Constructive Aspects on the Structural Behaviour of Masonry Cross Vaults*, in «International Journal of Architectural Heritage», Vol. 17, Issue 6, 868-891, DOI: 10.1080/15583058.2021.1992534
- [31] N. Bianchini, N. Mendes, C. Calderini, P. B. Lourenço (2023), *Modelling of the dynamic response of a reduced scale dry joints groin vault*, in «Journal of Building Engineering», Vol. 66, DOI:10.1016/j.job.2023.105826
- [32] B. Torres, E. Bertolesi*, P. A. Calderón, J. J. Moragues, J. M. Adam (2019), *A full-scale timber cross vault subjected to vertical cyclical displacements in one of its supports*, in «Engineering Structures», Vol. 183, pp. 791-804
- [33] N. Bianchini, N. Mendes, C. Calderini, P. Candeias, P. B. Lourenço (2023), *Shaking Table Testing of an Unstrengthened and Strengthened with Textile Reinforced Mortar (TRM) Full-Scale Masonry Cross Vault*, in «International Journal of Architectural Heritage», <https://doi.org/10.1080/15583058.2023.2295900>
- [34] N. Bianchini, N. Mendes, C. Calderini, P. X. Candeias, M. Rossi, P. B. Lourenço (2021), *Seismic response of a small-scale masonry groin vault: experimental investigation by performing quasi-static and shake table tests*, in «Bulletin of Earthquake Engineering», Vol. 20, <https://doi.org/10.1007/s10518-021-01280-0>
- [35] A. Becchi, F. Foce (2002), *Degli archi e delle volte: arte del costruire tra meccanica e stereotomia*, Marsilio, Venezia

[36] M. Alforno, F. Venuti, A. Monaco (2020), *The structural effects of micro-geometry on masonry vaults*, in «Nexus Network Journal», Vol. 22, Issue 4, pp. 1237-1258

[37] D. Chhabra (2017), *Comparison and analysis of different 3d-printing techniques*, in «International Journal of Latest Trends in Engineering and Technology», Vol. 8, Issue 4, pp. 264-272, DOI: <http://dx.doi.org/10.21172/1.841.44>